# INFORMATION TO USERS

This manuscript has been reproduced from the microfilm master. UMI films the text directly from the original or copy submitted. Thus, some thesis and dissertation copies are in typewriter face, while others may be from any type of computer printer.

**The quality of this reproduction is dependent upon the quality of the copy submitted.** Broken or indistinct print, colored or poor quality illustrations and photographs, print bleedthrough, substandard margins, and improper alignment can adversely affect reproduction.

In the unlikely event that the author did not send UMI a complete manuscript and there are missing pages, these will be noted. Also, if unauthorized copyright material had to be removed, a note will indicate the deletion.

Oversize materials (e.g., maps, drawings, charts) are reproduced by sectioning the original, beginning at the upper left-hand corner and continuing from left to right in equal sections with small overlaps. Each original is also photographed in one exposure and is included in reduced form at the back of the book.

Photographs included in the original manuscript have been reproduced xerographically in this copy. Higher quality 6" x 9" black and white photographic prints are available for any photographs or illustrations appearing in this copy for an additional charge. Contact UMI directly to order.

**UMI**

A Bell & Howell Information Company
300 North Zeeb Road, Ann Arbor MI 48106-1346 USA
313/761-4700 800/521-0600

Université d'Ottawa · University of Ottawa

# Properties of the Resting Membrane Potential in Central Myelinated Axons During Normoxic Conditions and Metabolic Inhibition

by

Lisa Leppanen

A thesis submitted to the
School of Graduate Studies and Research
in partial fulfillment of the requirements for the degree of
Master of Science

Department of Anatomy and Neurobiology
University of Ottawa
Ottawa, Ontario
April, 1997

## ABSTRACT

Anoxia/ischemia impairs the ability of CNS myelinated axons to maintain resting membrane potential, resulting in membrane depolarization. Subsequent irreversible damage occurs from a rise in $[Ca^{2+}]_i$ with $Ca^{2+}$ entering via reverse operation of the $Na^+/Ca^{2+}$ exchanger (Stys et al., 1992c). Exchanger mediated $Ca^{2+}$ entry is strongly modulated by membrane potential and therefore the degree of depolarization will influence the extent of deleterious $Ca^{2+}$ influx.

Compound resting membrane potential was studied in the rat optic nerve, a representative model of myelinated CNS axons, using the grease gap recording technique which measures a reliable fraction of the true intra-axonal potential. Studies were performed during 1) normoxic conditions, 2) glycolytic inhibition, or 3) chemical anoxia at 37 °C, in order to characterize ions and channels promoting membrane depolarization.

Ouabain, an antagonist of $Na^+,K^+$-ATPase, caused strong depolarization, showing that membrane potential is critically dependent on $Na^+,K^+$-ATPase. In addition, inhibiting energy metabolism during ouabain exposure produced further depolarization, suggesting additional ATP-dependent, ouabain-insensitive ion transport systems.

Glycolysis was blocked with iodoacetate or deoxyglucose, evoking a response consisting of four distinct phases. An initial transient hyperpolarization (phase 1) preceded a rapid depolarizing response (phase 2). Phase 2 was interrupted by a second brief hyperpolarization (phase 3) which was followed by a gradual depolarization (phase 4). Chemical anoxia (cyanide) immediately depolarized the nerve, with only a small inflection introducing a final slow depolarizing response. Addition of ouabain to cyanide-treated nerves caused an additional depolarization indicating a minor glycolytic contribution to $Na^+,K^+$-

ATPase, which seems preferentially fueled by mitochondrial ATP in optic nerve. Hyperpolarizing phases 1 and 3 induced by iodoacetate exposure and the inflection during cyanide treatment were abolished by zero-$Ca^{2+}$/EGTA treatment. Activation of a $Ca^{2+}$-dependent $K^+$ conductance during the hyperpolarizing phases is postulated.

Block of $Na^+$ channels with tetrodotoxin, the local anesthetics, procaine or QX-314, or replacement of $Na^+$ with the impermeant cation choline significantly reduced depolarization during iodoacetate or cyanide application, indicating that axonal membrane depolarization requires $Na^+$ influx which secondarily allows electroneutral $K^+$ efflux and depolarization.

The $Ca^{2+}$-dependent hyperpolarizing phases leading to abrupt reductions in depolarization rates may reflect intrinsic mechanisms designed to limit axonal injury during energy deprivation.

## TABLE OF CONTENTS

## LIST OF TABLES

## LIST OF FIGURES

## LIST OF ABBREVIATIONS

[ ]: concentration

$[\ ]_o$: extracellular concentration

$[\ ]_i$: intracellular concentration

aCSF: artificial cerebral spinal fluid

AMPA: alpha-amino-3-hydroxy-5-methyl-4-isoxazolepropionic acid

4-AP: 4-aminopyridine

APH: 2-amino-7-phosphonoheptanoic acid

APV: D-(-)-2-amino-5-phosphonopentanoate

ATP: adenosine triphosphate

$Ba^{2+}$: barium

$Ca^{2+}$: calcium

CAP: compound action potential

$Cd^{2+}$: cadmium

CNQX: 6-cyano-7-nitro-quinoxaline-2,3-dione

CNS: central nervous system

$Co^{2+}$: cobalt

$CO_2$: carbon dioxide

$Cs^+$: cesium

cyanide: $CN^-$

DG: 2-deoxyglucose

ECS: extracellular space

EGTA: ethylene glycol-bis(b-amino ethyl ether)-N,N,N',N'-tetraacetic acid

$E_K$: $K^+$ equilibrium potential

$E_{Na}$: $Na^+$ equilibrium potential

GM: gray matter

$H^+$: proton

IAA: iodoacetic acid - $Na^+$ salt

$InsP_3$: inositol-1,4,5-trisphosphate

$K^+$: potassium

$K_{ATP}$: ATP sensitive $K^+$ conductance

$K_{Ca}$: $Ca^{2+}$ activated $K^+$ conductance

$K_{fast}$: fast $K^+$ channel

$K_{IR}$: inward rectifier channel

$K_{Na}$: $Na^+$ activated $K^+$ channel

$K_{slow}$: slow $K^+$ channel

$Li^+$: lithium

μm: micron

μM: micromolar

$Mg^{2+}$: magnesium

min: minute

mM: millimolar

ms: millisecond

$Na^+$: sodium

NADH: nicotinamide adenine dinucleotide (reduced form)

NBQX: 2,3-dihydroxy-6-nitro-7-sulfamoyl-benzo quinoxaline

nM: nanomolar

NMDA: *N*-methyl-D-aspartate

NMDG: *N*-methyl-D-glucamine

$O_2$: oxygen

$P_K$: $K^+$ permeability

$P_{Na}$: $Na^+$ permeability

$R_e$: external resistance

$R_g$: trans-gap resistance

$R_i$: internal axoplasmic resistance

RMP: resting membrane potential

RON: rat optic nerve

ROS: reactive oxygen species

TCA: tricarboxylic acid

TEA: tetraethylammonium chloride

TTX: tetrodotoxin

$V_g$: recorded membrane potential

$V_m$: absolute membrane potential

WM: white matter

## ACKNOWLEDGEMENTS

I would like to give my sincere gratitude to Dr. Peter Stys for his guidance; excellent (and patient) teaching; generously lending "Huey" for an unlimited amount of time; and his *personal* support. I know that I have received exceptional scientific training (you have turned me into a monster); not to mention that my writing skills have also improved exponentially. Your suggestions improved the research project from excellent to *great*, and for this I am truly grateful.

I would like to thank the members of my advisory committee, Dr. Bin Hu and Dr. Howard Lesiuk, for their very helpful suggestions during my studies.

My greatest thanks to: Meister for *always* listening and just being there; Belley (let's re-hash); Dort (Calmez); James (my friend who was always just 3 feet apart, making those long hours fun; not to mention the great *life* discussions); Isabella (someone who really enjoys food as much as I do; I very much appreciated your help); Moe (I will truly miss our morning chats - the memories I will take with me); the Toronto Contingent; and my dinner gang in Ottawa - I always looked forward to those planned Sat nights (after long hours at the lab) and enjoyed myself immensely. A special thank-you to A and M.

I know that this thesis *definitely* would not have been possible without the never-ending love and support from my family, especially my parents. I appreciated the *constant* encouragement on those really difficult days.

***To Eric***

# CHAPTER 1

## INTRODUCTION

The central nervous system (CNS) is a complex network of well organized neuronal connections functioning to elicit physiological responses. A diverse group of structures present in the CNS, including the neuronal cell somata, axons, synaptic terminals, and glial cells, allows for efficient signal processing and transmission. Neurons (collectively the gray matter (GM)) communicate via synaptic connections using neurotransmitters, while signal propagation across distances is effected by axons (collectively the white matter (WM)).

Axonal dysfunction occurring from neurological disorders will have a dramatic impact on signal transmission because axons are a key component underlying information transfer between neurons. Stroke is one of the leading causes of death in the population. Moreover, approximately 20% of strokes affect WM only (Fisher, 1982; Bamford et al., 1987). Other prevalent diseases affecting mainly WM are spinal cord injury, ischemic optic neuropathy and radiation-induced WM necrosis (Stys et al., 1995a). It is for these reasons that the study of CNS axon physiology and pathophysiology is of prime importance. The goal of the present study was to examine CNS axons subjected to various experimental conditions designed to investigate the mechanisms causing damage induced by an anoxic/ischemic insult.

## 1.1 Gray Matter

### 1.1.1 Neuronal Signaling in Gray Matter

In mammalian GM, neuronal signaling generally consists of a stereotyped sequence of events. Initially, the cell soma receives stimuli via synaptic input from other neurons and processes the input by integrating the various signals to generate an action potential (Kandel and Schwartz, 1991). The action potential then propagates along the axon and arrives at the synaptic terminal, where it opens voltage gated $Ca^{2+}$ channels. $Ca^{2+}$ entry through these channels and into the presynaptic nerve terminal causes the release of a neurotransmitter.

The excitatory amino acid glutamate has been shown to act at several different receptors, including the *N*-methyl-D-aspartate (NMDA), alpha-amino-3-hydroxy-5-methyl-4-isoxazolepropionic acid (AMPA), and kainate receptors. These receptors are permeable to $Na^+$ and $K^+$, and the NMDA and some types of AMPA/kainate receptors are also permeable to $Ca^{2+}$ (Kandel and Schwartz, 1991; Brorson et al., 1994), which is why they, particularly the NMDA receptor, have been implicated in the pathogenesis of ischemic neuronal injury (Rothman and Olney, 1987; Choi, 1988).

The NMDA receptor channel is gated by glutamate and by the membrane potential. Both glutamate binding and depolarization, which removes the $Mg^{2+}$ block normally present in the NMDA channel (Kandel and Schwartz, 1991), are necessary for channel opening. Following receptor activation, glutamate must be removed from the synaptic cleft to terminate its physiological effect. Removal of glutamate from the extracellular space (ECS) is performed by a $Na^+$, $K^+$, and potential dependent glutamate transporter present in neurons (Nicholls and Attwell, 1990) and glia, specifically astrocytes (Chiu and Kriegler, 1994).

Since $Ca^{2+}$ is instrumental in neurotransmitter release and acts as a second messenger to activate various enzyme systems, a number of regulatory pathways exist in the neuron to re-establish and maintain $Ca^{2+}$ homeostasis. Theoretically, a low $[Ca^{2+}]_i$ can be maintained by 1) extrusion via the plasmalemmal proteins, $Ca^{2+}$-ATPase and $Na^+/Ca^{2+}$ exchanger, 2) uptake by intracellular storage organelles such as the endoplasmic reticulum (sarco(endo)plasmic reticulum calcium (SERCA) pump) and mitochondria, and 3) adsorption by cytosolic buffers such as calmodulin, calsequestrin and calbindin (Kostyuk and Verkhratsky, 1994). $Ca^{2+}$ stores, such as the endoplasmic reticulum, are controlled either by $Ca^{2+}$ itself or by inositol-1,4,5-trisphosphate ($InsP_3$) (Kostyuk and Verkhratsky, 1994). Since most of these systems are either directly or indirectly dependent on cellular energy production, anoxia/ischemia can rapidly and seriously disrupt the homeostasis of this key regulatory cation.

### 1.1.2 Energy Metabolism

The return to the resting levels of various ions following nerve excitation is an energy dependent process. Energy is generated by glycolytic and mitochondrial production of ATP. One molecule of glucose yields 2 molecules of ATP via glycolysis and 34 or 36 molecules of ATP from oxidative phosphorylation (Erecinska and Silver, 1989). Glycolysis functions in an $O_2$ independent manner, metabolically converting glucose to pyruvate in the cytosol (Stryer, 1988). Although glycolysis generates some energy, it more importantly synthesizes the substrate, pyruvate, that is obligatory for the subsequent production of mitochondrial ATP via the tricarboxylic acid (TCA) cycle and electron transport chain. Pyruvate is converted to acetyl coenzyme A, the compound that enters the TCA cycle located within the matrix of the mitochondria to yield NADH (nicotinamide adenine dinucleotide (reduced form)).

Of note, other substrates including various amino acids will produce NADH, but pyruvate is the primary substrate utilized by the TCA cycle (Stryer, 1988). NADH provides the essential electrons that are transferred to $O_2$. As the flow of electrons occurs via enzyme complexes (NADH-Q reductase, cytochrome reductase and cytochrome oxidase) located on the cristae of the inner mitochondrial membrane, $H^+$ ions are moved across this membrane with energy released by electron flow, thus creating a membrane potential. Consequently, $H^+$ returns to the inner matrix because of the electrochemical driving force. It is the re-entry of $H^+$ that drives the formation of ATP (Stryer, 1988). It is apparent that the mitochondria plays a critical role in maintaining ion homeostasis in the neuron since it synthesizes a substantial portion of the ATP. Neural tissue is not equipped with abundant stores of ATP (Siesjö, 1984), essentially depending on the continuous activity of glycolysis and oxidative phosphorylation to generate energy. Lack of glucose or $O_2$ will lead to rapid depletion of cellular energy stores (Siesjö, 1984), eventually resulting in cell damage.

### 1.1.3 Anoxic/Ischemic Injury of Gray Matter Tissue

Unlike many other tissues, GM is exquisitely dependent on a continuous supply of energy. Oxygen and glucose deprivation ultimately leads to GM injury, but the manner in which GM is damaged differs from WM. The difference in the anatomical structure of the cell soma and myelinated axon, specifically the lack of synapses in a myelinated tract, becomes of significant importance with respect to the mechanism of anoxic/ischemic injury. During GM ischemia, $[glutamate]_o$ rises to damaging levels in the rat hippocampus (Benveniste et al., 1984) and rat striatum (Obrenovitch et al., 1993). Glutamate may be released via exocytosis which would occur in response to $Ca^{2+}$ entry through pre-synaptic voltage gated $Ca^{2+}$ channels activated by $[K^+]_o$ mediated depolarization. The rise in

$[glutamate]_o$ could also occur by reverse operation of the glutamate transporter following membrane depolarization and/or increases in $[Na^+]_i$ or $[K^+]_o$ (Taylor et al., 1992). Under these conditions, glutamate becomes a toxic substance by producing overstimulation of the NMDA receptor, permitting excessive ion flux (discussed in next section). Evidence for a link between synaptic activity, specifically the NMDA receptor, and neurotoxicity during metabolic stress has been previously demonstrated in cultured hippocampal neurons that survived exposure to cyanide ($CN^-$) or anoxia if the $[Mg^{2+}]_o$ was elevated (Rothman, 1983), indicating that $Mg^{2+}$ exerts a protective effect by blocking the NMDA receptor pore. The protective effect of $Mg^{2+}$ has more recently been reported in studies using cortical cell cultures (Choi, 1987; Goldberg and Choi, 1993).

*NMDA Receptor Mediated Damage*

Evidence that neurotoxicity is mediated, at least in part, by glutamate was demonstrated by preventing anoxic damage of cultured hippocampal cells with the antagonist, γ-D-glutamylglycine (Rothman, 1984). Additional evidence for glutamate and NMDA receptor mediated cell death was obtained from results showing a reduction in ischemic damage by using the NMDA antagonists, 2-amino-7-phosphonoheptanoic acid (APH) in hippocampal cells *in vivo* (Simon et al., 1984), and MK-801, D-(-)-2-amino-5-phosphonopentanoate (APV), or dextrorphan in cortical cell cultures (Goldberg and Choi, 1993). These findings demonstrated that glutamate acted on postsynaptic NMDA receptors to mediate injurious ion influx (Goldberg and Choi, 1993). One component glutamate neurotoxic action at the NMDA receptor is through osmotic swelling which is a $Ca^{2+}$-independent effect. Removal of $Cl^-$ from a glutamate containing perfusate in hippocampal cells prevented swelling, thus it was suggested that a passive flux of $Na^+$, $Cl^-$ and $H_2O$ was responsible for swelling (Rothman, 1985). In addition to

the damaging effects of $Ca^{2+}$-independent neuronal swelling, there is also a $Ca^{2+}$-dependent component. Ischemic damage in cortical cell cultures was prevented by blocking $[Ca^{2+}]_i$ accumulation with NMDA antagonists (Goldberg and Choi, 1993).

In addition to glutamate, depolarization is necessary to open the NMDA receptor channel because it removes the voltage sensitive $Mg^{2+}$ plug in the channel pore. It was suggested that $Na^+$ influx was responsible for initiating membrane depolarization (Rothman, 1985). Increased permeability of the membrane to $Na^+$ and $K^+$ by glutamate activating both NMDA and non-NMDA receptors may intensify membrane depolarization.

*Injury Mediated by Non-NMDA Receptors*

NMDA receptor activation and subsequent $Ca^{2+}$ influx have been the focus of elucidating the mechanism of GM injury induced by anoxia/ischemia. However, complete protection of the neuron is not afforded by simply blocking the NMDA receptor during prolonged exposure to ischemia (Lynch et al., 1995), indicating that other mechanisms are partially responsible for injury. The non-NMDA glutamate agonists, kainate or AMPA, induced damage in cortex (Frandsen et al., 1989) and in cortical cell cultures (Koh et al., 1990). Application of the AMPA antagonist, 6-cyano-7-nitro-quinoxaline-2,3-dione (CNQX), blocked the deleterious effect of these agonists (Frandsen et al., 1989). Moreover, survival of cortical cells challenged with glutamate was greatest when CNQX and APV were applied together (Frandsen et al., 1989). The effect of non-NMDA antagonists were examined during energy depletion. During ischemia, CNQX failed to provide a beneficial effect to cortical cells (Goldberg and Choi, 1993). The possibility that the damaging effects of NMDA concealed injury by AMPA or kainate receptors was suggested, citing the rapidity of the NMDA

response as a factor (Goldberg and Choi, 1993). In support of this notion, hippocampal cells exposed to ischemia were protected, although not completely, using the AMPA antagonist, 2,3-dihydroxy-6-nitro-7-sulfamoyl-benzo quinoxaline (NBQX) (Buchan, 1992; Pulsinelli, 1996). This suggests that in addition to activation of the NMDA receptor, AMPA receptor activation produces significant deleterious effects during an ischemic insult.

*$Ca^{2+}$ Flow Through Voltage Gated $Ca^{2+}$ Channels*

In addition to $Ca^{2+}$ flux occurring through activated NMDA receptors and certain AMPA/kainate receptors, the rise in cytosolic $Ca^{2+}$ that occurs during anoxia/ischemia may be derived from other transmembrane pathways. The extent to which $Ca^{2+}$ entry through L-type voltage gated $Ca^{2+}$ channels on the postsynaptic membrane contributes to cell injury was explored. The L-type $Ca^{2+}$ channel blocker, nifedipine, attenuated injury in cortical neurons challenged with kainate or AMPA and, also, partially, but significantly reduced injury following exposure to NMDA (Weiss et al., 1990), indicating that this channel contributes to the toxic rise in $[Ca^{2+}]_i$.

Another transmembrane $Ca^{2+}$ influx component that may exacerbate glutamate neurotoxicity may occur via N-, P-, or Q-type voltage gated $Ca^{2+}$ channels. Protection was reported in hippocampal neurons exposed concomitantly to chemical ischemia and the N-, P-, and Q-type channel antagonist, ω-conotoxin MVIIC (Small et al., 1997), presumably due to indirect reduction of synaptic glutamate release.

*Intracellular $Ca^{2+}$ Stores*

Although the increase in $[Ca^{2+}]_i$ is primarily supplied by the ECS, intracellular $Ca^{2+}$ stores were also examined as a potential contributor to the cytosolic $Ca^{2+}$ overload. Elevated $[Ca^{2+}]_i$ evoked by glutamate in cortical neurons was reduced to 30% when dantrolene, a blocker of $Ca^{2+}$ release from intracellular storage organelles, was applied concomitantly with glutamate (Frandsen and Schousboe, 1991). Further support for release from intracellular stores was shown when dantrolene abolished the glutamate induced increase in $[Ca^{2+}]_i$ without extracellular $Ca^{2+}$ present. Although dantrolene significantly improved recovery from glutamate treatment, neuronal loss was still high probably because dantrolene is specific for only one type of receptor. However, the results demonstrate its use as a possible neuroprotective agent. Moreover, the hyperpolarizing response produced by anoxia in hippocampal cells, which is thought to be via a $Ca^{2+}$ activated $K^+$ channel ($K_{Ca}$) (Leblond and Krnjevic, 1989), was abolished with dantrolene (Belousov et al., 1995). Together, the findings show that the release of $Ca^{2+}$ from intracellular stores may be induced by the influx of $Ca^{2+}$ from the ECS which subsequently may amplify the increase in the $[Ca^{2+}]_i$ to cause more damage (Mody and MacDonald, 1995).

*$Na^+$-Dependent Mechanisms of Injury in Gray Matter*

Neuronal loss during anoxia/ischemia is also $Na^+$ dependent which led to the hypothesis that blockade of $Na^+$ influx through any of several pathways may be neuroprotective. Hippocampal slices subjected to anoxia in the presence of TTX showed significantly enhanced recovery compared to anoxia alone, showing that $Na^+$ influx through TTX-sensitive $Na^+$ channels is deleterious (Boening et al., 1989). Rothman (1983) also found protection by treating a hippocampal culture exposed to $CN^-$ with TTX. Lynch et al. (1995) reported similar results in cortical

cell cultures challenged with *in vitro* ischemia. In addition, TTX or QX-314 (another compound that blocks $Na^+$ conductance), enhanced the neuroprotective effect of the NMDA antagonist, MK-801 (Lynch et al., 1995). $Na^+$ influx mediated through TTX-sensitive, voltage gated $Na^+$ channels is not responsible for cell swelling (Choi, 1987). Kiedrowski et al. (1994) confirmed these findings by reporting that $Na^+$ enters mainly through NMDA channels since MK-801 blocked the rise in $[Na^+]_i$. However, the depolarizing response evoked in isolated perfused rat brain during ischemia was delayed by treatment with TTX. The delay may exert a protective effect by preventing excess neurotransmitter release and $Ca^{2+}$ influx (Xie et al., 1994).

*$Ca^{2+}$-Dependent Targets in Gray Matter Injury*

Maintenance of $Ca^{2+}$ homeostasis becomes impaired during ischemia because the regulatory systems are energy dependent. Evidence showed that delayed neuronal death possessed a $Ca^{2+}$ component where sustained elevation of cytosolic $[Ca^{2+}]$ was a primary causal event. $Ca^{2+}$ subsequently activates pathways that are deleterious to the cell.

One injurious pathway is the production of free radicals or reactive oxygen species (ROS). In cultured hippocampal neurons, exposure to glutamate caused an increase in ROS which depended on the presence of extracellular $Ca^{2+}$ (Mattson et al., 1995). This rise was prevented by the antioxidant, vitamin E, as well as by APV. $Ca^{2+}$ may cause ROS production by generating nitric oxide or by activating xanthine oxidase or by promoting arachidonic acid metabolism via activation of phospholipase $A_2$ (Dugan and Choi, 1994). A ROS exerts damaging effects by causing membrane disruption, by affecting glutamate transport in glia, and by altering the functional ability of $Ca^{2+}$ regulating membrane proteins including ion channels and transporters (Dugan and Choi, 1994).

Another damaging effect produced by the neurotoxicity of excitatory amino acids and the subsequent rise in $[Ca^{2+}]_i$ is stimulation of the $Ca^{2+}$ dependent protease, calpain I which degrades structural and functional proteins such as the cytoskeleton (Siman et al., 1989), $Ca^{2+}$-ATPase (Salamino et al., 1994), and myelin proteins (Banik et al., 1987).

*Beneficial Effect of $Na^+/Ca^{2+}$ Exchanger During Anoxia/Ischemia*

The $Na^+/Ca^{2+}$ exchanger may be utilized by the neuron to extrude $Ca^{2+}$ from the cytosol to reduce $Ca^{2+}$ mediated damage during metabolic stress. A study by Andreeva et al. (1991) found that a $Na^+$ free solution or blockade of the exchanger with 3',4'-dichlorobenzamil in cerebellar granule cells exacerbated the toxic effect of glutamate. The results were in agreement with findings in hippocampal neurons (Mattson et al., 1989). Cortical neurons challenged with glutamate in $Na^+$ free conditions were less able in their ability to restore intracellular $Ca^{2+}$ homeostasis (White and Reynolds, 1995). The findings showed that the $Na^+$ dependent $Ca^{2+}$ extrusion mechanism of the neuron is an important protective component during $Ca^{2+}$ overload. Compromise of this system, such as during reduction of the $Na^+$ gradient, will reduce its ability to remove $Ca^{2+}$ from the cytosol and will ultimately exacerbate cell injury. This is in direct contrast to the role of the $Na^+/Ca^{2+}$ exchanger in axons (see section 1.3.2), underscoring the unique pathophysiological mechanisms in GM versus WM.

*Role of Glia During an Anoxic/Ischemic Insult*

There is evidence that glia offer neuroprotection during an anoxic/ischemic insult. Under ischemic conditions or treatment with glutamate, cortical neurons with glia present were less sensitive to the insults than neurons without glia (Vibulsreth et al., 1987; Dugan et al., 1995). Interestingly, glia do not succumb to

the toxic effect of an ischemic insult for hours (Goldberg and Choi, 1993). Why are glia, specifically astrocytes, resistant to anoxia/ischemia? Does this resistance play a role in determining survival of the neuron? Perhaps, glia are resistant for an extended time in comparison to the neuron because they derive energy from their glycogen stores which are much more limited in neurons (Cataldo and Broadwell, 1986). By virtue of their greater resistance, it is possible that astrocytes are able to minimize damage or prolong neuronal survival by performing such functions as removing $K^+$ (Walz et al., 1993) and glutamate (Vibulsreth et al., 1987; Kraig et al., 1995) from the ECS during the insult.

*Apoptosis*

In contrast, support exists for $Ca^{2+}$ in a neuroprotective role (Choi, 1995; Sweeney et al., 1995). Removal of $Ca^{2+}$ was actually more detrimental to cortical cell cultures exposed to an ischemic insult (Goldberg and Choi, 1993). The deleterious effect of zero $Ca^{2+}$ was intensified with the addition of the $Ca^{2+}$ chelator ethylene glycol-bis(b-amino ethyl ether)-N,N,N',N'-tetraacetic acid (EGTA) in the perfusate. Other neurotoxic effects including cell swelling were potentiated by the removal of $Ca^{2+}$ (Goldberg and Choi, 1993). Incubating cerebral cortical cultures with either zero $Ca^{2+}$ perfusate or antagonists of voltage gated $Ca^{2+}$ channels induced neuronal injury which was prevented by applying the protein synthesis inhibitor, cycloheximide (Koh and Cotman, 1992). This suggested that low levels of $Ca^{2+}$ may signal apoptosis, implicating that reducing $Ca^{2+}$ below a certain level may be paradoxically injurious (Koh and Cotman, 1992).

Apoptosis, or programmed cell death, has been observed to occur in cortical cells exposed to ischemia (Gwag et al., 1995). Cells treated with MK-801 and CNQX were examined 24 and 48 hours after an ischemic insult. Minimal loss

occurred at 24 hours, but at 48 hours cell lysis was prevalent. By applying cycloheximide simultaneously with the glutamate receptor antagonists, damage to the neuron was significantly reduced (Gwag et al., 1995). The findings indicate that neurons may degenerate regardless of the protective therapies applied immediately following an anoxic or ischemic insult.

## 1.2 Axon Structure and Function

### 1.2.1 Structure of the Central Myelinated Axon

The axon is a cylindrical structure, maintained by cytoskeletal proteins including neurofilaments and microtubules (Waxman, 1995). The structure is covered by myelin which is an extension of the oligodendroglial plasmalemma. One oligodendrocyte will ensheath several different axons by wrapping its processes repeatedly around the fiber (Hirano, 1968). The astrocyte is a second glial cell present in the CNS. It extends processes which contain large amounts of glycogen (Cataldo and Broadwell, 1986), adjacent to the node of Ranvier (Waxman and Black, 1984).

*Ion Channels in the Axon*

Axonal ion channels are strikingly segregated in myelinated axons, in order to efficiently support action potential conduction. The voltage dependent, rapidly inactivating $Na^+$ channel is located primarily at the node of Ranvier, an interruption of the myelin along the length of the axon and the only component of the axon cylinder directly exposed to the ECS. Immunostaining with an antibody against $Na^+$ channels in rat optic nerve (RON) axons, revealed high densities at the node while the paranodal and internodal areas did not display any immunoreactivity (Black et al., 1989). Further support for clustering of the $Na^+$

channel at the node was shown in peripheral axons in a binding study using the labeled $Na^+$ channel antagonist, [$^3$H]saxitoxin (Ritchie and Rogart, 1977). It has been proposed that the $Na^+$ channel is anchored to the node of Ranvier by the cytoskeletal proteins ankyrin and spectrin (Srinivasan et al., 1988; Hirano and Llena, 1995). In addition to the voltage dependent $Na^+$ channel at the nodal axolemma, there is evidence for the presence of the slow $K^+$ channel ($K_{slow}$) in rat central axons (Baker et al., 1987). Baker et al. (1987) suggested that the $K_{slow}$ channel is localized at the node since tetraethylammonium chloride (TEA), an antagonist of the $K_{slow}$ channel affected a component of an electrotonic response. In rat sciatic nerve, voltage clamp experiments of myelinated and demyelinated axons also determined that the density of $K_{slow}$ channel is concentrated at the node and decreases to a small fraction at the internode (Roper and Schwarz, 1989).

In the paranodal and internodal region of myelinated axons, another distinct type of $K^+$ channel, the fast $K^+$ channel ($K_{fast}$), exists in greater abundance than the $K_{slow}$ channel. Roper and Schwarz (1989) showed that demyelination of the axon produced an outward $K^+$ current sensitive to the $K_{fast}$ channel antagonist, 4-aminopyridine (4-AP), indicating the presence of $K^+$ channels underneath the myelin. The distribution of the $K_{fast}$ was estimated to be maximal in the paranode, while diminishing to 1/6 of the paranodal density at the node and internode (Roper and Schwarz, 1989).

Other channels present in mammalian axons include the inward rectifier channel ($K_{IR}$) (Eng et al., 1990); the persistent, TTX sensitive $Na^+$ channel (Stys et al., 1993); the ATP sensitive $K^+$ channel ($K_{ATP}$) (Safronov et al., 1993); the $K_{Ca}$ channel (Safronov et al., 1993; Scholz et al., 1993); and a relatively TEA-insensitive $K^+$ channel, with novel gating kinetics (Brismar and Schwarz, 1985).

A $Na^+$ activated $K^+$ channel ($K_{Na}$) has been identified in *Xenopus* peripheral myelinated axons (Koh et al., 1994; Poulter et al., 1995).

A voltage dependent $Ca^{2+}$ channel has also been suggested to exist in the RON. This was based on the findings that a rise in the $[Ca^{2+}]_i$, detected by the $Ca^{2+}$ indicator, Fura-2, occurred concomitantly with the compound action potential (CAP) (Lev-Ram and Grinvald, 1987). A zero-$Ca^{2+}$ solution abolished the response. Further support that the channel is present in RON was suggested by a study that demonstrated a beneficial effect using voltage dependent $Ca^{2+}$ channel blockers during anoxia (Fern et al., 1995a), but the presence of these channels in RON axons still remains controversial.

*Axonal and Glial Ion Transporters*

In addition to the various channels present on the axolemma, the axonal membrane is resident to the $Na^+/Ca^{2+}$ exchanger. The exchanger has been suggested to be located at both the node, paranode and myelin sheath in RON (Steffensen and Stys, 1995). Another membrane transport protein, the $Na^+/K^+/2Cl^-$ co-transporter, has been characterized in squid axon (Russell and Boron, 1990), in RON axons (Stys et al., in press), and in rat (Tas et al., 1987) and mouse (Walz, 1995) astrocytes. The ATP dependent pumps, $Ca^{2+}$-ATPase and $Na^+.K^+$-ATPase, are distributed in the nodal area in rat spinal cord (Mata and Fink, 1989) and at the internode in RON (Mata et al., 1991), respectively.

The types and distribution of various ion channels and transporters on axons are important as they will collectively shape the fiber's response to physiological and pathological stimuli.

### 1.2.2 Determinants of $V_m$ in the Axon

This section has reported data focusing essentially on the RON since this preparation has been studied most extensively of all CNS axons. As such, the RON is used here as a representative model of CNS axons.

Under resting conditions, $V_m$ is determined by the following equation:

$$V_m = \frac{RT}{F} \ln \frac{r[K]_o + b[Na]_o}{r[K]_i + b[Na]_i}$$

where b is the $Na^+$:$K^+$ permeability ratio and r is the stoichiometry of $Na^+$,$K^+$-ATPase (typically 1.5) (Nicolls et al., 1992). This equation, a modification of the Goldman-Hodgkin-Katz equation, determines the potential at which there is no net current flow across the axonal membrane. $Cl^-$ has been omitted from the equation for simplicity because its influence on $V_m$ is insignificant since the axonal membrane permeability to $Cl^-$ is thought to be small (Connors and Ransom, 1984). It is apparent that $V_m$ depends on several parameters including the concentration of ions and the permeability of the membrane to these ions.

*$K^+$ Channels Open at Rest*

$V_m$, estimated to be ≈ -80 mV in RON axons (Stys, 1996; Stys et al., in press), is primarily determined by $K^+$ permeability, thus $V_m$ is near the $K^+$ equilibrium potential ($E_K$), -105 mV. In most cases, the channels responsible for maintaining $V_m$ have not been well characterized. One channel in peripheral axons expected to contribute to $V_m$ is the nodal $K_{slow}$ channel, since the activation curve determined for this channel revealed that 35% of the channel population is open at the resting membrane potential (RMP) (Roper and Schwarz, 1989). Brismar and Schwarz (1985) reported that a $Cs^+$ sensitive, TEA insensitive voltage dependent nodal $K^+$ channel in rat peripheral axons also displayed

activity at rest. In *Xenopus* peripheral axons, a non voltage-gated $K^+$ channel was also TEA insensitive and $Cs^+$ sensitive (Koh et al., 1992).

*$Na^+$ Channels Open at Rest*

The deviation from $E_K$ indicates permeability to other ions, specifically $Na^+$. In the RON, a TTX sensitive $Na^+$ conductance was observed *at rest* and an estimate of the permeability ratio of $Na^+$:$K^+$ in RON was calculated at 1:35 (Stys et al., 1993). The source of this persistent $Na^+$ conductance, which was recorded even at depolarized potentials, is unknown, but a possibility includes the classic TTX-sensitive, rapidly inactivating, voltage dependent $Na^+$ channel responsible for the upstroke of the action potential. This channel could generate a persistent $Na^+$ current, referred to as a "window current", from the overlap of the steady-state activation and inactivation curves (French et al., 1990; Hille, 1992; Taylor, 1993). Other possibilities include a population of $Na^+$ channels that is capable of switching between different gating modes (Alzheimer et al., 1993) or that a distinct subpopulation of non-inactivating $Na^+$ channels exists (French et al., 1990) as was demonstrated in rat cortical and hippocampal neurons, respectively.

*$Na^+$,$K^+$,-ATPase*

At the RMP, neither $Na^+$ nor $K^+$ is at electrochemical equilibrium. (+61 mV and -105 mV, respectively, in RON axons (Stys et al., in press)), thus there is a constant flux of $Na^+$ and $K^+$ across the membrane as each ion attempts to reach steady state. The $Na^+$,$K^+$-ATPase handles this ionic leakage, thus maintaining $V_m$. However, activity of $Na^+$,$K^+$-ATPase is electrogenic since it transfers 1 net charge per ATP by transporting 3 $Na^+$ in exchange for 2 $K^+$ across the membrane. The contribution of this hyperpolarizing electrogenic factor to $V_m$ has been estimated to be 1-2 mV in squid giant axon (De Weer and Geduldig, 1973).

### 1.2.3 Function of the Axon During Signal Transmission

*Ion Channels Mediating Nerve Excitation*

The cell soma and axon coordinate their individual functions to achieve signal conduction. The cell soma processes excitatory and inhibitory synaptic stimuli it receives from other neurons to generate an action potential. The axon functions to propagate the signal generated by the cell soma (Koester, 1991). Membrane excitability begins with depolarization at the axon hillock by opening voltage sensitive $Na^+$ channels. This knowledge, originating from the classic studies by Hodgkin and Huxley (1952), determined that an inward $Na^+$ current is responsible for the upstroke of the action potential. The localization of voltage gated $Na^+$ channels at the axon hillock ensures that a sufficient amount of current will enter the cytoplasm to depolarize the next node of the axonal membrane. Propagation of the action potential along the fiber by each node occurs because 1) the $Na^+$ driving force maintained by the pump provides the abundant source of current required and 2) the insulating property of myelin at the internode prevents stray leakage of current across the internodal axolemma. Moreover, myelin also affects the velocity of an action potential. The velocity increases linearly with myelin thickness (Waxman, 1983) because it provides high resistance and lowers the capacitance of the internodal membrane. For these reasons, myelin reduces the energy required to propagate signals since less ions are needed to depolarize the membrane, and therefore fewer ions have to be transported by the pump (Ritchie, 1995).

The $K_{fast}$ channel located below the myelin assists in membrane repolarization in some myelinated fibers. The channel is voltage sensitive, activating at depolarized potentials with a $\tau \approx 0.5$ ms in peripheral axons (Baker et al., 1987). In RON, application of 4-AP prolonged the duration of the action

potential (Gordon et al., 1988). The channel also functions to prevent re-excitation that can occur by activating additional $Na^+$ channels located at the paranode which, in turn, may cause re-opening of nodal $Na^+$ channels (Ritchie, 1995). In this regard, 4-AP exposure evoked repetitive firing in RON following a single short stimulus (Gordon et al., 1988; Eng et al., 1990). In addition to the $K_{fast}$ channel, the rapid inactivation kinetics of voltage gated $Na^+$ channels terminate the depolarizing effect, thus helping to repolarize the membrane. Voltage clamp experiments of rat myelinated axons at the node showed that the $Na^+$ channel activation and inactivation time constants were less than 0.5 ms at 20 °C (Neumcke et al., 1987). Although repolarization is assisted by the $K_{fast}$ and $Na^+$ channels, it is evident that another mechanism is involved, attributed to a nodal leakage current through as yet unidentified channels (Hille, 1992).

The $K_{slow}$ channel does not participate in action potential repolarization in CNS myelinated axons (Gordon et al., 1988) since it possesses slow activation kinetics ($\tau \approx 15$ ms) (Baker et al., 1987), thereby requiring sustained membrane depolarization to open. A study using TEA reported that blockade of the channel induces bursts of firing, which, at times, occurred continually, in rat peripheral axons, determining that the channel regulates repetitive firing (Baker et al., 1987). Similar findings were also reported in RON with 4-AP. Baker et al. (1987) suggested that the axon responds to the type of stimulus where a single stimulus will open 4-AP sensitive channels and bursts of firing will activate TEA sensitive channels. The axon is also endowed with another safety device, the $K_{IR}$ channel. In RON, it is permeable to $Na^+$ and $K^+$ and voltage dependent, activating by prolonged (>80 ms) hyperpolarizing potentials (Eng et al., 1990). In a circumstance where a prolonged hyperpolarizing response occurs, such as excessive $Na^+$,$K^+$-ATPase activity after a high frequency train (Gordon et al., 1990), the channel clamps the membrane potential, preventing excessive pump-

induced hyperpolarization, maintaining $V_m$ close to rest, and thus preserving signaling (Eng et al., 1990).

*Axonal-Glial Interaction: Role of Glia During Signal Transmission*

$Na^+,K^+$-ATPase causes membrane hyperpolarization following nerve excitation as it re-establishes $Na^+$ and $K^+$ gradients. In addition to the axonal pump, the glia also remove $K^+$ from the ECS via the astrocytic $Na^+,K^+$-ATPase, $Na^+/K^+/2Cl^-$ co-transporter, and Donnan forces (Ransom and Sontheimer, 1992; Walz, 1995; Ransom and Orkand, 1996). Moreover, glia cause shrinkage of the ECS subsequent to neuronal activity. A study using RON showed that shrinkage of the ECS was correlated with a rise in $[K^+]_o$ following stimulation (Ransom et al., 1985). Glia were implicated as mediators of the fluid shift since a significant reduction of the ECS occurred due to glial swelling in adult optic nerve compared to the neonatal nerve (Ransom et al., 1985) which lacks a mature complement of glial cells (Foster et al., 1982), and therefore unable to induce shrinkage of the ECS. A glial anion transport system was suggested because a low $Cl^-$ solution and an inhibitor of the $Na^+/K^+/2Cl^-$ co-transporter, furosemide, reduced the activity-dependent shrinkage (Ransom et al., 1985).

Axonal-glial interaction was also demonstrated in RON by Kriegler and Chiu (1993). Using $Ca^{2+}$ sensitive dyes, their findings showed that electrical stimulation of the axon evoked a $[Ca^{2+}]_i$ response in glial cells (Krielger and Chiu, 1993). The source of $Ca^{2+}$ came from the ECS as well as from internal stores since the response remained without $Ca^{2+}$ in the perfusate (Krielger and Chiu, 1993). However, these results may not necessarily be generalized to adults since experiments were performed on neonatal optic nerves. Future studies on adult nerves will need to examine whether this $Ca^{2+}$ response still occurs in axons with mature properties.

### 1.2.4 $Ca^{2+}$ Dynamics in Myelinated Axons

$Ca^{2+}$ homeostasis is maintained by several mechanisms in the axon. $Ca^{2+}$ increases in the axoplasm by entering through $Na^+$ channels which have been shown to have a finite permeability to $Ca^{2+}$ in squid axons (DiPolo et al., 1982) and RON (Stys and LoPachin, Submitted). Similar to GM, the axon utilizes the following systems to regulate $[Ca^{2+}]_i$: $Ca^{2+}$-ATPase (DiPolo and Beaugé, 1988), $Na^+/Ca^{2+}$ exchanger (DiPolo and Beaugé, 1988), intracellular storage organelles, and cytosolic buffers (Kostyuk and Verkhratsky, 1994).

In comparative terms with the other homeostatic mechanisms, $Ca^{2+}$-ATPase plays a major role under normal physiological conditions. It is a high affinity protein ($\approx$ 200 nM) (DiPolo and Beaugé, 1988) that keeps the resting $[Ca^{2+}]_i$ low (free cytosolic $Ca^{2+}$ is in the range of 100 nM) by extruding $Ca^{2+}$ using ATP (Kostyuk and Verkhratsky, 1994). The $Na^+/Ca^{2+}$ exchanger also helps to regulate $[Ca^{2+}]_i$. The exchanger depends on an intact $Na^+$ gradient to export $Ca^{2+}$ from the intracellular space. It imports 3 $Na^+$ in exchange for 1 $Ca^{2+}$ by deriving energy from the transport of $Na^+$ across the membrane (Rasgado-Flores and Blaustein, 1987). By its stoichiometry, the exchanger is electrogenic and, therefore, it is modulated by membrane potential. Consequently, membrane depolarization as well as reduction of the axonal transmembrane $Na^+$ gradient will cause it to operate in reverse mode where $Na^+$ efflux is coupled to $Ca^{2+}$ influx. This membrane protein has a low affinity for $Ca^{2+}$ in comparison to $Ca^{2+}$-ATPase, transporting $Ca^{2+}$ when local $Ca^{2+}$ levels reach micromolar concentrations (DiPolo and Beaugé, 1988).

## 1.3 Anoxic/Ischemic Injury in CNS White Matter

### 1.3.1 Structural and Functional Damage Induced by Anoxia in Central Myelinated Axons

Electron microscope studies of RON subjected to anoxia revealed morphological damage including swollen mitochondria with loss of normal cristae; development of large empty vacuoles located within the myelin sheath adjacent to irregular shaped axons; and destruction of cytoskeleton proteins in large axons, particularly microtubules and neurofilaments (Waxman et al., 1992a). Astrocytes appeared dense with shrunken processes. Conversely, the myelin remained relatively unaffected by one hour of anoxia, showing retraction at only some paranodes. Similar results were found in another white matter tract, rat corpus callosum, that had been treated with $CN^-$ which induces chemical anoxia (Hirano et al., 1967).

In addition to structural damage, function of the axon is also severely compromised. The propagated CAP, recorded with suction electrodes in RON, was abolished within 6-8 min following induction of anoxia *in vitro*. Upon subsequent reoxygenation, the magnitude of the CAP showed only 30% recovery, indicating irreversible loss in the ability of the axon bundle to propagate a signal (Stys et al., 1990; Stys, 1996). Similar findings were reported in another WM preparation, rat dorsal column (Utzschneider et al., 1991; Lee et al., 1993). In the same WM tissue, anoxia also produced significant membrane depolarization (Utzschneider et al., 1991).

### 1.3.2 $Ca^{2+}$: Primary Factor Causing Axonal Damage During Anoxia

As in GM anoxic/ischemic injury, $Ca^{2+}$ plays a key role in causing structural and functional damage in WM during energy loss. Evidence for

deleterious effects of $Ca^{2+}$ overload in WM was obtained ultrastructurally, showing that excess $Ca^{2+}$ entry caused dissolution of neurofilaments in RON (Schlaepfer and Zimmerman, 1981; Waxman et al., 1993) and spinal cord (Schlaepfer and Zimmerman, 1981). In contrast, those tissues perfused with EGTA and zero $Ca^{2+}$ solutions were spared (Schlaepfer and Zimmerman, 1981; Waxman et al., 1993).

Using the CAP as a measure of functional integrity in RONs subjected to anoxia, Stys et al. (1990) reported that lowering the $[Ca^{2+}]_o$ in a graded manner increased axonal protection which was nearly complete in $Ca^{2+}$ free conditions. The results also showed that the accumulation of cytosolic $Ca^{2+}$ loading and its ensuing toxic effects occurred in a time-dependent manner. CAP recovery *progressively* diminished as the time at which the zero $Ca^{2+}$ solution was introduced began later during the anoxic insult (Stys et al., 1990). Zero $Ca^{2+}$ conditions also prevented degradation of the cytoskeletal proteins as well as the appearance of empty regions between the axon and myelin, but morphological changes in the mitochondria were still observed (Waxman et al., 1993). Electron probe x-ray microanalysis later supported the $Ca^{2+}$ hypothesis by showing that a gradual rise in intraaxonal $Ca^{2+}$ content occurred in RON axoplasm exposed to anoxia for 60 min (LoPachin and Stys, 1995).

Thus, it was evident that, similar to GM, $Ca^{2+}$ exerted damaging effects in WM. However, without glutamate activated receptors present in the axon, the mode of $Ca^{2+}$ entry into the axoplasm required further investigation. $Ca^{2+}$ influx via $Na^+$ channels was considered to be a minor route since perfusing the RON with a zero $Na^+$ solution containing $Ca^{2+}$ during anoxia resulted in axonal protection (Stys et al., 1992c). Injury should have still occurred if $Ca^{2+}$ had been entering through the channel. Moreover, increasing $Na^+$ permeability with veratridine significantly exacerbated the toxicity of anoxia. $Na^+$ free conditions

also provided a similar beneficial result to rat spinal cord subjected to compression injury (Agrawal and Fehlings, 1996). In addition, in the presence of TTX, less injury was induced by anoxia in RON axons (Stys et al., 1992c) or compression injury in rat spinal cord (Agrawal and Fehlings, 1996; Douglas et al., 1996). The cytoskeleton also remained intact by blocking $Na^+$ influx with TTX during anoxia in the RON (Waxman et al., 1994).

*$Na^+/Ca^{2+}$ Exchanger: Major Determinant of $Ca^{2+}$ Influx During Anoxia*

The above findings strongly suggested that anoxia elicited its detrimental effects in WM by a concomitant requirement of $Na^+$ and $Ca^{2+}$ flux. A plausible common link was the $Na^+/Ca^{2+}$ exchanger. The altered $Na^+$ gradient which occurred from the increased level of $[Na^+]_i$ in RON during anoxia (LoPachin and Stys, 1995), would cause the exchanger to operate in reverse, importing $Ca^{2+}$. Preventing a rise in $[Na^+]_i$ by TTX or zero $Na^+$ was protective, therefore supporting the $Na^+/Ca^{2+}$ exchanger hypothesis. Moreover, antagonists of the exchanger, benzamil, dichlorobenzamil, and bepridil, significantly improved recovery of function in RONs challenged with anoxia (Stys et al., 1992c). Very recent studies have directly confirmed the role of reverse $Na^+/Ca^{2+}$ exchange as the main $Ca^{2+}$ import mechanism in anoxic CNS axons (Stys and LoPachin, Submitted).

*$Ca^{2+}$ Flux Via Voltage Gated $Ca^{2+}$ Channels*

In addition to the $Na^+/Ca^{2+}$ exchanger, $Ca^{2+}$ may permeate the axolemma into the cytoplasm via voltage gated $Ca^{2+}$ channels to cause injury. Early findings suggested that transmembrane $Ca^{2+}$ flux via these channels was not a factor in WM injury (Stys et al., 1990). The study determined that $Ca^{2+}$ channel antagonists which included nifedipine (5 μM, 10 μM) and nimodipine failed to

provide protection to the RON challenged with anoxia. In the same preparation and similar conditions, Fern et al. (1995a) confirmed the results of nifedipine. However, nifedipine at 2.5 μM as well as other $Ca^{2+}$ channel antagonists, verapamil and diltiazem, were modestly protective (Fern et al., 1995a). Moreover, applying L-type (diltiazem) and N-type (SNX-124) $Ca^{2+}$ channel antagonists together, further enhanced neuroprotection compared to diltiazem alone.

*pH Regulation*

The primary pH regulating system of mammalian axons has not been clearly identified, but candidates include the $Na^+/H^+$ exchanger, $Na^+$-$HCO_3^-$ co-transporter, and $HCO_3^-$-$Cl^-$ exchanger (Khodorov et al., 1994; Stys et al., 1995b).

Inhibitors of the $Na^+/H^+$ exchanger, amiloride and harmaline, improved CAP recovery following mechanical trauma (compression) in rat spinal cord (Agrawal and Fehlings, 1996). This trauma induces several types of secondary injury including ischemia *in vivo*. The study suggested that through accumulation of axoplasmic $Na^+$, the $Na^+/H^+$ exchanger would induce intracellular acidosis by reverse operation of the exchanger. However, experiments were performed at 25 °C and some at 33 °C, but a protective effect of hypothermia has been demonstrated in WM at 33 °C (Stys et al., 1992b). In addition, although the findings indicate a possible role of $Na^+/H^+$ exchanger in the mechanism of WM injury, the potential effect of $Ca^{2+}$ was not considered. Further complicating the interpretation of these results is the fact that the blockers are not specific, and both have $Na^+$ channel blocking properties. Thus, it remains unknown if the neuroprotective effect is caused by blocking $Na^+$ influx directly.

### 1.3.3 Endogenous Neuroprotective Mechanisms in CNS WM

*Neurotransmitters: Beneficial Agents?*

Although disruption of $Ca^{2+}$ and $Na^{+}$ homeostasis cause axonal dysfunction, WM tissue may possess compensatory defense mechanisms. The role of the neurotransmitters, GABA and adenosine, were examined to determine possible endogenous protective properties of these compounds (Fern et al., 1994; Fern et al., 1995b). The observation that GABA and adenosine levels significantly increased extracellularly during ischemia in a WM tract (internal capsule of the cat) (Shimada et al., 1993) raised the possibility that they are involved in the anoxic response. In fact, the presence of adenosine or GABA prevented the usual extent of CAP loss in the RON preparation exposed to anoxic conditions. In addition, GABA actually reduced the concentration of adenosine required to elicit its beneficial effect, indicating that a synergistic mechanism may be operational (Fern et al., 1994). The neurotransmitters probably evoked their effect by activating a G-protein/protein kinase C pathway via GABA-B and adenosine receptors, since staurosporine, an inhibitor of the enzyme, abolished the improvement conferred by either compound (Fern et al., 1994; Fern et al., 1995b).

*Ion Channels Attempt to Maintain Membrane Polarization*

The axon possesses various channels including the $K_{ATP}$, $K_{Ca}$, and $K_{Na}$ channels which open in response to reduced concentrations of ATP or to elevated $Ca^{2+}$ or $Na^{+}$ levels, respectively. These events are similar to the ion gradient changes that occur during anoxia. For the $K_{ATP}$ channel, the ATP concentration required to induce half maximal inhibition of the channel is 35 μM in *Xenopus* peripheral axons (Jonas et al., 1991), a level reached during anoxia in

rat brain (Erecinska and Silver, 1994). Although various types of the $K_{Ca}$ channel have been identified based on different $Ca^{2+}$ sensitivities, the activating $[Ca^{2+}]_i$ is generally in the micromolar range for *Xenopus* (Jonas et al., 1991) and human (Scholz et al., 1993) peripheral axons. In addition to $Ca^{2+}$, the maxi or large conductance type of $K_{Ca}$ channel also requires membrane depolarization to open (Blatz and Magleby, 1987; Jonas et al., 1991; Scholz et al., 1993). Measurements of the $[Ca^{2+}]_i$ under pathophysiological conditions have been reported to reach the micromolar level in rat brain (Silver and Erecinska, 1990), sufficient to activate the $K_{Ca}$ channel. Finally, the $K_{Na}$ channel activates at $Na^+$ concentrations well above the level normally present in the cytosol ($K_{1/2} \approx 32.5$ mM (Koh et al., 1994)). It is evident that in the event of metabolic stress, the axon increases $K^+$ conductance to prevent or delay depolarization and, therefore, minimize damage by prolonging the inevitable depolarizing response and $Ca^{2+}$ influx.

### 1.3.4 Glia: Friend or Foe?

Interestingly, one hour of $O_2$ deprivation did not produce abnormal ultrastructure in RON myelin, which remained compact (Waxman et al., 1992a). The mechanism of this tolerance to anoxia has not been elucidated. Paradoxically, the process of myelination or the myelin itself may act to exacerbate injury by causing increased sensitivity to an anoxic insult. RON of myelin deficient rats were compared to normal RON to investigate this possibility. The findings showed that the CAP was never completely abolished even after 60 min of anoxia. Recovery of 71% upon reoxygenation was recorded in myelin deficient nerves treated with anoxia while only 33% recovery occurred for myelinated axons (Waxman et al., 1990). Ischemic exposure also failed to injure neonatal RONs (Fern and Ransom, 1996). Further evidence demonstrating that myelin induces harmful effects was observed in another CNS fiber tract, rat dorsal

column, when compared to peripheral axons which are myelinated with Schwann cells and devoid of astrocytes (Utzschneider et al., 1991). During anoxia, the typical reduction in CAP was observed in dorsal column while no change in the CAP was recorded in peripheral nerves.

Conversely, it is possible that the glycogen containing astrocytes potentiate axonal survival during an anoxic challenge (Ransom and Orkand, 1996). RON subjected to ischemia (anoxia and aglycemia) was less resistant to injury than those nerves exposed to zero glucose only (Fern and Ransom, 1996), suggesting that the axon may utilize energy generated from glycogen metabolism to prevent damage (Fern and Ransom, 1996). Support for a beneficial effect of astrocytic glycogen on neurons was demonstrated when survival was improved by elevating glycogen stores with insulin prior to exposing the culture to a zero glucose medium (Swanson and Choi, 1993).

### 1.3.5 $Na^+$ Conductance

The continued $Na^+$ influx induced by anoxia eventually caused the $Na^+/Ca^{2+}$ exchanger to operate in reverse in RON, mediating cytosolic $Ca^{2+}$ overload (Stys et al., 1992c; Waxman et al., 1992b). While TTX was effective at reducing anoxic damage in RON, the concentration required blocked nerve excitation. Therefore, for therapeutic reasons, minimizing the accumulation of $Na^+$ intracellularly with other $Na^+$ channel antagonists that could spare electrogenesis would be ideal. The tertiary (lidocaine, procaine) and quaternary (QX-314, QX-222) local anesthetics applied during anoxia provided significantly beneficial effects to RON. The quaternary compounds were particularly effective since they caused minimal reduction in the pre-anoxic CAP in contrast to lidocaine and procaine that reduce excitability (Stys et al., 1992a). These drugs are referred to as use-dependent $Na^+$ channel blockers, with quaternary drugs

exerting their effect by binding preferentially to open channels (Khodorov, 1991). Other compounds including certain antiarrhythmics (ajmaline, prajmaline, tocainide) (Stys, 1995) and anticonvulsants (phenytoin, carbamazepine, diazepam) (Fern et al., 1993) are $Na^+$ channel antagonists that are also neuroprotective in the anoxic RON.

## 1.4 Comparisons Between GM and WM Anoxic/Ischemic Injury

Glucose and $O_2$ deprivation for extended periods of time results in irreversible injury to the neuron. The toxic events begin with energy depletion and the subsequent failure of $Na^+$,$K^+$-ATPase (Fig. 1.1). Dissipation of the ion gradients leads to accumulation of $K^+$ in the ECS in both GM (Hansen, 1985) and WM (Ransom et al., 1992), causing the neuronal tissue to undergo membrane depolarization. Although $Ca^{2+}$ is ultimately the main pathogenic factor responsible for cell death, it is at this stage that the mechanisms causing damage to GM and WM diverge (Fig. 1.1).

In GM, neurotoxicity is caused in large part by synaptic mechanisms, particularly via activation of glutamate receptors by the excitatory amino acids (Choi, 1992) (see Section 1.1.3). A large number of studies has determined that there is not a primary causal agent producing GM injury, but a series of distinct mechanisms participating in the demise of the neuron. It is clear that without $Ca^{2+}$, a $Na^+$ dependent mechanism can still produce cell death or possibly initiate apoptosis (Gwag et al., 1995).

The mechanism of $Ca^{2+}$ mediated injury in WM is different from that in GM (Fig. 1.1). Ransom et al. (1990) reported that exposure of the RON to glutamate did not have a deleterious effect on axonal function which is not unexpected since synaptic connections are absent in WM. Instead, WM becomes damaged primarily by reverse mode of the $Na^+/Ca^{2+}$ exchanger which is caused

by accumulation of $Na^+$ intracellularly and membrane depolarization. The subsequent rise in $[Ca^{2+}]_i$ mediates irreversible injury in WM. Damage in WM likely occurs through overactivation of $Ca^{2+}$ activated systems, such as endonucleases, proteases, lipases, and others (Orrenius et al., 1989).

## 1.5 Research Objectives

An anoxic/ischemic insult in WM eventually leads to impaired function and loss of signal transmission which results from a rise in the axoplasmic $[Ca^{2+}]$. Energy depletion and the failure of axolemmal ion transport systems disrupts ion homeostasis. In particular, dissipation of the $K^+$ gradient results in $K^+$ mediated membrane depolarization. Membrane depolarization is an essential determinant mediating axonal injury because it stimulates the $Na^+/Ca^{2+}$ exchanger to operate in the $Ca^{2+}$ import mode, thus elevating toxic cytosolic $Ca^{2+}$ levels. Therefore, it is important to elucidate the mechanisms involved in causing the loss of $V_m$ during anoxia/ischemia.

The objective of this research project was to study the factors governing the changes in $V_m$ during physiological and pathophysiological conditions in mammalian central myelinated axons, with particular emphasis on determining the role of 1) $Na^+$,$K^+$-ATPase, 2) $Na^+$, 3) $Ca^{2+}$, 4) $Na^+$ and $K^+$ permeability, and 5) differences between chemical anoxia and glycolytic block. The grease gap recording technique was used to record the membrane potential during normoxic conditions and metabolic inhibition in RON.

Figure 1.1: Comparisons between WM and GM anoxic/ischemic injury. The pathways leading to neuronal and axonal damage begin in a similar manner. The loss of energy, ATP, and reduced activity of $Na^+$,$K^+$-ATPase, result in disruption of ion homeostasis and subsequent membrane depolarization. At this stage, the mechanisms leading to WM and GM injury diverge. GM damage is primarily mediated by activation of the NMDA receptors by the excitatory amino acid, glutamate, permitting excessive $Ca^{2+}$ influx. In contrast, elevated toxic levels of cytosolic $Ca^{2+}$ in WM is caused by reverse operation of the membrane transport system, the $Na^+/Ca^{2+}$ exchanger. Thereafter, the WM and GM mechanism of injury converge where various $Ca^{2+}$ activated enzymes, proteases, lipases, and endonucleases, are responsible for producing cell death.

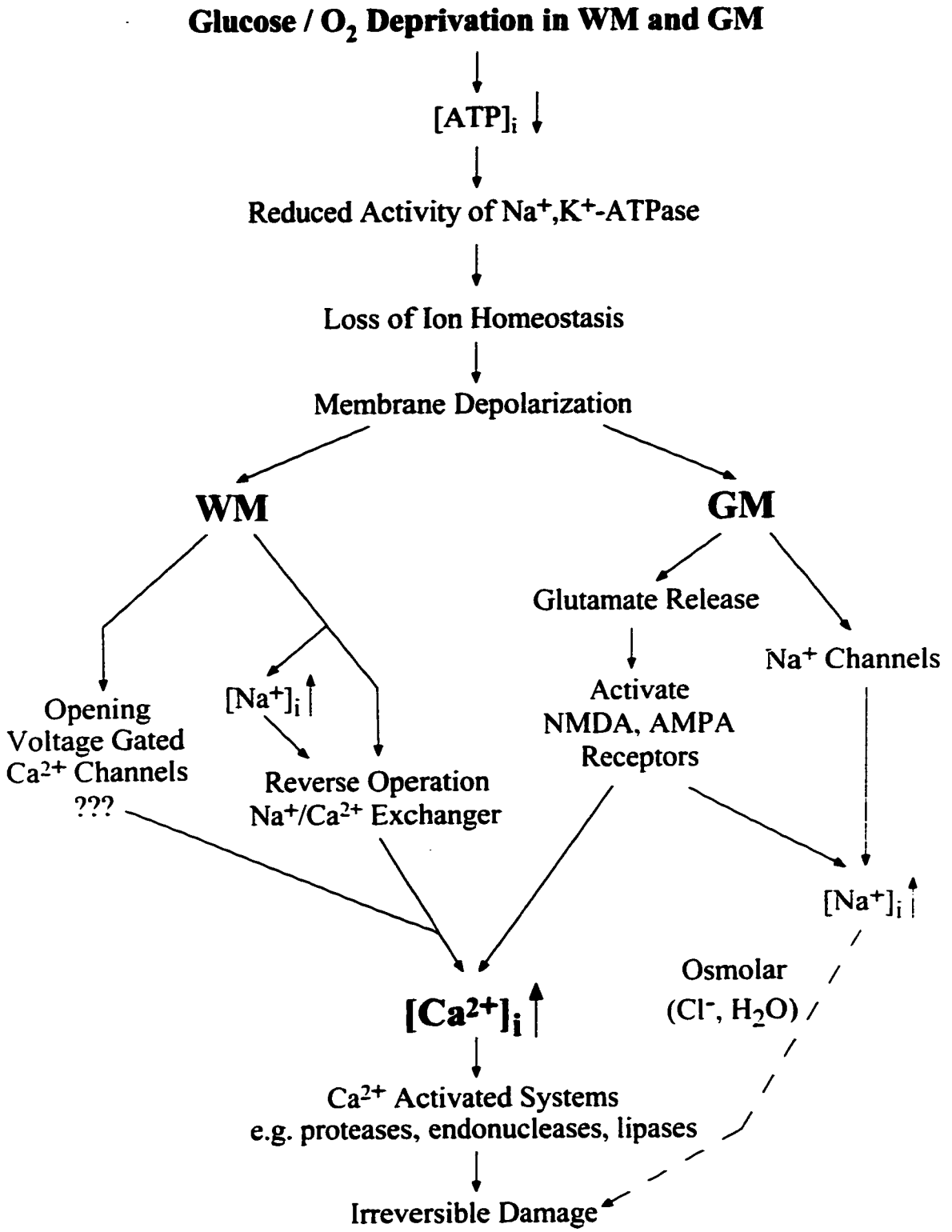
Glucose / $O_2$ Deprivation in WM and GM
$[ATP]_i$
Reduced Activity of $Na^+,K^+$-ATPase
Loss of Ion Homeostasis
Membrane Depolarization
WM
GM
Glutamate Release
$Na^+$ Channels
Activate NMDA, AMPA Receptors
Opening Voltage Gated $Ca^{2+}$ Channels ???
$[Na^+]_i$
Reverse Operation $Na^+/Ca^{2+}$ Exchanger
$[Na^+]_i$
Osmolar ($Cl^-$, $H_2O$)
$[Ca^{2+}]_i$
$Ca^{2+}$ Activated Systems e.g. proteases, endonucleases, lipases
Irreversible Damage

# CHAPTER 2

# MATERIALS AND METHODS

## 2.1 Preparation and Dissection

The RON is a representative model of central myelinated axons. It is a nerve bundle comprised of approximately 100,000 myelinated axons of 3 different sizes (De Juan et al., 1992), ranging from 0.3 μm to 2.2 μm with an average inner diameter of 0.77 μm (Foster et al., 1982). Long-Evans male rats (50-70 days old) were anesthetized with 80% $CO_2$ / 20% $O_2$, decapitated, and the optic nerves rapidly dissected out. At this age, the nerve had fully developed mature properties including complete myelination of the axons (Foster et al., 1982) and ion channel distribution at the node and internode (see section 1.2.1) (Waxman and Ritchie, 1993).

## 2.2 Grease Gap Recording Technique

The axonal compound RMP, $V_g$, was recorded *in vitro* with the grease gap technique (Fig. 2.1 A) (Stys et al., 1993). This technique provides a more stable recording in central mammalian axons at physiological temperatures than the conventional sucrose gap method (Stämpfli, 1954; Eng et al., 1990). The small diameter of optic nerve axons (mean < 1 μm (Foster et al., 1982)), and the long recording times required (up to 4 hrs), precluded the use of intracellular microelectrodes. The middle segment of one nerve was inserted into a silastic tube (≈ 2mm long, 0.64 mm in diameter) slit longitudinally, and filled with petroleum jelly for electrical isolation and to minimize intermixing of solutions from the two wells (Fig. 2.1 A). One end was perfused at 2 ml/min with oxygenated artificial cerebrospinal fluid (aCSF) or test solutions at 37 °C. The

opposite end was depolarized using an isotonic $K^+$ solution (NaCl replaced by KCl) containing 0.5 mM $CaCl_2$ (to reduce potential $Ca^{2+}$-mediated injury in strongly depolarized axon segments) flowing at 2 ml/min at room temperature. All solutions were gassed with 95% $O_2$ / 5% $CO_2$. To improve recording stability, the central nerve segment embedded in petroleum jelly was cooled by circulating a cold ($\approx$ 0° C) solution of 1:1 glycerol/water through tubing in contact with the silastic tube. $V_g$ was recorded with 3 M KCl/agar bridge electrodes. Junction potentials were determined at the beginning and end of each experiment by shorting the two wells with a strand of filter paper. These potentials, which were typically 1-3 mV, drifted linearly over time (data not shown). $V_g$ recorded during the course of an experiment was therefore corrected by subtracting estimated values of junction potentials obtained by linear interpolation between the readings obtained at the start and end of the experiment. The trans-gap resistance, $R_g$, was measured in some experiments by applying current steps (98 nA) across the two wells ($i_g$, Fig. 2.1 A), small enough to prevent activation of voltage-sensitive conductances. Following dissection, one nerve was recorded immediately ('nerve A'), while the second ('nerve B') was placed in an oxygenated chamber (95% $O_2$ / 5% $CO_2$) containing aCSF at room temperature for later study.

The experimental data was recorded by using customized software (Stys, 1994) on a Macintosh microcomputer. Errors were expressed as standard deviations and statistical differences were calculated using ANOVA with Dunnett's test.

## 2.3 Grease Gap Electrical Model

The potential recorded by the grease gap technique, $V_g$, is governed by the electrical circuit illustrated in a model axon in Fig. 2.1 B. If $V_m$ and $V_m'$ are unequal, a current $i_g$ will flow, and the recorded potential will be:

$$V_g = i_g R_e \qquad \text{(eq.1)}$$

The magnitude of the current will be:

$$i_g = (V_m - V_m') / (R_e + R_i) \qquad \text{(eq.2)}$$

As $V_m'$ approaches zero in isotonic KCl solution, and eliminating $i_g$ from equations 1 and 2, the expression reduces to (Stämpfli, 1954):

$$V_g = V_m R_e / (R_e + R_i) \qquad \text{(eq.3)}$$

where: $V_g$ is the recorded gap potential; $V_m$ is the absolute transmembrane potential; $R_i$ is the combined internal axoplasmic resistance and serial membrane resistance; $R_e$ is the external resistance, comprised of ECS, nerve sheath, residual solution and other parallel leakage pathways.

The term $R_e / (R_e + R_i)$, defined as the "short circuit factor" (Stämpfli, 1954; Jirounek and Straub, 1971), will tend to reduce $V_g$ to a constant fraction of the true transmembrane potential, $V_m$. When $R_e$ is assumed to be much greater than $R_i$ (as might occur in sucrose gap recordings of single fibers (Julian et al., 1962)). $V_g$ will approach $V_m$. In our preparation this assumption may not be valid. Independent estimates of $V_m$ in optic axons ($\approx$ -80 mV (Stys, 1996; Stys et al., in press)) differ from our typical grease gap potentials ($\approx$ -50 mV) by a factor of $\approx$

0.6, which represents an estimate of our short circuit factor (eq.3). Importantly, although absolute transmembrane potentials could not be recorded from optic axons using this technique, as long as the short circuit factor remains constant, $V_g$ will represent a reliable fraction of $V_m$ and will vary linearly with $V_m$. For this reason, $R_g$ measurements were a standard part of the experimental procedure. While $R_e$ or $R_i$ could not be recorded separately, $R_g$, which is the parallel combination of $R_e$ and $R_i$ ($R_g = R_e R_i / R_e + R_i$) provided an estimate of stability of the two resistances, and therefore of the short circuit factor. A stable $R_g$ reading is a reasonable indicator of true relative potential changes rather than artifactual drift. Our data showed that the potential recorded by the grease gap represented a reliable fraction of the true axonal compound RMP in a CNS myelinated axon bundle. Although the magnitude of $V_g$ was less than $V_m$ due to a short circuit factor less than unity, this disadvantage was offset by the long term stability of our recordings (refer to Chapter 3 and see Fig 3.1) essential for the questions to be addressed in this project.

The measured potential, $V_g$, originates from a voltage drop across $R_e$ produced by a current $i_g$ (Fig. 2.1 B). Current flow through each constituent fiber is inversely proportional to its axial resistance, and therefore directly proportional to the square of axon diameter. Because the RON is composed of a parallel bundle of fibres with different diameters ranging from 0.3 to 3 μm (Hildebrand and Waxman, 1984), it follows that the current contribution to the total current $i_g$, and therefore to recorded potential $V_g$, will be biased in favor of larger fibers.

## 2.4 Composition of Solutions

Composition of aCSF, solutions of 2-deoxyglucose (DG; Sigma, St. Louis, MO), KCN (Fisher Scientific, Ottawa, ON), TEA (Sigma, St. Louis, MO), zero-glucose, and zero-$Na^+$ solutions (cholineCl (BDH, Toronto, ON), LiCl (Sigma, St. Louis, MO), *N*-methyl-D-glucamine (NMDG; Sigma, St. Louis, MO)) are listed in Table 2.1. TTX (Sigma, St. Louis, MO) was diluted from stock solution in distilled water. Ouabain (Sigma, St. Louis, MO; RBI, Natick, MA), NaCN (BDH, Toronto, ON) and iodoacetate-$Na^+$ salt (IAA; Sigma, St. Louis, MO), pyruvate (Sigma, St. Louis, MO), EGTA (Sigma, St. Louis, MO), procaine (Sigma, St. Louis, MO), and QX-314 (a generous gift from Astra Pharma Inc., Westboro, MA) were dissolved in aCSF.

Figure 2.1: (**A**) Diagram of the grease gap recording chamber. A nerve is inserted into the slit silastic tube containing petroleum jelly, cooled for stability, with one end perfused with aCSF or test solutions and the other end is depolarized with isotonic $K^+$ solution. The potential, $V_g$, was recorded with 3 M KCl/agar bridge electrodes. Constant current steps ($i_g$) were applied across the wells to measure $R_g$. (**B**) Electrical model of the grease gap technique. $V_g$ is the recorded potential. $V_m$ and $V_m'$ are the absolute transmembrane potentials at each end of a model axon. $R_e$ is the external resistance, comprised of extracellular space, nerve sheath, residual solution and other parallel leakage pathways. $R_i$ is the combined internal axoplasmic resistance and membrane resistance. A current $i_g$ will flow when $V_m$ and $V_m'$ are unequal, and the resultant voltage drop ($V_g$) is recorded across $R_e$, representing a stable, constant fraction of the absolute transmembrane potential, $V_m$.

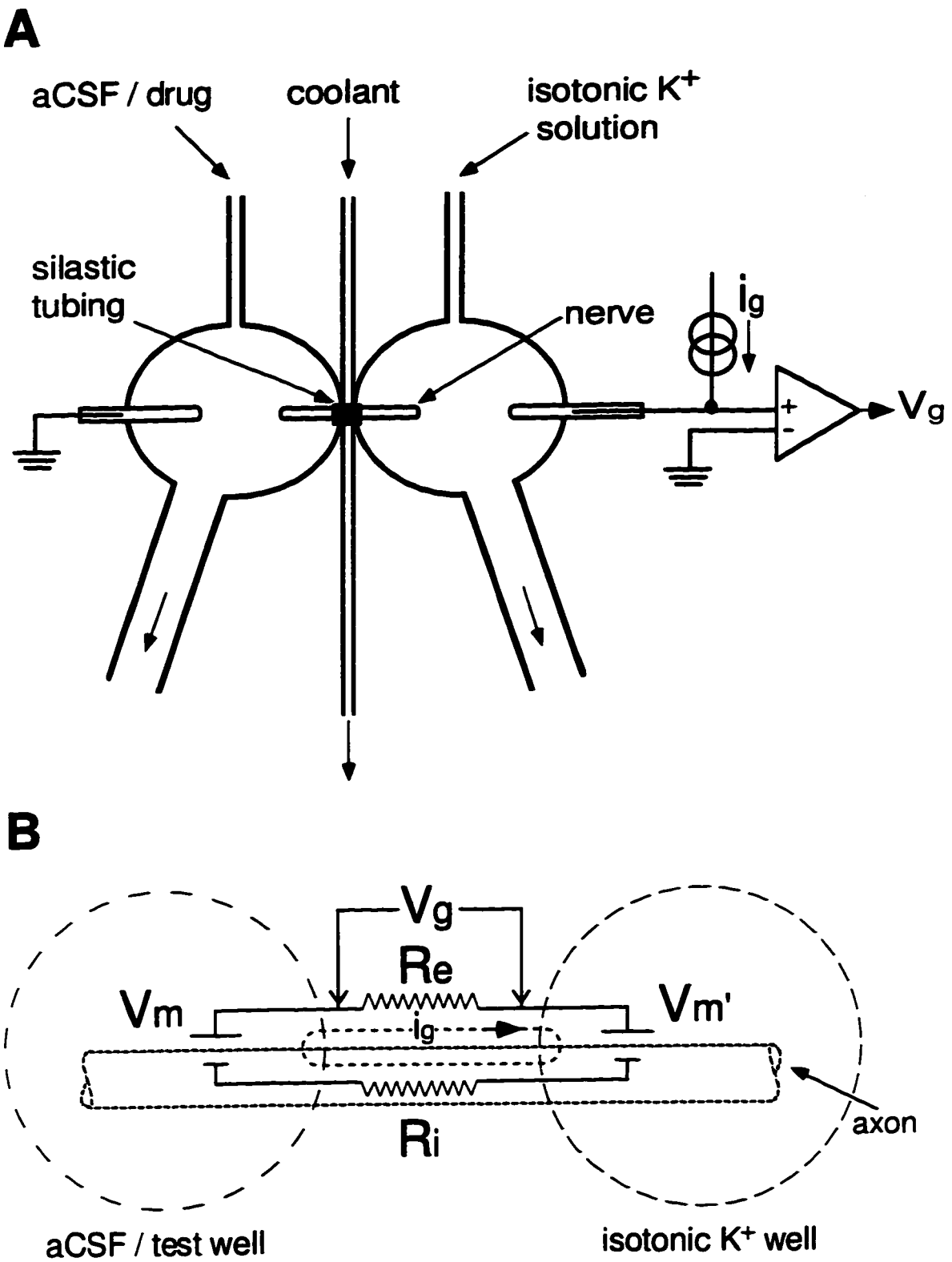
A
aCSF / drug
coolant
isotonic K+ solution
silastic tubing
nerve
ig
Vg
B
Vg
Re
Vm
Vm'
ig
Ri
axon
aCSF / test well
isotonic K+ well

Table 2.1: Composition of solutions (mM).

| | aCSF | Zero-$Na^+$/ Choline | Zero-$Na^+$/ $Li^+$ | Zero-$Na^+$/ NMDG | Zero Glucose | DG | KCN | TEA |
|---|---|---|---|---|---|---|---|---|
| NaCl | 126 | | | | 126 | 126 | 126 | 106 |
| KCl | 3 | 1.75 | 1.75 | 1.75 | 3 | 3 | 1 | 3 |
| $MgSO_4$ | 2 | 2 | 2 | 2 | 2 | 2 | 2 | 2 |
| $CaCl_2$ | 2 | 2 | 2 | 2 | 2 | 2 | 2 | 2 |
| $NaHCO_3$ | 26 | | | | 26 | 26 | 26 | 26 |
| Choline Bicarbonate | | 26 | 26 | 26 | | | | |
| $NaH_2PO_4$ | 1.25 | | | | 1.25 | 1.25 | 1.25 | 1.25 |
| $KH_2PO_4$ | | 1.25 | 1.25 | 1.25 | | | | |
| Dextrose | 10 | 10 | 10 | 10 | | | 10 | 10 |
| CholineCl | | 127 | | | | | | |
| LiCl | | | 127 | | | | | |
| NMDG | | | | 127 | | | | |
| Sucrose | | | | | 10 | | | |
| DG | | | | | | 10 | | |
| KCN | | | | | | | 2 | |
| TEA-Cl | | | | | | | | 20 |

# CHAPTER 3

# ION TRANSPORT AND MEMBRANE POTENTIAL IN CNS MYELINATED AXONS I: NORMOXIC CONDITIONS

## 3.1 Introduction

Axons play the critical role of conducting electrical signals within the nervous system with high fidelity and efficiency. In order to sustain electrogenesis, transmembrane $K^+$ and $Na^+$ gradients maintain axons in a polarized state, and provide energy for signaling, respectively. These electrochemical gradients are established by energy-dependent ion transport systems, the most important of which is $Na^+$,$K^+$-ATPase (Rossier et al., 1987; Horisberger et al., 1991; Sweadner, 1995). Because membrane conductances responsible for initiation and termination of the action potential are voltage dependent, resting properties of an axon such as membrane potential, ionic permeabilities and the various transporters that move ions against their gradients will influence its electrical behavior. Moreover, these same properties may affect the response of an axon to pathophysiological conditions, such as anoxia/ischemia, and may in turn modulate the degree of injury sustained by the fiber. For these reasons, it is important to define these properties as they will fundamentally influence the response of the axon to physiological and pathophysiological stimuli. We investigated the ionic determinants underlying the RMP in central myelinated axons of the RON, and explored some of the membrane transport systems involved. Preliminary results have been presented in abstract form (Leppanen and Stys, 1996).

## 3.2 Results

### 3.2.1 Resting Membrane Potential Recorded During Control Conditions

$V_g$ recorded from an optic nerve by the grease gap technique during control conditions is illustrated in Fig. 3.1. Following nerve insertion, $V_g$ usually stabilized within 90 min with potentials ranging from -40 to -55 mV (mean -47 ± 3 mV). No differences were noted between nerves A and B [see Methods] (-47.3 ± 3.5 vs. -46.6 ± 4.2 mV, $p = 0.18$). $R_g$ was typically about 60 kΩ. Both $V_g$ and $R_g$ remained relatively constant for several hours under control conditions (Fig. 3.1, Table 3.1). Probable variation in the short circuit factor (Stämpfli, 1954) from nerve to nerve resulted in different absolute values of $V_g$. For this reason, we routinely compared *ratios* of potentials over time, normalized to the baseline reading obtained at time zero (defined as 90 min after nerve insertion and stabilization). Using -80 mV as an estimate of true optic axon membrane potential (Stys, 1996; Stys et al., in press), these ratios were used to estimate $V_m$ over time in this (Table 3.1) and subsequent experiments. Normalizing the recorded potential, $V_g$, to -80 mV provided a measure of the effect of experimental conditions in relation to the true axonal membrane potential.

### 3.2.2 Effect of Inhibiting $Na^+,K^+$-ATPase on $V_m$

$Na^+,K^+$-ATPase plays a key role in maintaining transmembrane $Na^+$ and $K^+$ gradients. Ouabain (1 mM), an antagonist of the pump, caused a rapid depolarization which ended in a stable plateau at 39 ± 3% of control potential after 60 min or more of exposure (Fig. 3.2 A, Table 3.2). The initial rapid depolarization proceeded at a rate of 10 ± 3 mV/min. Higher ouabain concentrations (2 and 10 mM) did not produce statistically greater depolarization (Table 3.2). Lower concentrations of ouabain (10 and 100 μM) produced

proportionally less depolarization (Fig. 3.2 A, Table 3.2). The substantial membrane potential remaining after presumably complete pump inhibition with 1 - 10 mM ouabain was surprising. It was hypothesized that additional energy-dependent mechanisms, independent of $Na^+,K^+$-ATPase, may be in part responsible for maintenance of $V_m$. Nerves were depolarized by a 60 min exposure to ouabain (1 mM) as above. Mitochondrial and glycolytic ATP production were then blocked by adding $CN^-$ (2 mM) and IAA (1 mM), respectively, to the ouabain-containing perfusate. This treatment resulted in a further depolarization to 22 ± 4% of control (Fig. 3.2 B, Table 3.2) exceeding that seen with ouabain alone ($p<0.0001$). Similar results were obtained with 10 mM ouabain (Table 3.2).

### 3.2.3 Study of $Na^+$ Permeability in Central Myelinated Axons

The influence of membrane $Na^+$ permeability on $V_g$ was studied by substitution of bath $Na^+$ with other monovalent cations or pharmacological block of $Na^+$ channels. Replacing $Na^+$ with the impermeant cation choline elicited a transient hyperpolarizing response. The maximal hyperpolarization reached 109 ± 3% of control (Fig. 3.3 A, arrow, Table 3.3) for nerve A (the nerve recorded immediately after dissection), and was greater for nerve B (113 ± 3%, $p<0.002$). The hyperpolarization was followed by a slow depolarization to a stable potential (96 ± 8% of control, Table 3.3) within 60 min, with no difference between nerves A and B. The junction potential remained unaffected by the choline solution, indicating that this solution did not produce an artifactual change in $V_g$. NMDG-substituted zero-$Na^+$ solution produced similar results (Table 3.3). To test whether $Na^+,K^+$-ATPase was still operating after perfusion with zero-$Na^+$ solution, ouabain was added after 60 min, resulting in a prompt albeit limited

depolarization (Fig. 3.3 B) to 79 ± 5% of control potential in aCSF alone (Table 3.3).

Substituting bath $Na^+$ with $Li^+$, a cation permeable at the $Na^+$ channel (Richelson, 1977; Hille, 1992), resulted in a different voltage trajectory. In contrast to results with impermeant cations, zero-$Na^+$/$Li^+$ solution caused only a small, brief hyperpolarization (Fig. 3.3 C, arrow) which persisted in zero external $Ca^{2+}$ bath. This was followed by a steep, rapid depolarization (rate: 7 ± 2 mV/min) to a plateau of 65 ± 5% of control after 60 min (Table 3.3), significantly less depolarized than with 1 mM ouabain (39 ± 3%, $p<0.0001$, Table 3.2). In several nerves, a small hyperpolarizing 'sag' was also noted (Fig. 3.3 C, double arrow). To examine whether the $Na^+$,$K^+$-ATPase was operating during $Li^+$-substituted conditions, ouabain (1 mM) was added after 60 min of zero-$Na^+$/$Li^+$ exposure, resulting in a substantial additional depolarization to 32 ± 3% of control (Fig. 3.3 D, Table 3.3).

The $Na^+$ substitution data provided evidence that ouabain-induced depolarization was dependent to a large extent on extracellular $Na^+$ or $Li^+$. The role of voltage-gated $Na^+$ channels in isolation was studied by applying TTX (1 μM), which evoked a small hyperpolarizing response (Fig. 3.4 A) to 104 ± 1% of control membrane potential after 20 min (Table 3.3). The TTX-induced hyperpolarization was significantly smaller than that produced by zero-$Na^+$/choline perfusion ($p<0.001$), suggesting the presence of $Na^+$ influx pathway(s) other than TTX-sensitive $Na^+$ channels. Blocking TTX-sensitive $Na^+$ conductance during zero-$Na^+$/$Li^+$ perfusion resulted in depolarization to 75 ± 10% of control, which proceeded at a significantly slower rate of 1 ± 1 mV/min compared to $Li^+$ alone ($p<0.0001$) (Fig. 3.4 B, Table 3.3). TTX blunted, but did not abolish, the depolarizing response, providing additional support for a TTX-insensitive route(s) of $Na^+$ and $Li^+$ entry. The hypothesis was supported by

applying ouabain to nerves pretreated for 20 min with TTX (Fig. 3.4 C). This still resulted in a marked depolarization to 58 ± 5% of control, less than with ouabain alone (39 ± 3% after 60 min, $p<0.001$, Table 3.2) and, also occurring at a considerably slower rate (2 ± 0.1 vs. 10 ± 3 mV/min, $p<0.005$).

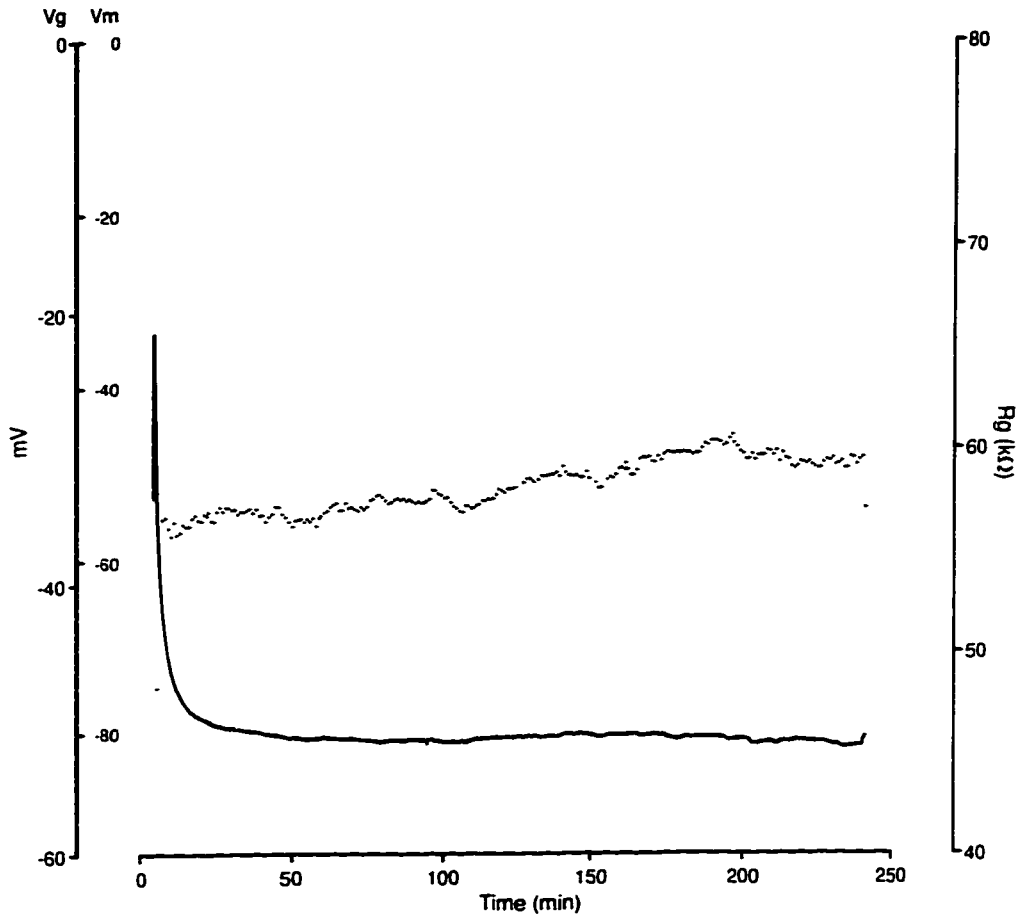


Figure 3.1: Recorded ($V_g$) and calculated absolute ($V_m$) compound resting membrane potential in rat optic nerve measured by the grease gap technique during control conditions. Representative trace of membrane potential under control conditions. $V_g$ typically stabilized within 90 min following insertion, ranging from -40 to -55 mV, and remained constant for 2-3 hrs. These and subsequent tracings were normalized to the estimated absolute resting membrane potential ($V_m$, -80 mV; see text). $R_g$ (dotted line) typically fluctuated to a minimal degree without concomitant change in $V_m$ (see 4.3.2 for explanation).

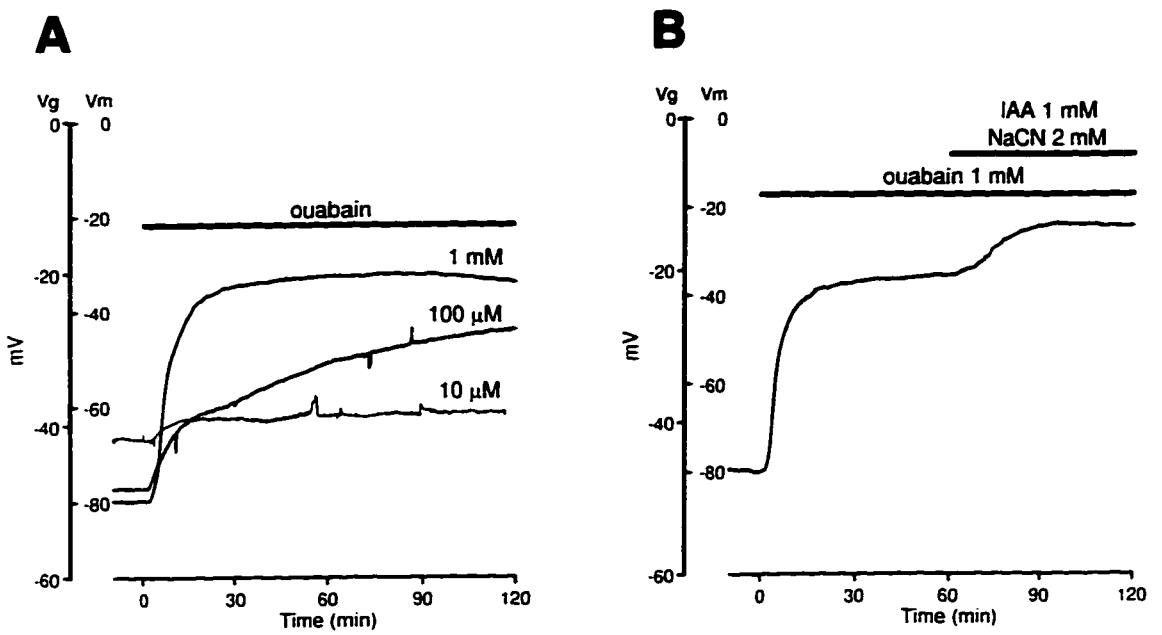


Figure 3.2: $V_g$ recorded during $Na^+,K^+$-ATPase inhibition with ouabain. (**A**) Ouabain (10 µM - 1 mM) evoked nerve depolarization in a dose-dependent manner, indicating a significant (although not exclusive, see B) dependence of RON axonal resting potential on continued pump operation. (**B**) Metabolic inhibition with NaCN (2 mM) and IAA (1 mM) caused further depolarization following ouabain application (1 mM), suggesting additional ATP-dependent ion transport mechanisms (see text).

Figure 3.3: Effect of $Na^+$ substitution experiments on resting membrane potential. (**A**) Replacement of $Na^+$ with the impermeant cation, choline, caused a hyperpolarizing response (arrow), followed by modest depolarization to a constant potential, which typically stabilized within 60 min. (**B**) Ouabain added to the zero-$Na^+$/choline perfusate evoked a small, but limited depolarization indicating continued pump operation under zero-$Na^+$ conditions. (**C**) Application of the permeant cation, $Li^+$, in the absence of $Na^+$, elicited a small, brief hyperpolarization (arrow). The nerve then depolarized rapidly, followed by a hyperpolarizing sag (double arrow). (**D**) Zero-$Na^+$/$Li^+$ application for 60 min produced a similar response described in trace C. Addition of ouabain to zero-$Na^+$/$Li^+$ conditions elicited a substantial additional depolarization indicating continued pump operation under these $Na^+$-substituted conditions.

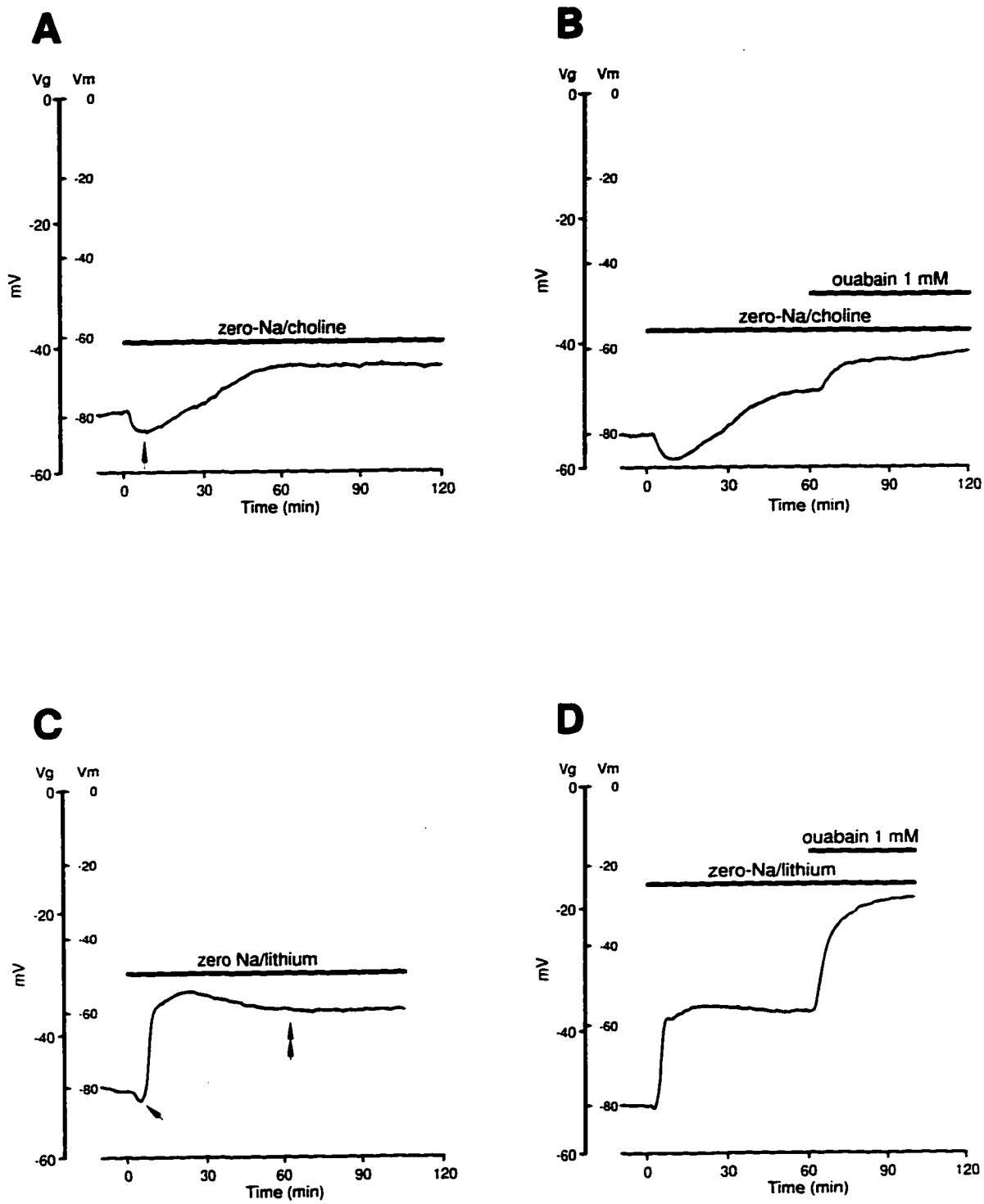
A
Vg
Vm
0
-20
-40
-60
-80
mV
zero-Na/choline
0
30
60
90
120
Time (min)
B
ouabain 1 mM
zero-Na/choline
C
zero Na/lithium
D
ouabain 1 mM
zero-Na/lithium

Figure 3.4: Effects of the $Na^+$ channel blocker TTX. **(A)** TTX alone had a hyperpolarizing effect on $V_m$, reaching a stable potential within 20 min, indicating a finite, TTX-sensitive $Na^+$ conductance in resting RON axons. **(B)** Applying zero-$Na^+$/$Li^+$ perfusate caused a depolarization that was more gradual and limited compared to the same exposure without TTX (Fig. 3.3 C). **(C)** TTX also reduced the rate of nerve depolarization during ouabain treatment. Together these results suggest additional, TTX-insensitive $Na^+$ influx pathways in resting RON axons.

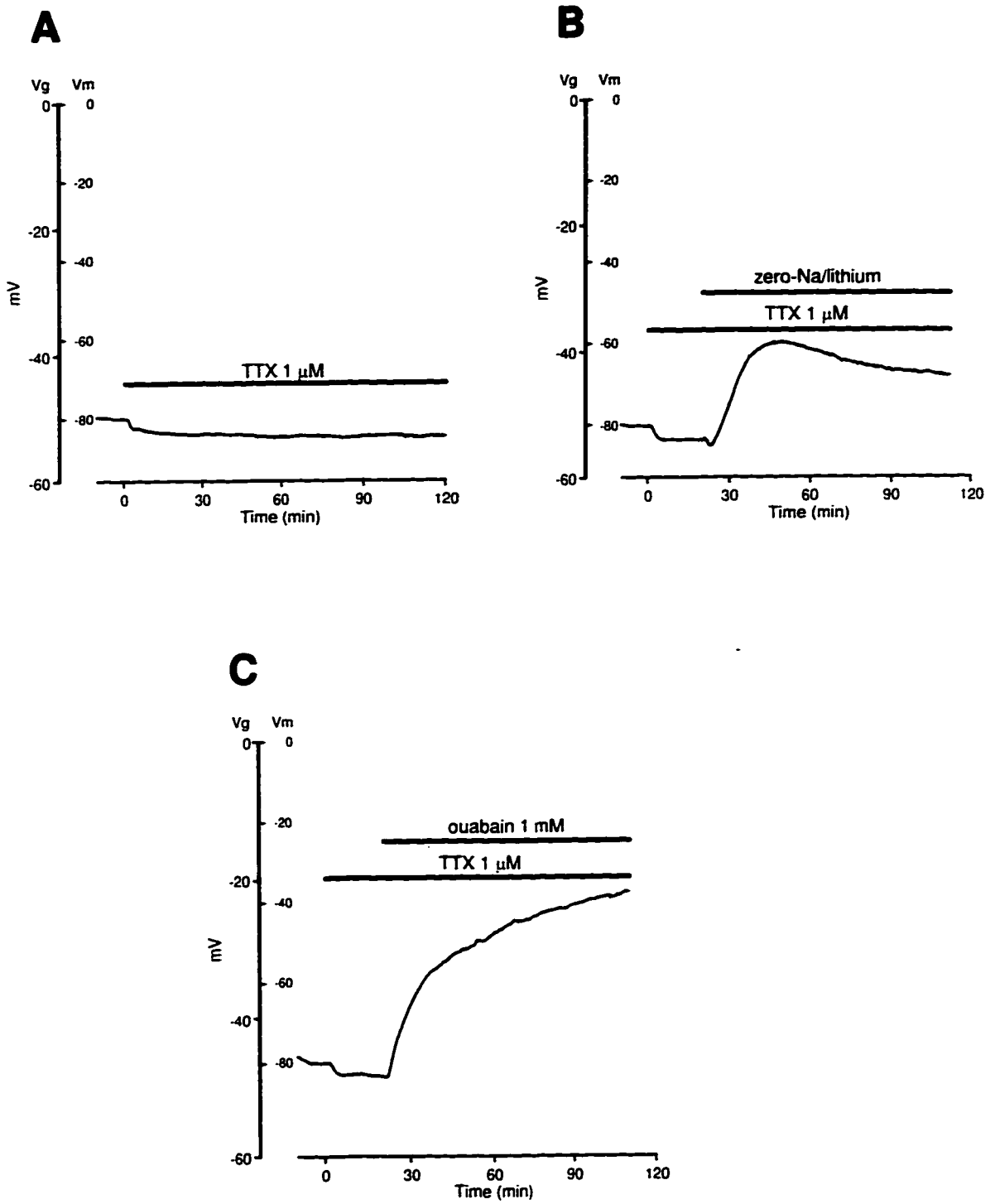
A
Vg
Vm
0
0
-20
-20
-40
-60
-40
-80
-60
mV
TTX 1 µM
0
30
60
90
120
Time (min)
B
Vg
Vm
0
0
-20
-20
-40
-40
-60
-80
-60
mV
zero-Na/lithium
TTX 1 µM
0
30
60
90
120
Time (min)
C
Vg
Vm
0
0
-20
-20
-40
-60
-40
-80
-60
mV
ouabain 1 mM
TTX 1 µM
0
30
60
90
120
Time (min)

Table 3.1: Resting membrane potential recorded during control conditions in aCSF by the grease gap technique.

| Time (min) | Ratio (%) ±S.D. | $V_g$ (mV) ±S.D. | $V_m$ (mV) ±S.D. | n |
|---|---|---|---|---|
| 0* | 100 | -47 ±3 | -80 | 284 |
| 60 | 102 ±3 | -49 ±3 | -81 ±2 | 20 |
| 90 | 101 ±3 | -49 ±3 | -81 ±3 | 20 |
| 120 | 101 ±4 | -48 ±3 | -81 ±3 | 20 |
| 150 | 100 ±4 | -48 ±3 | -80 ±3 | 18 |

All times corrected for dead space.
Ratios, $V_g$ and $V_m$ are corrected for junction potentials.
Ratio was calculated by dividing the potential at 60, 90, 120, 150 min by the time 0 potential.
*Time zero was determined after 90 min of stabilization after insertion into recording chamber.

Table 3.2: Effect of $Na^+$,$K^+$-ATPase inhibition with ouabain on membrane potential.

| Condition | Time (min) | Ratio (%) ±S.D. | $V_g$ (mV) ±S.D. | $V_m$ (mV) ±S.D. | Rate of Initial Rapid Phase (mV/min) ±S.D. | n |
|---|---|---|---|---|---|---|
| Ouabain 10 µM | 60 | 93 ±2 | -41 ±5 | -74 ±2 | | 5 |
| Ouabain 100 µM | 60 | 67 ±5 | -32 ±3 | -53 ±4 | | 6 |
| Ouabain 1 mM | 60 | 39 ±3 | -18 ±2 | -31 ±2 | 10 ±3 | 10 |
| | 120 | 34 ±3 | -16 ±2 | -27 ±2 | | 6 |
| Ouabain 2 mM | 60 | 34 ±6 | -15 +3 | -27 ±5 | | 6 |
| Ouabain 10 mM | 60 | 34 ±1 | -16 ±1 | -27 ±1 | | 3 |
| Ouabain 1 mM, add NaCN 2 mM + IAA 1 mM* | 30 | 22 ±4 | -10 ±2 | -18 ±3 | | 4 |
| Ouabain 10 mM, add NaCN 2 mM + IAA 1 mM* | 30 | 23 ±3 | -10 ±1 | -18 ±3 | | 3 |
| TTX, add Ouabain 1 mM† | 60 | 58 ±5 | -28 ±3 | -46 ±4 | 2 ±0.1 | 2 |

All times are corrected for dead space.
*NaCN and IAA were applied together for 30 min following 60 min of ouabain.
†TTX applied 20 min prior to 60 min of ouabain.

Table 3.3: Effect of $Na^+$ substitution on $V_m$ during various conditions.

| Condition | Time (min) ±S.D. | Ratio (%) ±S.D. | $V_g$ (mV) ±S.D. | $V_m$ (mV) ±S.D. | Rate of Initial Rapid Phase (mV/min) ±S.D. | n |
|---|---|---|---|---|---|---|
| Zero-$Na^+$/choline | 60 | 96 ±8 | -46 ±4 | -77 ±7 | | 30 |
| Zero-$Na^+$/choline @ Trough* | A†: 5 ±2 | A: 109 ±3 | A: -52 ±3 | A: -87 ±2 | | 18 |
| | B†: 7 ±2 | B: 113 ±3 | B: -52 ±4 | B: -90 ±3 | | 16 |
| Zero-$Na^+$/choline, add Ouabain 1 mM‡ | 60 | 79 ±5 | -37 ±3 | -63 ±4 | | 8 |
| Zero-$Na^+$/NMDG, add Ouabain 1 mM‡ | 60 | 80 ±3 | -36 ±1 | -64 ±3 | | 3 |
| Zero-$Na^+$/$Li^+$ | 60 | 65 ±5 | -31 ±2 | -52 ±4 | 7 ±2 | 8 |
| Zero-$Na^+$/$Li^+$, add Ouabain 1 mM‡ | 40 | 32 ±3 | -15 ±1 | -25 ±2 | | 2 |
| TTX 1 µM, add zero-$Na^+$/$Li^+$§ | 60 | 75 ±10 | -34 ±5 | -60 ±8 | 1 ±1 | 4 |
| TTX 1 µM | 20 | 104 ±1 | -49 ±3 | -83 ±2 | | 23 |

All times corrected for dead space.
*Trough is maximal hyperpolarization induced by zero-$Na^+$/choline perfusion.
†A = nerve A; B = nerve B.
‡Ouabain application following 60 min of zero-$Na^+$/choline or zero-$Na^+$/NMDG or zero-$Na^+$/$Li^+$.
§TTX applied 20 min prior to 60 min of zero-$Na^+$/$Li^+$.

## 3.3 Discussion

### 3.3.1 Effect of $Na^+$,$K^+$-ATPase Inhibition in CNS Myelinated Axons

The importance of $Na^+$,$K^+$-ATPase in maintaining $V_m$ was illustrated by the effect of the inhibitor, ouabain. The loss of ion gradients resulted in rapid nerve depolarization in a dose-dependent manner, which was exacerbated by $CN^-$ and IAA suggesting a ouabain insensitive, ATP dependent transport mechanism for partial maintenance of $V_m$. Similar observations were made using rat hypoglossal neurons (Jiang and Haddad, 1991). Given that the $Na^+$,$K^+$-ATPase may also be located at the internodal axolemma (Mata et al., 1991), it is possible that some pump molecules were shielded from bath-applied ouabain by the myelin sheath, and continued to operate: these then failed when nerves were poisoned with $CN^-$ and IAA. Alternatively, activation of $P_{Na}$ and/or reduction of $P_K$ by metabolic inhibition, which would cause additional depolarization, cannot be excluded. A finite potential remained following combined ouabain and metabolic block, which may be partly due to a passive Donnan equilibrium (Junge, 1981), diffusion of $K^+$ from the isotonic $K^+$ well to the test well contributing to a higher $[K^+]_i$ in the latter compartment, and/or a poorly explained hyperpolarizing shift caused by low-conductance media such as sucrose, observed in sucrose gap recordings (Julian et al., 1962; Jirounek et al., 1981).

### 3.3.2 $Na^+$ Permeability in CNS White Matter

TTX reduced resting $Na^+$ permeability producing a hyperpolarizing response which was shown previously (Stys et al., 1993). Replacing $Na^+$ with an impermeant cation caused a greater hyperpolarization, indicating additional, TTX-insensitive resting $Na^+$ permeability in RON axons. The estimated absolute hyperpolarization of 7 mV in zero-$Na^+$/choline (-87 mV (Table 3.3) versus -80 mV

(Table 3.1)) was identical to that observed by Morita et al. (1993) in peripheral lizard axons recorded intra-axonally under the same conditions. Using $Na^+$-replacement data (from nerve A only), the resting $P_K$:$P_{Na}$ ratio was estimated at 20:1 using (Stys et al., 1993):

$$\frac{P_K}{P_{Na}} = \frac{E_K - E_{Na} R_V}{E_K R_V - E_K}$$

where:

$R_V = V_{zero\text{-}Na^+} / V_m$, i.e. the ratio of membrane potentials after and before $Na^+$ permeability blockade with zero-$Na^+$ solutions.

$E_K$ and $E_{Na}$ are ionic reversal potentials, calculated from measurements of axoplasmic concentrations (LoPachin and Stys, 1995; Stys et al., in press).

This ratio was lower than a previous estimate of 35 which reflected only TTX-sensitive permeability (Stys et al., 1993). Interestingly, the $P_K$:$P_{Na}$ ratio calculated using nerves B (subject to several additional hours of incubation in aCSF at room temperature) was significantly lower at 15:1 ($p<0.01$). In contrast, TTX-induced hyperpolarizations were not different between nerves A and B, indicating that the different $P_K$:$P_{Na}$ ratios were either due to a higher TTX-insensitive $Na^+$ permeability or a reduced $K^+$ permeability in nerves B. Because $P_{Na}$ is less than $P_K$ at rest, $Na^+$ permeability will be rate limiting for electroneutral $K^+$ and $Na^+$ exchange across the membrane during pump inhibition. Therefore, one would expect a more rapid depolarization during ouabain exposure or metabolic inhibition (see chapter 4) in nerves B if their lower $P_K$:$P_{Na}$ ratio was due to an absolute increase in $P_{Na}$. Instead we found that neither the rate nor the extent of depolarization were different during ouabain or $CN^-$ treatment between

the two sets of nerves ($p>0.2$), suggesting that the lower $P_K$:$P_{Na}$ ratio in nerves B was due to a reduction of $P_K$ rather than increase in $P_{Na}$. The reasons for the difference are not known, but may be related to transient exposure to lower temperature or washout of a soluble modulator (see below and chapter 4).

Curiously, despite the observed difference in $P_K$:$P_{Na}$ ratios between nerves A and B, resting membrane potentials were virtually identical. It is likely that hyperpolarizing influences increased with incubation time negating the depolarizing effect of a smaller $P_K$:$P_{Na}$ ratio; for example axonal $[K^+]_i$ has been shown to rise with *in vitro* incubation (LoPachin and Stys, 1995) or washout of an endogenous ouabain-like substance (Blaustein, 1993) might increase $Na^+$,$K^+$-ATPase activity. Using a $P_K$:$P_{Na}$ ratio of 20:1, the contribution of the pump to $V_m$ at rest was calculated to be -7 mV (Martin and Levinson, 1985).

All nerves depolarized to a variable extent after the zero-$Na^+$/choline-induced hyperpolarization, which we interpret as partial pump inhibition due to depletion of axoplasmic $Na^+$ (Stys et al., in press). A new steady state was reached with reduced pump activity and parallel reduction of membrane $Na^+$ conductance. The small depolarization that occurred following the addition of ouabain (Fig. 3.3 B) indicates that $Na^+$,$K^+$-ATPase was not totally inhibited by 60 min of zero-$Na^+$ perfusion, consistent with reports that extensive depletion of intracellular $Na^+$ is difficult to attain (Dunham and Senyk, 1977; Stys et al., in press). It is likely that a small proportion of extracellular $Na^+$ ions were continuously recycled back into the axon to supply the pump at this new steady state, rather than negotiating the sinuous ECS of the nerve to be removed by the perfusate.

In contrast to zero-$Na^+$/choline, the nerve depolarized markedly during zero-$Na^+$/$Li^+$ because $Li^+$ permeates the $Na^+$ channel, partially inhibiting $Na^+$,$K^+$-ATPase and allowing electroneutral $K^+$ efflux. $Li^+$ is not equally permeable to

$Na^+$ at the $Na^+$ channel ($P_{Na}$:$P_{Li}$ is 0.9 (Hille, 1992)), therefore, a decrease in $[Na^+]_o$ may have evoked the brief hyperpolarizing response typically seen (Fig. 3.3 C, arrow). The hyperpolarizing sag noted after depolarization may have resulted from a reduction of $[K^+]_o$, caused by a slow washout of the ion. The extent of depolarization with zero-$Na^+$/$Li^+$ was less than expected, given that $Li^+$ inhibits $Na^+$,$K^+$-ATPase (Halm and Dawson, 1983). The additional depolarization caused by ouabain after zero-$Na^+$/$Li^+$ application suggested the pump was maintaining $V_m$ by utilizing residual $Na^+$. Electron microprobe data showed that $[Na^+]_i$ remained at $\approx$ 6 mM after 60 min of zero-$Na^+$/$Li^+$ perfusion (Stys et al., in press) and, at this concentration, the pump is still able to operate at approximately 20% capacity (Shyjan et al., 1990). It is also possible that the pump substituted $Li^+$ for $Na^+$ (Thomas et al., 1975; Dunham and Senyk, 1977; Ritchie and Straub, 1980). The application of TTX during zero-$Na^+$/$Li^+$ did not prevent nerve depolarization which suggested the presence of a TTX-insensitive $Li^+$/$Na^+$ influx pathway in RON axons. $Na^+$ channel blockade with TTX during ouabain exposure supported this notion since this blocker did not eliminate ouabain-induced depolarization, the extent of which exceeded the maximal steady-state hyperpolarizing contribution of pump current ($\approx$ -10 mV for a coupling ratio of $3Na^+ : 2K^+$ (Thomas, 1972; Martin and Levinson, 1985)), indicating transmembrane ion flux rather than mere elimination by ouabain of pump contribution to $V_m$. However, for both zero-$Na^+$/$Li^+$ or ouabain exposure, TTX reduced the rate of depolarization, due to partial reduction of resting TTX-sensitive $Na^+$ permeability, with gradients dissipating more gradually because of the slowed exchange of $Na^+$ and $K^+$.

Taken together, $Na^+$ influx into RON axons is a key step mediating membrane depolarization during $Na^+$,$K^+$-ATPase inhibition. Although the primary $Na^+$ influx path is the TTX-sensitive $Na^+$ channel, our data support the

existence of additional, TTX-insensitive $Na^+$ influx pathways that may have important implications for axonal responses to physiological and pathological stimuli.

# CHAPTER 4

# ION TRANSPORT AND MEMBRANE POTENTIAL IN CNS MYELINATED AXONS II: EFFECTS OF METABOLIC INHIBITION

## 4.1 Introduction

Mammalian CNS axons are susceptible to anoxic injury, and sustain irreversible damage from an increase in $[Ca^{2+}]_i$ (Stys et al., 1990; Waxman et al., 1991; Ransom et al., 1994; LoPachin and Stys, 1995). $Ca^{2+}$ homeostasis becomes disrupted as a result of energy depletion and the subsequent loss of ion gradients. Under normal physiological conditions, the low $[Ca^{2+}]_i$ is maintained by two membrane proteins, the $Na^+/Ca^{2+}$ exchanger and $Ca^{2+}$-ATPase (Blaustein, 1988), as well as buffering by intracellular stores and $Ca^{2+}$ binding proteins (Kostyuk and Verkhratsky, 1994). The $Na^+/Ca^{2+}$ exchanger normally extrudes 1 $Ca^{2+}$ in exchange for 3 $Na^+$ by utilizing the free energy available through the $Na^+$ gradient (Steffensen and Stys, 1996). As described in section 1.2.4, factors influencing the rate and direction of exchanger operation include the transmembrane $Na^+$ gradient and membrane potential. The exchanger will mediate $Ca^{2+}$ influx when 1) the transmembrane $Na^+$ gradient is reduced and/or 2) the membrane depolarizes. The exchanger is sensitive to membrane potential because its ion transport is electrogenic, transferring one net charge per cycle (Rasgado-Flores and Blaustein, 1987). For these reasons, given that the exchanger is the main pathway for anoxic $Ca^{2+}$ overload in optic nerve axons (Stys et al., 1992c; Waxman et al., 1992b), the rate and extent of depolarization during metabolic stress will influence the degree of exchanger-mediated $Ca^{2+}$ entry, and thus ultimate cellular injury. Therefore, the ions and channels involved

in mediating membrane depolarization were examined during glycolytic inhibition and chemical anoxia in optic nerve. Preliminary results have been published in abstract form (Leppanen and Stys, 1996).

## 4.2 Results

### 4.2.1 Effect of Glycolytic Inhibition in CNS Myelinated Axons

Several methods of inducing glycolytic inhibition were examined in the RON. In Fig. 4.1 A, the effect of zero-glucose (sucrose substitution) on RMP is shown. A delay of 28 ± 6 min preceded the onset of a monotonic, gradual depolarization proceeding at 2 ± 1 mV/min (Table 4.3), to 55 ± 10% of control after 60 min (Table 4.1). In contrast to simple omission of glucose, substitution of glucose with deoxyglucose (DG) (a competitive antagonist of the glycolytic enzyme, hexokinase (Devlin, 1992)), induced an initial hyperpolarizing response in 5 of 7 nerves (Fig. 4.1 B). This hyperpolarization, termed phase 1, together with the delay prior to hyperpolarizing lasted for 38 ± 8 min after application of DG before nerves began to gradually depolarize (phase 2) at 3 ± 1 mV/min (Table 4.3). Again, in contrast to zero-glucose alone, the gradual depolarization was interrupted by a hyperpolarizing response in 4 of 7 nerves studied (phase 3), finally terminating in a slow depolarization (phase 4) to 75 ± 9% of control after 60 min of application (Table 4.1). Because energy production could still occur from residual glucose in the ECS or from glycogen stores in astrocytes (Cataldo and Broadwell, 1986), IAA (1 mM), a relatively specific irreversible inhibitor of glyceraldehyde 3-phosphate dehydrogenase (Sabri and Ochs, 1971), was used to directly inhibit glycolytic metabolism. As with DG, four phases were observed (Fig. 4.1 C): an initial distinct hyperpolarizing response (phase 1, in 14/24 nerves) was followed by a rapid depolarization (phase 2) at a rate of 7 ± 3 mV/min (Table

4.3). Phase 2 began 20 ± 3 min after IAA application (Table 4.3), which was significantly faster than in zero-glucose/sucrose, 28 ± 6 min ($p<0.001$), or in DG/zero-glucose, 38 ± 8 min ($p<0.01$). As with DG, a second hyperpolarizing response, phase 3, interrupted phase 2. Finally, a gradual depolarization following phase 3 (at a reduced rate in comparison to phase 2) reached 55 ± 6% of control potential after 60 min (Table 4.1). $R_g$ remained relatively constant throughout the application of IAA. Addition of pyruvate (10 mM) completely prevented the IAA-induced changes (Fig. 4.1 D, Table 4.1).

### 4.2.2 Chemical Anoxia in CNS White Matter

Differences were observed between glycolytic block and chemical anoxia induced with 2 mM $CN^-$, an inhibitor of mitochondrial cytochrome oxidase (Albaum et al., 1946; Kauppinen and Nicholls, 1986a; Tadic, 1992). $CN^-$ resulted in a rapid depolarization (phase 2) at 7 ± 4 mV/min (Table 4.3) with minimal delay after application; in contrast to IAA and DG, the transient initial hyperpolarization (phase 1) was never seen (Fig. 4.2 A). A small inflection (Fig. 4.2 A, arrow), which was far less pronounced than with IAA, followed the rapid depolarizing response, leading to an abrupt slowing of the rate of depolarization. Nerves depolarized to 34 ± 4% of control after 60 min (Table 4.1). $R_g$ measurements increased by approximately 20 kΩ, but the change *followed* the phase 2 response. To test the hypothesis that $Na^+,K^+$-ATPase was still partially active during $CN^-$ poisoning, ouabain (1 mM) was added to the perfusate after 90 min of $CN^-$. An additional depolarization confirmed that residual pump activity was present during chemical anoxia (Fig. 4.2 B, Table 4.1). In contrast, no change in voltage trajectory was observed by adding ouabain to IAA-poisoned nerves (Fig. 4.2 C, Table 2).

### 4.2.3 Role of $Ca^{2+}$ During Glycolytic Inhibition and Chemical Anoxia

The hyperpolarizing inflections observed with IAA and to a far lesser extent, $CN^-$, were unexpected and may reflect interesting underlying mechanisms of axonal response to energy failure. $Ca^{2+}$-activated $K^+$ conductances have been implicated in other tissues (Leblond and Krnjevic, 1989), therefore we investigated the role of $Ca^{2+}$ on potential trajectories during IAA and $CN^-$ treatment. In Fig. 4.3 A, simultaneous application of IAA and nominally zero $Ca^{2+}$ caused an accelerated *onset* of depolarization, beginning within 5 ± 2 min, compared with 20 ± 3 min in IAA alone (Table 4.3). The depolarizing response, at a rate of 4 ± 1 mV/min (Table 4.3), was interrupted by a less prominent phase 3 (Fig. 4.3 A, arrow). Resting potential depolarized to 65 ± 2% and 44 ± 2% of control at 30 and 60 min (Table 4.2), respectively, significantly more than with IAA alone at these times (79 ± 7% and 55 ± 6%, $p<0.01$ and $p<0.05$, respectively). Pretreating the nerves with nominally zero $Ca^{2+}$ for 60 min prior to IAA application caused phase 3 to become a brief response without a distinct hyperpolarization (Fig. 4.3 B, arrow, Table 4.2) after the addition of IAA. A 60 min application of zero-$Ca^{2+}$/EGTA (5 mM) elicited a small but rapid depolarization to 96 ± 1% of control (Fig. 4.3 C, Table 4.5). As with nominally zero $Ca^{2+}$ and IAA, the nerve depolarized quickly, beginning within 3 ± 1 min (Table 4.3), but distinct phases were not observed in the voltage trajectory. Exposure to zero-$Ca^{2+}$/EGTA plus IAA resulted in a slower rate of depolarization (2 ± 0.2 mV/min) compared to IAA alone (7 ± 3 mV/min, $p<0.05$, Table 4.3). Although zero-$Ca^{2+}$/EGTA slowed the rate of depolarization, because of a more rapid onset in $Ca^{2+}$-depleted conditions, nerves depolarized to a greater degree at 30 and 60 min, 61 ± 3% and 43 ± 4%, respectively, versus IAA alone, 79 ± 7% and 55 ± 6%, ($p<0.0001$ and $p<0.001$, respectively) (Table 4.2). Similarly, the *abrupt alteration* in the depolarization rate following phase 3 was progressively

reduced as the $Ca^{2+}$ removal became more severe (compare Figs. 4.1 C, 4.3 A-C), until the trajectory became monotonic under zero-$Ca^{2+}$/EGTA conditions.

TEA (20 mM), a non-specific $K^+$ channel antagonist (including the $K_{Ca}$ channel) (Hille, 1992), depolarized nerves modestly when applied alone (Fig. 4.3 D, Table 4.5). TEA exposure during IAA application reduced phase 1 and eliminated phase 3, with depolarization beginning within 17 ± 2 min (similar to IAA alone, 20 ± 3 min) (Table 4.3) to 61 ± 4% of control after 60 min (similar to IAA alone, 55 ± 6%) (Table 4.2). Although phase 3 was abolished, a distinct change in the rate of depolarization from phase 2 to phase 4 was still present.

During chemical anoxia and a nominally zero $Ca^{2+}$ perfusate which was applied 60 min prior to $CN^-$, nerves depolarized at a rate of 14 ± 3 mV/min (Table 4.3) to 30 ± 7% of control at 60 min (Table 4.2) with an inflection apparent (Fig. 4.4 A). Similar to the voltage trajectory observed with IAA and zero-$Ca^{2+}$/EGTA, addition of $CN^-$ after 60 min of zero-$Ca^{2+}$/EGTA treatment evoked a depolarization at a rate of 15 ± 4 mV/min, without an inflection, to 27 ± 4% at 60 min (Fig. 4.4 B, Table 4.2). For both nominally zero $Ca^{2+}$ and zero-$Ca^{2+}$/EGTA treatments, nerves depolarized at a significantly faster rate than with $CN^-$ alone (7 ± 4 mV/min, $p<0.05$).

### 4.2.4 Role of $Na^+$ During Glycolytic Inhibition and Chemical Anoxia

The role of transmembrane $Na^+$ flux during metabolic inhibition was studied using a specific $Na^+$ channel blocker and ion substitution experiments. In Fig. 4.5 A, TTX (1 μM) alone elicited a hyperpolarizing response and with IAA addition, the extent of depolarization (to 95 ± 6% of control after 60 min, Table 4.4), was greatly reduced in comparison to IAA alone. This gradual depolarization continued for at least two hours after IAA addition and did not attain a steady state level during the times examined. Notably, no

hyperpolarizing inflections were ever seen (i.e. phases 1 or 3) in IAA-poisoned nerves pre-treated with TTX. Further support for $Na^+$ mediated depolarization was provided by experiments where $Na^+$ was replaced with the impermeant cation choline. Zero-$Na^+$/choline alone caused a prompt hyperpolarization followed by depolarization to a stable plateau (Fig. 4.5 B; see also Fig. 3.3 A). Addition of IAA produced a small but prompt hyperpolarization (Fig. 4.5 B, arrow) with little depolarization during 60 min of application (Table 4.4).

For IAA and TTX, the trajectory of $V_g$ was similar for nerves A (studied immediately following dissection) and nerves B (maintained in oxygenated aCSF at room temperature for several additional hours), which was not the case for $CN^-$. For TTX-treated nerves A, addition of $CN^-$ resulted in a fast, albeit limited (compared to $CN^-$ without TTX, $p<0.0001$) depolarization to 76 ± 13% of control after 60 min of treatment (Table 4.4). In contrast, nerves B failed to depolarize after $CN^-$ was added to the TTX perfusate ($V_g$ = 99 ± 7% of control after 60 min of $CN^-$) which was significantly different than nerve A ($p<0.05$) (Fig. 4.5 C, Table 4.4). The nerve A and B difference was also observed for $CN^-$ and zero-$Na^+$/choline ($p<0.001$). Similar to the $CN^-$ and TTX nerves A, $CN^-$ exposure after 60 min of zero-$Na^+$/choline produced an immediate, but slow depolarization (Fig. 4.5 D) to 81 ± 5% of control after 60 min of $CN^-$ (Table 4.4). In contrast to nerves A, nerves B responded by hyperpolarizing (Fig. 4.5 D, arrow) in $CN^-$, then modestly depolarized to 98 ± 4% of control (Table 4.4). Results were similar regardless of whether $CN^-$ was applied as the $Na^+$ or $K^+$ salt, indicating that the small amounts of $Na^+$ from NaCN had little effect on the nominally zero-$Na^+$/choline responses (data not shown).

$V_g$ was studied during chemical anoxia with the use-dependent $Na^+$ channel blockers, procaine and QX-314. In Fig. 4.6 A, procaine (1 mM) applied for 60 min had a hyperpolarizing effect on $V_g$ to 106 ± 2% of control (Table 4.5).

Procaine greatly reduced the $CN^-$ -induced depolarization ($V_g$ = 84 ± 11% of control after 60 min, Table 4.5). QX-314 (300 μM, a concentration that does not block action potential generation (Stys et al., 1992a)), a quaternary analog of lidocaine, hyperpolarized $V_g$ to 105 ± 2%; this effect developed much more slowly than that of procaine (Fig. 4.6 B, Table 4.5). The nerve A and B difference observed during $CN^-$ / TTX and $CN^-$ / zero-$Na^+$/choline treatment also occurred for $CN^-$ and QX-314. Nerves A depolarized to 80 ± 9% of control whereas $V_g$ for nerves B remained unchanged at 101 ± 6% ($p<0.05$, Table 4.4).

Figure 4.1: Effect of glycolytic inhibition on recorded ($V_g$) and calculated absolute ($V_m$) compound resting membrane potential in RON. $V_m$ was normalized to -80 mV for this and all subsequent figures. (**A**) Zero glucose/sucrose application evoked a gradual depolarization after a delay of ≈ 30 min. DG substituted zero-glucose (**B**) or IAA (**C**) both elicited a characteristic response consisting of four distinct phases: an initial hyperpolarizing phase, P-1, which was followed by a more rapid depolarization (P-2). P-2 was interrupted by a second hyperpolarization (P-3) and the voltage trajectory then entered a final, more gradual depolarization at a lower rate (P-4). The final levels of depolarization were similar at the end of two hours for IAA and zero-glucose. The extent of depolarization was less for deoxyglucose than for IAA or zero-glucose. (**D**) Pyruvate (10 mM) completely prevented IAA-induced depolarization.

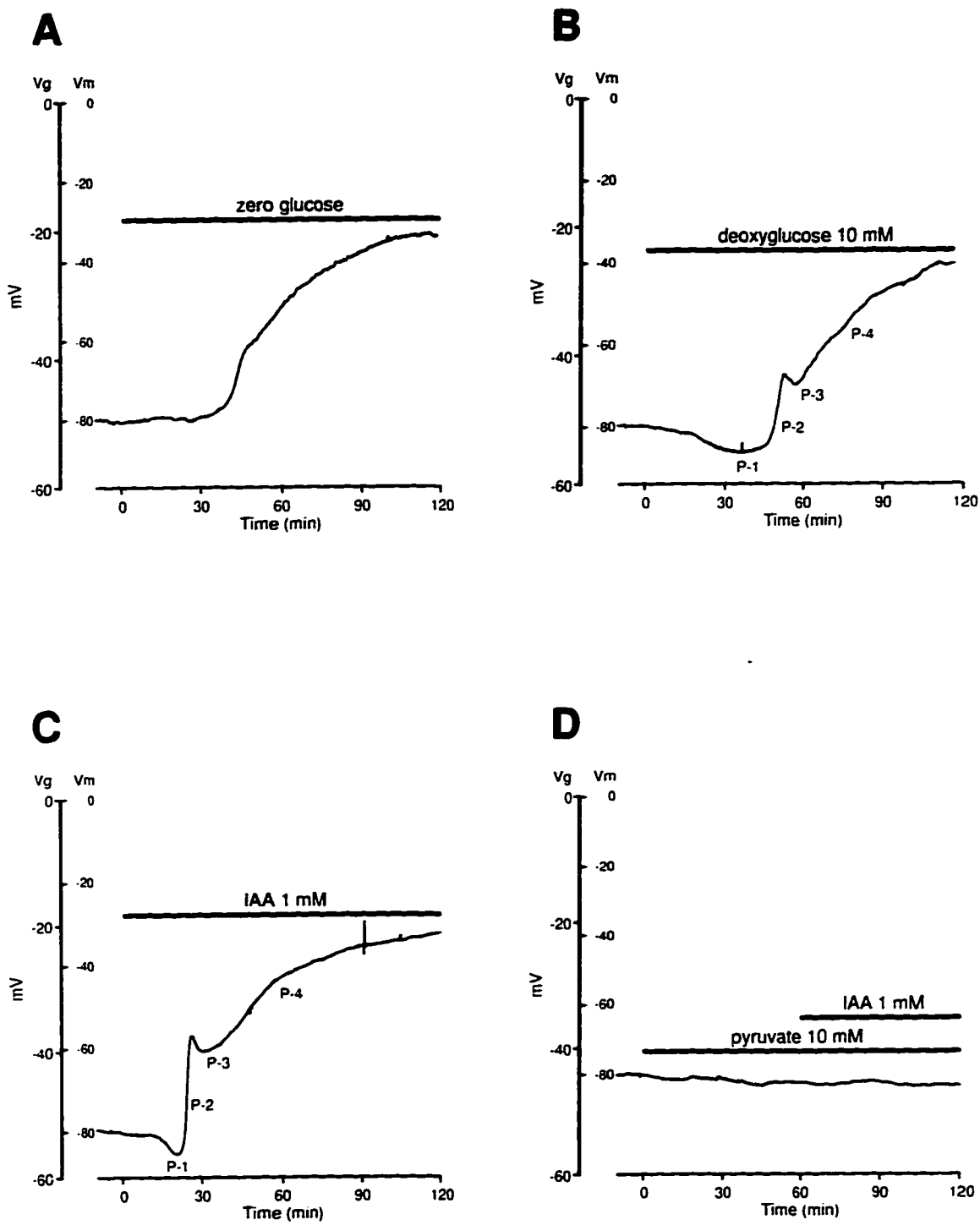
A
Vg
Vm
0
-20
-40
-60
-80
mV
zero glucose
0
30
60
90
120
Time (min)
B
deoxyglucose 10 mM
P-1
P-2
P-3
P-4
C
IAA 1 mM
D
IAA 1 mM
pyruvate 10 mM

Figure 4.2: Effect of chemical anoxia and ouabain on resting membrane potential in RON. (**A**) NaCN (2 mM) caused an immediate depolarizing response commonly interrupted by an inflection in the voltage trajectory (arrow), followed by a slower depolarization. The rise in $R_g$ (dotted line) occurred following the initial, rapid depolarization. (**B**) Addition of ouabain (1 mM) produced an additional, although minor depolarization, in chemically anoxic nerves. (**C**) Glycolytically-inhibited RON's were unaffected by ouabain. $R_g$ (dotted line) remained relatively stable (see Figure 3.1 for comparison to control conditions). The data suggest that glycolysis is able to fuel the $Na^+,K^+$-ATPase to a minor extent during chemical anoxia.

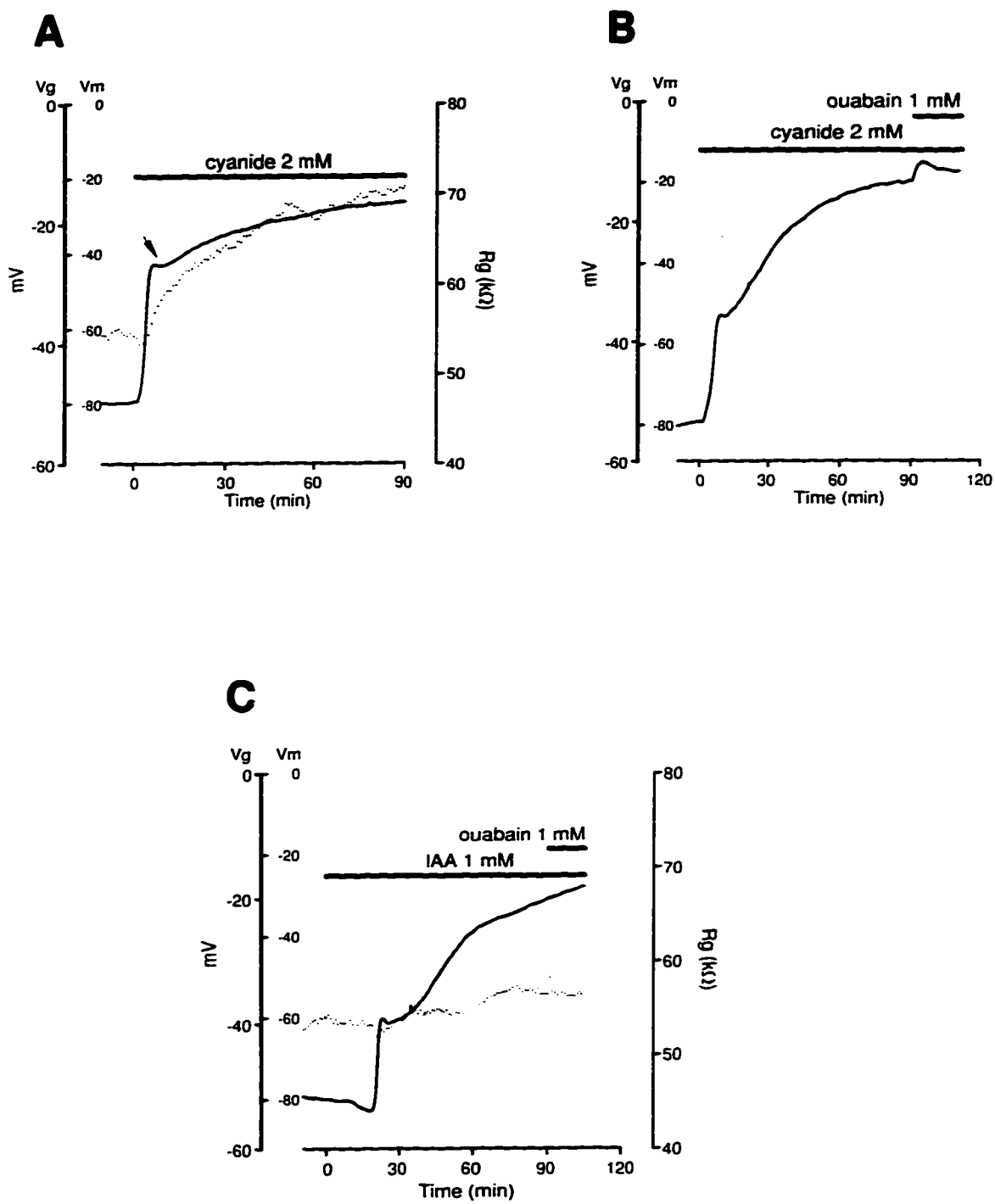
A
Vg
Vm
0
0
-20
-40
-60
-80
-20
-40
-60
mV
cyanide 2 mM
80
70
60
50
40
Rg (kΩ)
0
30
60
90
Time (min)
B
Vg
Vm
ouabain 1 mM
cyanide 2 mM
120
C
ouabain 1 mM
IAA 1 mM

Figure 4.3: Effect of $Ca^{2+}$- depleted perfusate on membrane potential during glycolytic inhibition with IAA (1 mM). (**A**) Exposure of nerves to IAA and nominally zero $Ca^{2+}$ simultaneously, accelerated the onset of depolarization and also eliminated phase 1 (see Fig. 4.1 C), and reduced the size of phase 3 compared to IAA alone. (**B**) Pretreatment with zero $Ca^{2+}$ for 60 min caused phase 3 to become even less pronounced (arrow). (**C**) Addition of a $Ca^{2+}$ chelator eliminated all hyperpolarizing phases. Zero-$Ca^{2+}$/EGTA solution alone elicited a small depolarization (arrow). (**D**) TEA (20 mM) alone depolarized nerves modestly due to its broad spectrum $K^+$ channel blocking properties [Hille, 1992 #231]. In addition, TEA reduced the first hyperpolarizing response, P-1, and abolished the second hyperpolarizing response, P-3, without affecting the delay prior to depolarization characteristic of glycolytic blockers. Together, these data point to a possible contribution of a $Ca^{2+}$-dependent $K^+$ conductance(s) as a mechanism for the hyperpolarizing phases induced by glycolytic block in RON.

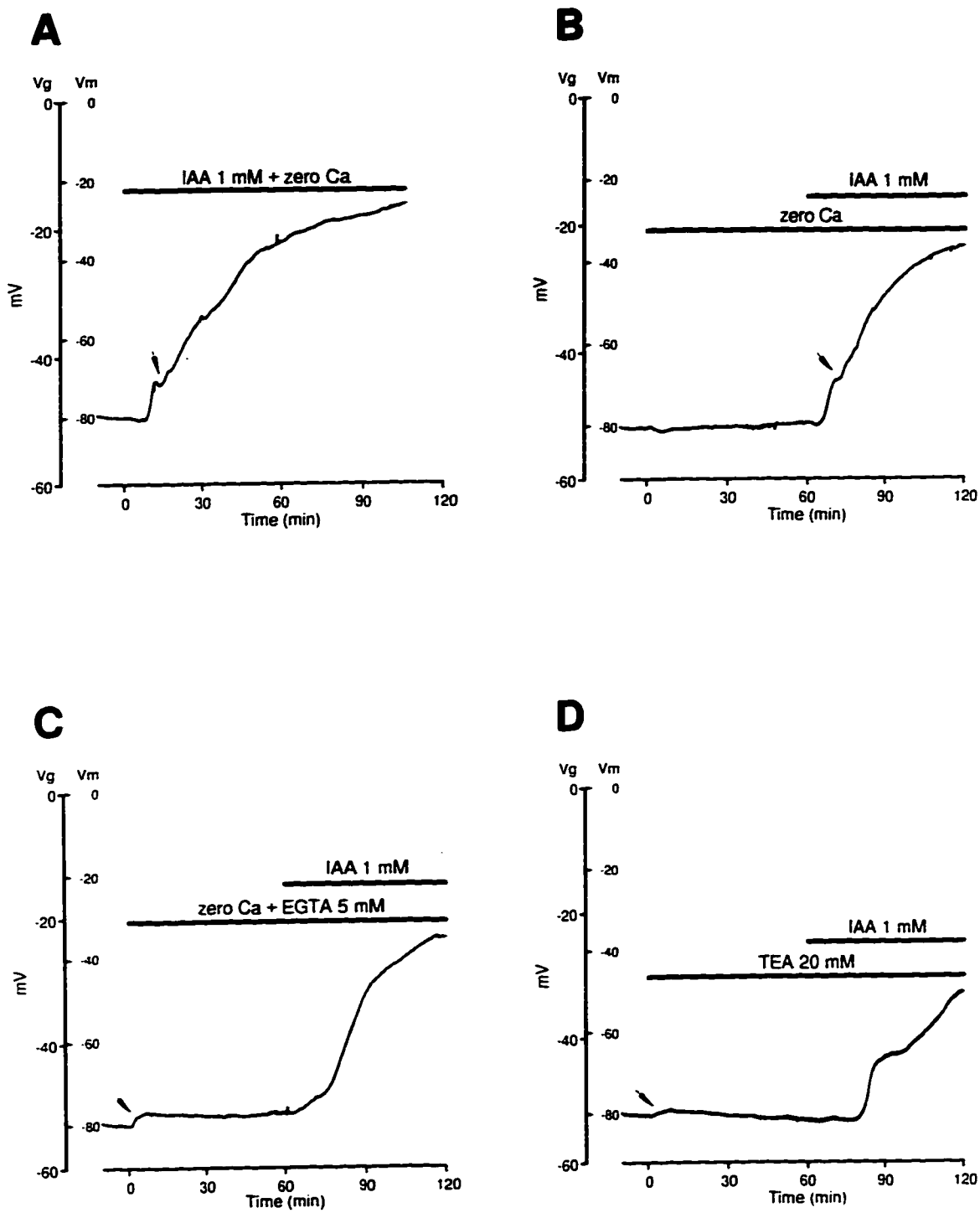
A
Vg
Vm
0
0
-20
-40
-60
-80
mV
IAA 1 mM + zero Ca
0
30
60
90
120
Time (min)
B
Vg
Vm
0
0
-20
-40
-60
-80
mV
IAA 1 mM
zero Ca
0
30
60
90
120
Time (min)
C
Vg
Vm
0
0
-20
-40
-60
-80
mV
IAA 1 mM
zero Ca + EGTA 5 mM
0
30
60
90
120
Time (min)
D
Vg
Vm
0
0
-20
-40
-60
-80
mV
IAA 1 mM
TEA 20 mM
0
30
60
90
120
Time (min)

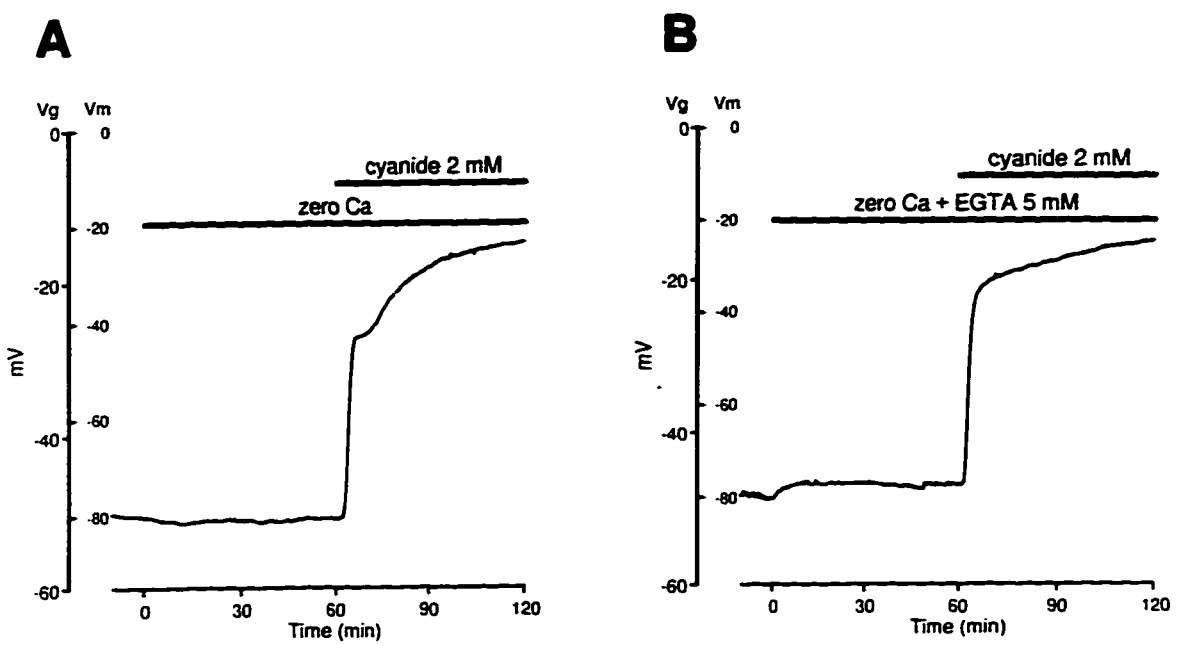


Figure 4.4: Effect of zero $Ca^{2+}$ and zero-$Ca^{2+}$/EGTA on membrane potential during chemical anoxia. (**A**) Nominally zero $Ca^{2+}$ significantly accelerated the rate of $CN^-$ - induced depolarization (Table 4), but inflections, characteristic of induction of chemical anoxia alone, were preserved. (**B**) In contrast, addition of EGTA also caused accelerated depolarization with $CN^-$, and also abolished inflections in the voltage trajectory, suggesting the possible modulation of $Ca^{2+}$-dependent conductances during anoxia, which were less pronounced than with glycolytic inhibition (compare with Figs. 4.1 C and 4.3 A-D).

Figure 4.5: **Role of $Na^+$ during glycolytic inhibition and chemical anoxia. (A)** Block of TTX-senstive $Na^+$ channels elicited a small hyperpolarizing effect. Under these conditions, glycolytic inhibition with iodoacetate (1 mM) resulted in a greatly reduced depolarization. **(B)** Replacement of $Na^+$ with the impermeant cation choline caused a transient hyperpolarizing response. Addition of IAA caused a prompt hyperpolarization (arrow) with complete preservation of membrane potential for at least 60 min. **(C)** In contrast, TTX and NaCN application elicited significantly different responses between nerves A (recorded immediately) and nerves B (recorded after several additional hours of *in vitro* incubation, see text). For nerves A, NaCN application evoked a prompt depolarization which was much less extensive that without TTX. In contrast, nerves B failed to depolarize. These results suggest an additional $Na^+$ influx pathway into RON axons, distinct from TTX-sensitive $Na^+$ channels. This pathway appears to be downregulated after several hours of *in vitro* incubation (see text). **(D)** Similarly, NaCN and zero-$Na^+$/choline solution caused a blunted but consistent depolarization for nerves A. Nerves B ($V_m$ not normalized to -80 mV baseline) instead hyperpolarized slightly (arrow) after addition of $CN^-$ with little further depolarization.

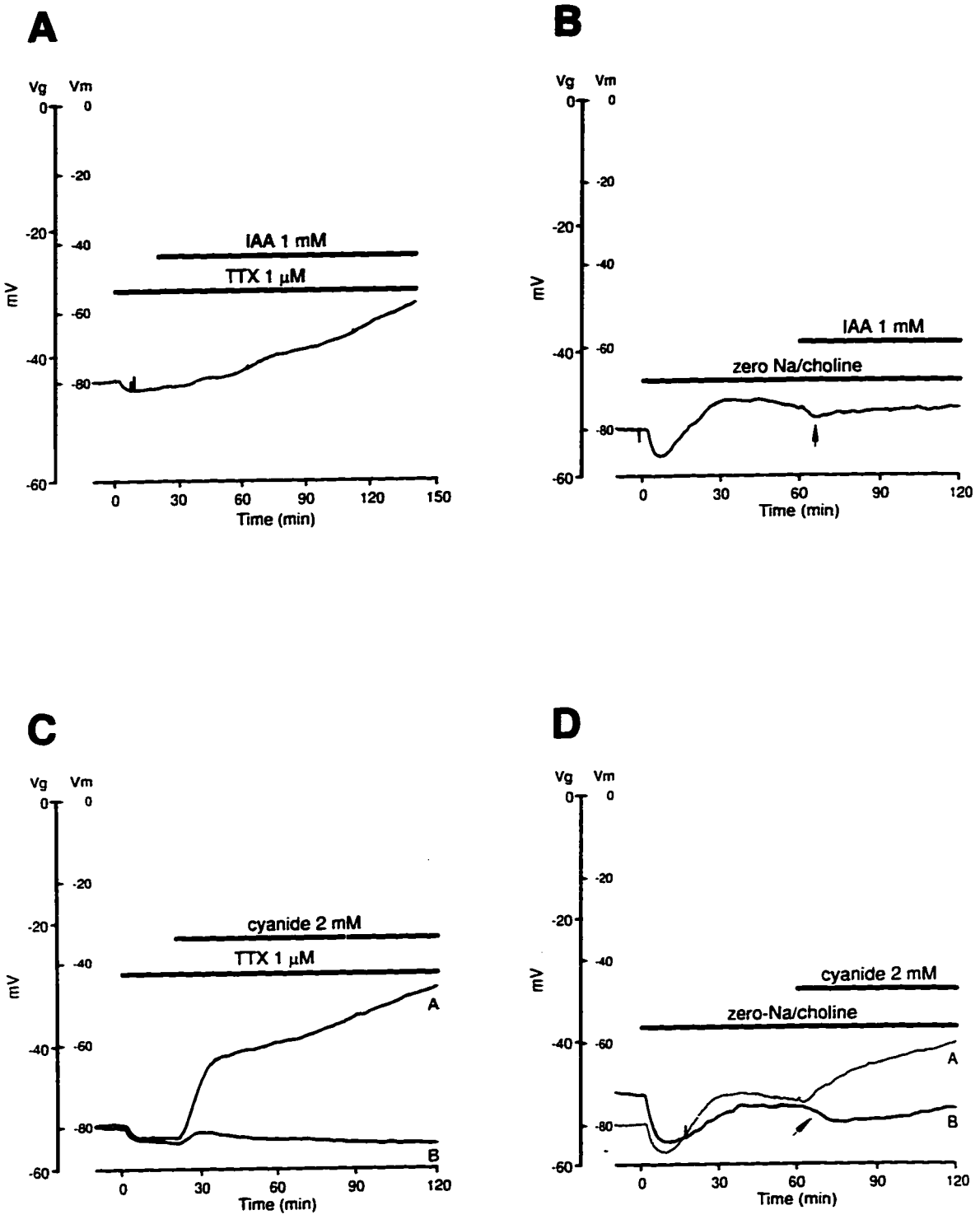
A
Vg
Vm
0
-20
-40
-60
-80
mV
IAA 1 mM
TTX 1 µM
0
30
60
90
120
150
Time (min)
B
Vg
Vm
IAA 1 mM
zero Na/choline
Time (min)
C
cyanide 2 mM
TTX 1 µM
A
B
Time (min)
D
cyanide 2 mM
zero-Na/choline
A
B
Time (min)

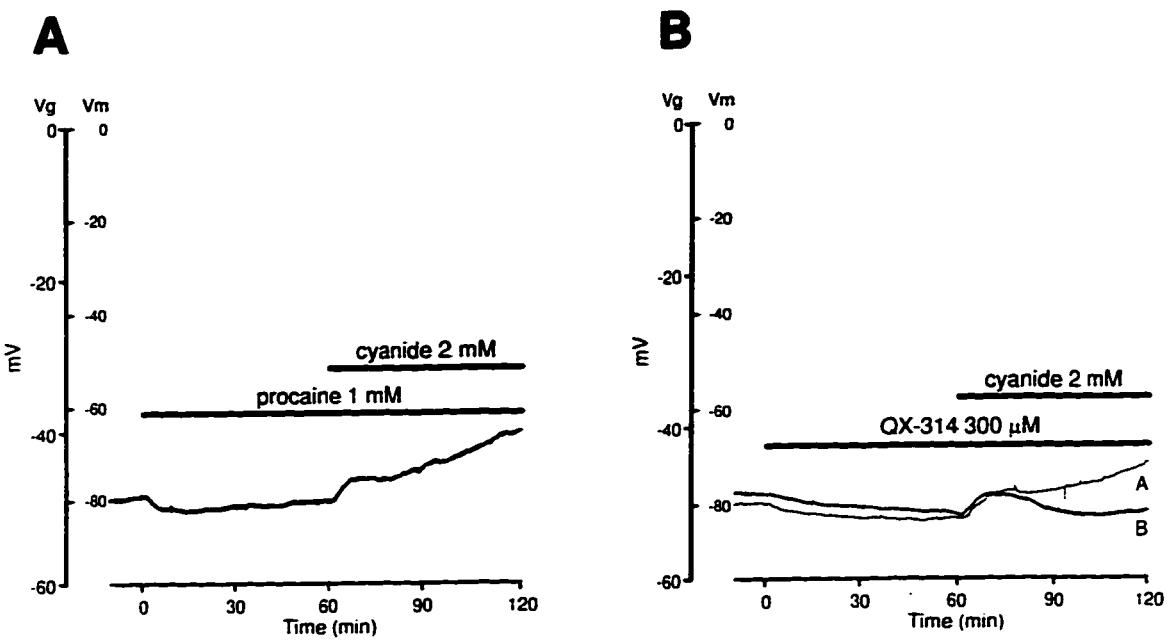


Figure 4.6: Local anesthetics reduce anoxic RON depolarization. (**A**) Procaine (1 mM) alone had a rapid hyperpolarizing effect on membrane potential, and blunted the depolarizing effect of chemical anoxia. (**B**) QX-314 (300 µM) alone also elicited a small hyperpolarization, which developed much more slowly that with procaine, likely reflecting the limited rate at which this permanently charged compound could cross the axolemma to gain access to the cytosolic side of the $Na^+$ channel. Differences were observed for nerves A and B (see Fig. 4.5 legend and text for details) after $CN^-$ was applied, causing limited depolarization in nerves A which was further reduced for nerves B.

Table 4.1: The effect of glycolytic block or chemical anoxia on optic nerve membrane potential.

| Condition | Time (min) | Ratio (%) ±S.D. | $V_g$ (mV) ±S.D. | $V_m$ (mV) ±S.D. | n |
|---|---|---|---|---|---|
| Zero Glucose | 60 | 55 ±10 | -25 ±5 | -44 ±8 | 6 |
| Deoxyglucose 10 mM | 60 | 75 ±9 | -35 ±4 | -60 ±7 | 7 |
| IAA 1 mM | 30 | 79 ±7 | -38 ±4 | -63 ±5 | 24 |
| | 60 | 55 ±6 | -26 ±3 | -44 ±5 | 24 |
| | 120 | 37 ±3 | -18 ±2 | -29 ±3 | 19 |
| Pyruvate 10 mM, add IAA 1 mM* | 60 | 104 ±2 | -49 ±5 | -83 ±2 | 2 |
| IAA 1 mM, add Ouabain 1 mM† | 20 | 35 ±5 | -16 ±1 | -28 ±4 | 2 |
| NaCN 2 mM | 30 | 51 ±6 | -24 ±3 | -41 ±5 | 15 |
| | 60 | 34 ±4 | -16 ±2 | -27 ±3 | 15 |
| NaCN 2 mM, add Ouabain 1 mM† | 20 | 26 ±6 | -11 ±1 | -20 ±5 | 3 |

All times corrected for dead space.
*Pyruvate applied 60 min prior to IAA.
†Ouabain applied after 90 min of IAA or NaCN.

Table 4.2: Role of $Ca^{2+}$ during glycolytic inhibition and chemical anoxia.

| Condition | Time (min) | Ratio (%) ±S.D. | $V_g$ (mV) ±S.D. | $V_m$ (mV) ±S.D. | n |
|---|---|---|---|---|---|
| Zero $Ca^{2+}$, add IAA 1 mM (applied simultaneously) | 30 | 65 ±2 | -31 ±0.2 | -52 ±2 | 3 |
| | 60 | 44 ±2 | -21 ±2 | -35 ±2 | 3 |
| Zero $Ca^{2+}$, add IAA 1 mM* | 30 | 60 ±2 | -29 ±1 | -48 ±2 | 4 |
| | 60 | 42 ±1 | -20 ±1 | -34 ±1 | 4 |
| Zero $Ca^{2+}$ + EGTA 5 mM, add IAA 1 mM* | 30 | 61 ±3 | -30 ±2 | -49 ±2 | 4 |
| | 60 | 43 ±4 | -21 ±1 | -34 ±3 | 4 |
| TEA 20 mM, add IAA 1 mM* | 60 | 61 ±4 | -30 ±2 | -49 ±3 | 4 |
| Zero $Ca^{2+}$, add NaCN 2 mM† | 30 | 38 ±7 | -17 ±1 | -31 ±5 | 3 |
| | 60 | 30 ±7 | -13 ±2 | -24 ±6 | 3 |
| Zero $Ca^{2+}$ + EGTA 5 mM, add NaCN 2 mM† | 30 | 34 ±7 | -16 ±3 | -27 ±5 | 3 |
| | 60 | 27 ±4 | -13 ±1 | -21 ±3 | 3 |

All times corrected for dead space.
*Zero $Ca^{2+}$, zero $Ca^{2+}$/EGTA or TEA were applied 60 min prior to IAA.
†Zero $Ca^{2+}$ or zero $Ca^{2+}$/EGTA were applied 60 min prior to NaCN.

Table 4.3: Time to onset and rate of rapid depolarization induced by glycolytic inhibition and chemical anoxia.

| Condition | Time to Onset (min) ±S.D. | Rate of Initial Rapid Phase (mV/min) ±S.D. | n |
|---|---|---|---|
| Zero Glucose | 28 ±6 | 2 ±1 | 6 |
| Deoxyglucose 10 mM | 38 ±8 | 3 ±1 | 7 |
| IAA 1 mM | 20 ±3 | 7 ±3 | 24 |
| IAA 1 mM + zero $Ca^{2+}$ (applied simultaneously) | 5 ±2 | 4 ±1 | 3 |
| Zero $Ca^{2+}$, add IAA 1 mM* | 3 ±1 | 2 ±1 | 4 |
| Zero $Ca^{2+}$ + EGTA 5 mM, add IAA 1 mM* | 3 ±1 | 2 ±0.2 | 4 |
| TEA 20 mM, add IAA 1 mM* | 17 ±2 | — | 4 |
| NaCN 2 mM | — | 7 ±4 | 15 |
| Zero $Ca^{2+}$, add NaCN 2 mM† | — | 14 ±3 | 3 |
| Zero $Ca^{2+}$ + EGTA 5mM, add NaCN 2 mM† | — | 15 ±4 | 3 |

All times corrected for dead space.
*Zero $Ca^{2+}$, zero $Ca^{2+}$/EGTA and TEA were applied 60 min prior to IAA.
†Zero $Ca^{2+}$ and zero $Ca^{2+}$/EGTA were applied 60 min prior to NaCN.

Table 4.4: Role of $Na^+$ during glycolytic inhibition and chemical anoxia.

| Condition | Time (min) | Ratio (%) ±S.D. | $V_g$ (mV) ±S.D. | $V_m$ (mV) ±S.D. | n |
|---|---|---|---|---|---|
| TTX 1 μM, add IAA 1 mM* | 60 | 95 ±6 | -46 ±5 | -76 ±4 | 6 |
| Zero-$Na^+$/choline, add IAA 1 mM† | 60 | 97 ±7 | -47 ±3 | -77 ±6 | 4 |
| TTX 1 μM, add NaCN 2 mM* | 60 | A‡: 76 ±13 | A: -38 ±7 | A: -61 ±10 | 3 |
| | | B‡: 99 ±7 | B: -49 ±4 | B: -80 ±5 | 3 |
| Zero-$Na^+$/choline, add NaCN 2 mM† | 60 | A: 81 ±5 | A: -39 ±2 | A: -65 ±4 | 6 |
| | | B: 98 ±4 | B: -47 ±1 | B: -79 ±3 | 4 |
| Procaine 1 mM, add NaCN 2 mM§ | 60 | 84 ±11 | -38 ±5 | -67 ±9 | 4 |
| QX-314 300 μM, add NaCN 2 mM§ | 60 | A: 80 ±9 | A: -37 ±7 | A: -64 ±7 | 3 |
| | | B: 101 ±6 | B: -48 ±2 | B: -81 ±5 | 3 |

All times corrected for dead space.
*TTX applied 20 min prior to 60 min of IAA or NaCN.
†IAA or NaCN were applied following 60 min of zero-$Na^+$/choline.
‡A = nerve A; B = nerve B.
§Procaine or QX-314 were applied 60 min prior to NaCN.

Table 4.5: Effect of various experimental conditions on $V_m$.

| Condition | Time (min) | Ratio (%) ±S.D. | $V_g$ (mV) ±S.D. | $V_m$ (mV) ±S.D. | n |
|---|---|---|---|---|---|
| Pyruvate 10 mM | 60 | 102 ±2 | -48 ±5 | -81 ±2 | 2 |
| TEA 20 mM | 60 | 98 ±2 | -48 ±1 | -78 ±1 | 4 |
| Zero $Ca^{2+}$ + EGTA 5 mM | 60 | 96 ±1 | -45 ±4 | -77 ±1 | 8 |
| Procaine 1 mM | 60 | 106 ±2 | -47 ±1 | -85 ±2 | 4 |
| QX-314 300 μM | 60 | 105 ±2 | -49 ±2 | -84 ±2 | 6 |

All times corrected for dead space.

## 4.3 Discussion

### 4.3.1 Effect of Glycolytic Inhibition or Chemical Anoxia on $V_m$

Glucose and $O_2$ are instrumental in sustaining adequate cellular energy metabolism since ATP is derived almost exclusively from a continuous supply of glucose in the brain (Erecinska and Silver, 1989). A large proportion of the ATP synthesized from glycolysis and oxidative phosphorylation is utilized by $Na^+,K^+$-ATPase to maintain $V_m$ in neural cells (Ritchie, 1967; Erecinska and Silver, 1989). The effect of inhibiting glycolysis or oxidative phosphorylation on $V_m$ was investigated in CNS myelinated axons.

Unexpectedly, differences existed between various methods of blocking glycolysis, that, in theory, possessed similar modes of action. IAA likely blocked glycolysis profoundly, causing a more synchronous disruption of energy-dependent mechanisms, eliciting a response consisting of four distinct phases. Conversely, the energy depletion from zero glucose exposure occurred more gradually (probably due to slow removal of glucose from the ECS), resulting in a less severe insult and consequently a more gradual collapse of ion gradients and $V_m$. Axons may have also derived energy from the degradation of astrocytic glycogen (Cataldo and Broadwell, 1986; Dringen and Hamprecht, 1992; Swanson and Choi, 1993), possibly via lactate transfer (Tsacopoulos and Magistretti, 1996). Adding DG, an inhibitor of hexokinase, may have produced a somewhat harsher disruption of glycolysis, with emergence of the four characteristic phases typical of IAA (Fig. 4.1 A). Interference with glial glycogen breakdown by DG (Dringen and Hamprecht, 1993) may have also contributed to the observed differences. DG also induced cell death at a slower rate in cultured rat astrocytes in comparison to sodium fluoride, an inhibitor of the glycolytic enzyme, enolase (Pappas and Ransom, 1995). Interestingly, pyruvate completely prevented nerve

depolarization induced by IAA, making it unlikely that non-specific effects of this inhibitor were responsible for $V_m$ changes, in agreement with previous reports (Ochs and Smith, 1971; Sabri and Ochs, 1971). The results also indicated that RON axons are fueled preferentially by aerobic metabolism which generates the majority of required ATP at rest, as in other parts of the CNS (Erecinska and Dagani, 1990); glycolysis contributed insufficient and only minor amounts of ATP for the maintenance of $V_m$ (Fig. 4.2 C).

A feature common to all three methods of glycolytic inhibition was a significant delay (20-30 min) before any effect on $V_m$ was noticeable. While it could be argued that slow washout of glucose was responsible for zero-glucose (± DG) treatments, a delayed penetration of IAA into the cells is unlikely as this inhibitor produced almost immediate effects under zero-$Ca^{2+}$/EGTA conditions (Fig. 4.3 C). Instead, it is thought that operation of the TCA cycle/oxidative phosphorylation continued temporarily, using alternate substrates such as amino acids (Stryer, 1988). Evidence for persistent oxidative phosphorylation activity during glycolytic inhibition was shown in cultured rat astrocytes and neurons (Pauwels et al., 1985) and guinea pig synaptosomes (Kauppinen and Nicholls, 1986b). These studies suggested that the cells generated energy using substrates other than glycolytically-derived pyruvate. Further support for maintenance of $V_m$ mainly by aerobic metabolism (with minimal glycolytic contribution) was provided by the observation that nerves depolarized at a similar rate (phase 2) with IAA and $CN^-$, despite a delayed onset with the former.

### 4.3.2 $R_g$ During Cyanide Exposure

Unlike the stable $R_g$ measurements recorded during control conditions (see Fig. 3.1) or IAA (see Fig. 4.2 C) application, the trans-gap resistance, $R_g$, increased during $CN^-$ exposure. Since the $R_g$ shift largely occurred *following* the rapid

depolarizing response (phase 2), it was concluded that the $V_m$ change (phase 2) was not artifactual. The voltage trajectory occurring after phase 2 must be examined with the knowledge that the response may be inaccurate because $R_g$ may artifactually influence $V_g$ (see section 2.3: Grease Gap Electrical Model). $R_g$ is determined by a change in $R_i$ or $R_e$. $R_i$ will increase by shrinkage of the axons, and RON axons have been shown to shrink by exposure to an anoxic challenge (Waxman et al., 1992a). Glial swelling will cause $R_i$ or $R_e$ to rise by either compressing the axon or by reducing the area of the ECS, respectively. Swelling may result from concomitant uptake of $K^+$, $Cl^-$, and $H_2O$ (Walz et al., 1993).

However, evidence that the depolarizing response following phase 2 induced by $CN^-$ is not artifactual was provided by the similar voltage trajectory observed with IAA and $CN^-$. Both $CN^-$ and IAA characteristically displayed an abrupt change in the rate of membrane depolarization with an inflection or hyperpolarization, respectively. Moreover, the slow depolarization following the inflection is also similar to that of IAA. Considering these observations, it is reasonable to conclude that the $V_m$ response recorded during $CN^-$ application is real, but the *extent* to which the nerve depolarized must be interpreted with caution. From these findings, it is evident that $R_g$ measurements are important for quantitative recording with this type of electrophysiological technique.

### 4.3.3 Role of $Ca^{2+}$ During Metabolic Insult

The distinct hyperpolarizing response (phase 1) observed in the majority of nerves during glycolytic inhibition with IAA and DG raised the possibility of an activated $K^+$ conductance. These results are similar to guinea pig (Hansen et al., 1982) and rat (Fujiwara et al., 1987; Leblond and Krnjevic, 1989; Belousov et al., 1995) hippocampal neurons in which hyperpolarization occurred during anoxia secondary to $K^+$ conductance increase. It was suggested that a rise in $[Ca^{2+}]_i$

was responsible for the hyperpolarizing response stimulating the $K_{Ca}$ channel (Leblond and Krnjevic, 1989). Our data are also consistent with such a mechanism since phase 1 was $Ca^{2+}$ dependent. Phase 3, which interrupted the rapid nerve depolarization with a hyperpolarizing inflection during glycolytic inhibition, was also dependent on $Ca^{2+}$. Moreover, reduction or elimination of these responses by TEA further supports the notion of a mechanism involving activation of a $K_{Ca}$ channel. These hyperpolarizing responses were progressively reduced with more severe $Ca^{2+}$-depleting treatments (Fig. 4.3 A-C), suggesting that a relatively inaccessible source of $Ca^{2+}$ may have been the trigger, perhaps originating from internal $Ca^{2+}$ stores (Belousov et al., 1995) known to be present in myelinated axons (Takei et al., 1992). The absence of hyperpolarizing responses during $CN^-$ treatment, despite rapid and massive depolarization, may indicate preferential maintenance of internal $Ca^{2+}$ stores by glycolytically derived ATP (Xu et al., 1995).

$Ca^{2+}$-depleted conditions accelerated the rate of depolarization during chemical anoxia, consistent with a more rapid loss of RON excitability (Stys, unpublished). This may be due to removal of charge screening by the divalent cation, resulting in a leakier membrane (Woodhull, 1973; Hille et al., 1975). However, zero $Ca^{2+}$ conditions markedly slowed the depolarization rates in *glycolytically inhibited* nerves, suggesting that $Ca^{2+}$ depletion has more complex effects than simple charge screening removal at the membrane. It was concluded that the hyperpolarizing responses were probably not due to activation of the $K_{ATP}$ channel (Jonas et al., 1991) because phases 1 and 3 were abolished during zero $Ca^{2+}$ conditions and, in addition, the $K_{ATP}$ channel antagonist, glibenclamide, failed to blunt the hyperpolarizing phases (data not shown).

Phase 1 occurred without delay during zero-$Na^+$/choline and IAA exposure as well as during zero-$Na^+$/choline and $CN^-$ (nerve B) application. Moreover, it was absent during the concomitant application of IAA and the $Na^+$ channel antagonist, TTX. The findings suggest a mechanism dependent on $Na^+$ channels, but, not on $Na^+$ influx (the response was still present with zero-$Na^+$/choline application). It is possible that during IAA alone, the $Na^+/Ca^{2+}$ exchanger removed $Ca^{2+}$ entering through $Na^+$ channels (DiPolo et al., 1982; Stys and LoPachin, Submitted) or $Ca^{2+}$ channels (Fern et al., 1995a) delaying the rise in $[Ca^{2+}]_i$. During zero-$Na^+$ perfusion, the exchanger was unable to buffer $Ca^{2+}$, thereby permitting a faster increase in $[Ca^{2+}]_i$ and activation of the $K_{Ca}$ channel. We propose a dual role for the $Na^+/Ca^{2+}$ exchanger: at the beginning of metabolic stress, it operates to extrude $Ca^{2+}$, but in the later stages of anoxia/ischemia, when the $Na^+$ gradient has collapsed, it imports damaging quantities of $Ca^{2+}$ (Stys et al., 1990; Stys et al., 1992c). The inflection recorded during $CN^-$ exposure alone may be analogous to the hyperpolarization in $CN^-$ and zero-$Na^+$/choline (Fig. 4.5 D, nerve B), truncated by the massive and rapid depolarization.

The abrupt reduction in depolarization rate coinciding with phase 3 (Fig. 4.1 C), persisted in TEA despite the abolition of distinct hyperpolarizations by this blocker. This suggests that the mechanisms underlying the *rate change* are distinct from those mediating the *hyperpolarizing phenomena*, although both appear to be relatively $Ca^{2+}$-dependent. While the hyperpolarizing shifts were likely due to $K^+$ conductance activation, given the rate limiting effect on depolarization of $Na^+$ conductance (see below), it is likely that shifts in rate of decay of $V_m$ were due to reductions in $Na^+$ conductance, rather than increases in $K^+$ conductance. Other studies have shown that anoxia decreased $Na^+$ permeability and shifted the steady state inactivation curve to increasingly

negative potentials (Brismar, 1981; Brismar, 1983; Cummins et al., 1991; Haddad and Jiang, 1993; O'Reilly and Haddad, 1996). The mechanism for this presumed conductance change is unknown, but may involve $Ca^{2+}$-dependent phosphorylation of $Na^+$ channels by protein kinase (Li et al., 1993). The reduction of $Na^+$ permeability may represent a stereotyped response to metabolic stress, which would at the same time reduce the drain on already strained energy reserves and diminish the degree of depolarization and deleterious $Na^+/Ca^{2+}$ exchange-mediated $Ca^{2+}$ influx.

### 4.3.4 Role of $Na^+$ During Metabolic Inhibition

The immediate depolarizing response elicited by $CN^-$ demonstrated a major dependence of axonal polarization on aerobic metabolism, consistent with the rapid loss of excitability previously observed within minutes of anoxia (Stys et al., 1990; Stys, 1996). Nerve depolarization by glycolytic inhibition or chemical anoxia was reduced by blocking TTX-sensitive $Na^+$ channels. One explanation may be that $Na^+$ influx is rate limiting, and will in turn affect the rate of $K^+$ loss, for reasons of electroneutrality: reducing $Na^+$ influx will therefore reduce loss of internal $K^+$ and accumulation of extracellular $K^+$ (Ransom et al., 1992), thereby maintaining membrane polarization. Relative preservation of membrane potential during metabolic inhibition where $Na^+$ was replaced with the impermeant cation choline further supports this possibility. An intriguing alternative explanation, for which we have preliminary evidence (Stys and LoPachin, Submitted), may involve the induction of $K^+$ and $Cl^-$ co-efflux when $Na^+$ entry is prevented: osmotically obligated water loss would concentrate remaining internal $K^+$ and in turn blunt the membrane depolarization.

Nerves A (studied immediately following dissection) and nerves B (stored in oxygenated aCSF at room temperature for several additional hours) exposed to

$Na^+$ channel blockers (TTX, QX-314) or $Na^+$-depleted perfusate responded very differently to the addition of $CN^-$: nerves A depolarized (although not nearly to the same extent as with $CN^-$ alone), whereas nerves B did not (Fig. 4.5 C-D). Curiously, glycolytic inhibition did not distinguish between the two nerve populations. The persistent, albeit blunted, depolarization observed during anoxia in nerves studied promptly, despite $Na^+$ channel block with TTX, may suggest an additional $Na^+$ influx path, which appeared to be downregulated with prolonged *in vitro* incubation. Together with indications that axonal $K^+$ permeability is also reduced with time (see section 3.3.2), these findings suggest that a common mechanism may be downregulation of the mixed $Na^+$- and $K^+$-permeable $K_{IR}$ channel (Eng et al., 1990; Karst et al., 1993; Solomon and Nerbonne, 1993), perhaps due to washout of modulatory factors (Zhang and Krnjevic, 1993).

The local anesthetics, procaine and QX-314, had similar effects to TTX. Both agents caused a small but reproducible hyperpolarization indicating block of a persistent $Na^+$ conductance at rest (Stys et al., 1993). These compounds act at the cytoplasmic side of the $Na^+$ channel; the onset of the procaine effect was rapid likely due to its ability to permeate the membrane in its uncharged form. In contrast, the time of onset of the permanently charged QX-314 was much longer reflecting the much slower movement across the axolemma by this molecule. As with TTX, both compounds greatly reduced nerve depolarization during chemical anoxia. Unlike TTX however, QX-314 does not abolish electrogenesis at the concentration used (Stys et al., 1992a), and its membrane potential sparing effect is likely due to this drug's preferential action at open, non-inactivating $Na^+$ channels (Wang et al., 1987; Khodorov, 1991). QX-314 appeared to reduce the extent of depolarization for nerves A even more effectively than TTX alone (compare Figs. 4.5 C and 4.6 B), similar to complete $Na^+$ replacement with

impermeant choline (Fig. 4.5 D). Given the evidence suggesting additional $Na^+$ influx pathways in RON axons (see above), perhaps QX-314 has activity at these as yet unidentified influx routes. One possibility is the $K_{IR}$ channel, known to be present on RON axons (Eng et al., 1990) and to possess finite $Na^+$ permeability (Karst et al., 1993; Solomon and Nerbonne, 1993). This idea is further supported by observations that blocking this channel with $Cs^+$ was highly protective against RON anoxia (Stys and Hubatsch, 1996), likely due to a reduction of depolarization and $Na^+$ influx.

In conclusion, it was determined that the resting potential of the RON depends on energy generated primarily from aerobic metabolism with a minor contribution from glycolytic ATP. The effects of glycolytic inhibition alone were delayed, suggesting a limited ability of axons to generate aerobic ATP from alternate substrates. The inevitable massive depolarization was largely, although not exclusively, dependent on $Na^+$ influx through TTX-sensitive $Na^+$ channels (likely the noninactivating $Na^+$ conductance previously demonstrated in the RON (Stys et al., 1993)), with evidence for additional TTX-insensitive $Na^+$ influx pathways. The membrane potential-sparing effect of local anesthetics likely contributes to their neuroprotective actions. Finally, CNS axons may possess autoprotective mechanisms (Fern et al., 1996), including probable activation of a $Ca^{2+}$-dependent $K^+$ conductance(s) to delay depolarization onset, and a controlled reduction of $Na^+$ permeability to slow the decay of $V_m$, also $Ca^{2+}$-dependent. We therefore suggest that during the initial stages of metabolic insult, the presumed rise in free $[Ca^{2+}]_i$ may be transiently beneficial, reflecting the axon's intrinsic mechanism designed to limit injury during anoxia/ischemia.

# CHAPTER 5

# GENERAL DISCUSSION

## 5.1 Significance of the Findings

### 5.1.1 Research Summary

The axon is an essential structure in the CNS, permitting neurons to communicate. Irreversible damage to axons results in impairment of a vital CNS function i.e. signal transmission. Thus, the mechanisms leading to axonal injury by diseases such as stroke and spinal cord injury are important to elucidate. The main pathogenic agent, $Ca^{2+}$, is ultimately responsible for axonal dysfunction induced by anoxia/ischemia. The anoxic/ischemic insult begins with extensive depolarization of $V_m$, resulting from energy deprivation and the ensuing reduced activity of $Na^+$,$K^+$-ATPase. Importantly, $Ca^{2+}$ influx in optic nerve axons occurs mainly via the $Na^+/Ca^{2+}$ exchanger (Stys et al., 1992c; Waxman et al., 1992b), a structure that is functionally influenced by the $Na^+$ gradient and membrane potential (Rasgado-Flores and Blaustein, 1987; Steffensen and Stys, 1996). The ions and channels involved in mediating this depolarizing response are not known. A rise in $[K^+]_o$ has been determined (Ransom et al., 1992), but the counterion and channel(s) allowing $K^+$ efflux have not been identified. The research project was designed to identify this ion and its influx pathway(s) during pathophysiological conditions.

We first explored the effect on $V_m$ of pharmacological blockers and ion substitution under *normoxic* conditions. The grease gap technique recorded a fraction (≈ -50 mV) of the true compound RMP (≈ -80 mV (Stys, 1996; Stys et al., in press)) at 37 °C for several hours. The stability of the recording enabled the

reliable study of $V_m$ for prolonged time periods, while $R_g$ measurements ensured that observed changes in $V_m$ were not artifactual. The depolarizing response observed with ouabain application determined that $V_m$ critically depended on the continuous function of $Na^+,K^+$-ATPase due to the constant and, obviously, rapid leak of $Na^+$ and $K^+$ across the axonal membrane. Moreover, further depolarization produced by metabolic inhibition following ouabain exposure suggested that $V_m$ is also maintained by an ATP-dependent, ouabain-insensitive ion transport system.

$Na^+$ substitution studies identified the ion and channels involved in mediating this membrane depolarization. Perfusion with zero-$Na^+$/choline, an impermeant cation, caused a transient hyperpolarization, that was greater than with TTX alone, indicating the presence of both TTX sensitive and insensitive $Na^+$ influx pathways in resting RON axons. Using the $Na^+$ substitution data, the resting $P_K$:$P_{Na}$ ratio was estimated at 20:1 and with this ratio, the contribution of the electrogenic pump to the resting axonal potential was estimated at -7 mV. In contrast to zero-$Na^+$/choline solution, $Li^+$ substituted zero-$Na^+$ perfusate caused a rapid depolarization due to failure of $Na^+,K^+$-ATPase and the ability of $Li^+$ to permeate the $Na^+$ channel. TTX reduced, but did not prevent, ouabain- or zero-$Na^+$/$Li^+$- induced depolarization. It was concluded that the primary $Na^+$ influx path in *resting* RON axons is the TTX-sensitive $Na^+$ channel, with evidence for additional TTX-insensitive routes permeable to $Na^+$ and $Li^+$.

$V_m$ was subsequently examined during energy depletion. Glycolytic inhibition with IAA and DG evoked a voltage response consisting of four phases. A distinct hyperpolarizing response (phase 1) was followed by a rapid depolarization (phase 2). Phase 2 was interrupted by a second hyperpolarizing response (phase 3) which led to an abrupt reduction in the rate of potential change, with $V_m$ then gradually depolarizing (phase 4). The delay preceding

depolarization was probably due to continued, temporary oxidative phosphorylation using alternate substrates through the TCA cycle.

Conversely, chemical anoxia induced with $CN^-$ immediately caused a rapid depolarizing response, and phase 1 was never observed. Similar to that of IAA, this rapid depolarization was terminated by an inflection (not as pronounced as the phase 3 response of IAA) which was followed by a slow depolarizing response. Application of ouabain to $CN^-$ treated nerves caused additional depolarization, indicating a minor glycolytic contribution to the $Na^+$,$K^+$-ATPase, which is preferentially fueled by ATP generated by oxidative phosphorylation.

Phases 1 and 3 during IAA exposure and the inflection during $CN^-$ treatment were abolished by perfusing the RON with zero-$Ca^{2+}$/EGTA. TEA also reduced phase 1 and eliminated phase 3. Thus, a $Ca^{2+}$ activated $K^+$ conductance is thought to be responsible for these hyperpolarizing inflections.

The $Na^+$ channel antagonists, TTX, procaine and QX-314, and replacement of $Na^+$ with choline significantly reduced depolarization during glycolytic inhibition with IAA as well as during chemical anoxia. The potential-sparing effects of TTX were less than those of choline-substituted perfusate, suggesting additional, TTX-insensitive $Na^+$ influx pathways in *metabolically compromised* axons. Taken together, depolarization of metabolically stressed axons is heavily dependent on external $Na^+$.

### 5.1.2 Significance of the Findings

*Conductance at the Resting Membrane Potential*

This research study characterized a part of $Na^+$ permeability *at rest* in optic nerve axons. Previously, a TTX-sensitive $Na^+$ channel was shown in RON (Stys

et al., 1993) which was also found with the present data. There is also support for a novel TTX-insensitive $Na^+$ influx path in RON axons.

*$Na^+$,$K^+$-ATPase*

The findings demonstrated that $Na^+$,$K^+$-ATPase is the primary ion transport system maintaining 1) ion homeostasis and 2) membrane potential in optic nerve axons, similar to that found in other mammalian neuronal preparations (Rossier et al., 1987; Erecinska and Dagani, 1990). In turn, this enzyme functions only in the presence of ATP and, thus it was not unexpected that subjecting the RON to energy deprivation by either glycolytic inhibition or chemical anoxia led to a rapid change in $V_m$ due to collapse of ion gradients. The results signified the extreme sensitivity of axons exposed to metabolic stress. The data also showed that a continuous supply of energy substrates is essential, indicating that minimal energy reserves are present. These results are in agreement with data in other tissues (Hansen, 1985; Erecinska and Silver, 1994; Martin et al., 1994; Ransom et al., 1994).

*$Na^+$ Mediated Membrane Depolarization*

We concluded that membrane depolarization caused by block of $Na^+$,$K^+$-ATPase or metabolic inhibition is mediated by electroneutral exchange of $K^+$ efflux and $Na^+$ influx with $Na^+$ entering via TTX-sensitive and TTX-insensitive $Na^+$ pathways. Continuous $Na^+$ influx has been found to cause injury in the RON by inducing a rise in $[Ca^{2+}]_i$ through reverse operation of the $Na^+/Ca^{2+}$ exchanger (Waxman et al., 1991; Stys et al., 1992c; Ransom et al., 1994). Therefore, $Na^+$ flux elicits two deleterious effects which are 1) causing reverse mode of the exchanger from the reduced $Na^+$ gradient and 2) permitting $K^+$

efflux, which, in turn, produces membrane depolarization, further stimulating intracellular $Na^+$ dependent $Ca^{2+}$ import.

*$Na^+$ Channel Antagonists*

By preventing $Na^+$ entry with $Na^+$ channel antagonists, axonal damage can be reduced (Stys et al., 1992a; Stys et al., 1992c). This corresponds with the data reported here, where membrane depolarization was drastically blunted by using the same compounds. Decreasing the $Na^+$ load intracellularly will also diminish $Na^+$,$K^+$-ATPase activity, thus preserving ATP levels. The ATP could be utilized for other cellular energy dependent systems, such as maintaining $Ca^{2+}$ homeostasis by $Ca^{2+}$-ATPase.

*Autoprotective Mechanisms*

The axon has demonstrated a limited ability to protect itself from anoxic/ischemic damage. In other preparations (Hansen et al., 1982; Fujiwara et al., 1987; Leblond and Krnjevic, 1989; Belousov et al., 1995) and likely in this preparation, a $Ca^{2+}$ dependent $K^+$ conductance is activated in response to anoxic exposure which delays membrane depolarization and, thus reduces damage.

An altered $Na^+$ permeability may represent an attempt to exert a similar beneficial effect. The voltage trajectory of $CN^-$ and IAA showed a distinct decrease in the rate of depolarization, suggesting a reduction in membrane permeability. A lower permeability to $Na^+$ has been shown to occur (Brismar, 1981; Brismar, 1983; Cummins et al., 1991; Haddad and Jiang, 1993). The results demonstrate that the axon is extremely sensitive to its metabolic state, allowing it to adapt in a rapid fashion in an effort to protect itself from injury.

## 5.2 Criticism of Methodology

### 5.2.1 Grease Gap Technique

The grease gap recording technique is an excellent methodological tool, providing stable long-term recordings of $V_m$. Therefore, subjecting the preparation to various conditions allowed observation of the trajectory of the potential and examination of the mechanisms of the response.

Several sources of error are inherent in this method. Junction potentials were constantly present, but remained small by performing routine procedures including chlorinating electrodes and preparing new agar. More importantly, the junction potentials were measured and subtracted from the recorded potential for each experiment, thus reducing the error. Although the grease gap is a modification of the sucrose gap, an unexplained hyperpolarizing shift present in sucrose gap recordings (Jirounek et al., 1981) may influence the grease gap as well, thus causing some inaccuracies in the recordings.

Another potential problem with the grease gap technique is the effect of pharmacological agents on the short circuit factor which could artifactually change $V_m$. For this reason, $R_g$ measurements were recorded concomitantly with the membrane potential, providing a means of assessing this potential inaccuracy. $CN^-$ application was the only experimental situation that showed a change in $R_g$ and, therefore, the data involving $CN^-$ was interpreted accordingly (see section 5.2.3). For example, in qualitative terms, it is reasonable to conclude that the large reduction of membrane depolarization caused by $CN^-$ in the presence of TTX was not artifactual. However, more quantitative analysis may not be justified.

The grease gap technique records the compound RMP where the recorded potential is biased in favor of large diameter fibers (see section 2.3) The effect of metabolic inhibition (see section 4.3) was discussed assuming that the RON is a

homogeneous bundle of fibers, but the preparation is composed of axons with varying diameters (Foster et al., 1982). It is possible that individual axons possess different electrophysiological properties which would cause an axon to respond differently to experimental conditions. Previous study of the RON has reported that exposure to anoxia and reoxygenation alters the shape of the three-peak CAP where smaller fibers recovered from an anoxic insult while loss of function was observed in larger axons (Stys et al., 1992c). However, structural analysis of the RON has revealed that single axons share similar properties including complete myelination (Foster et al., 1982) and localization of the $Na^+$ channel at the node (Black et al., 1989). Although there is high structural homogeneity in the RON, it was not possible to discern the potential differences between individual axons during metabolic inhibition.

### 5.2.2 Effect of Axotomy

In addition to the few drawbacks of the grease gap technique, the effect of severing the RON upon dissection must be considered since it may have influenced the response of the nerve to experimental manipulations. Axotomy likely did not elicit substantial deleterious effects based on the evidence that ion levels in the axons and glia of RON recovered to *in situ* levels following *in vitro* incubation (120 min) (LoPachin and Stys, 1995), similar to the standard 90 min equilibration period performed in these experiments. In squid giant axon, the cut end constricted within 60 min, retaining it's axoplasm, and remained constricted for hours (Gallant, 1988). Perhaps, the RON has a similar autoprotective mechanism, preventing further injury. However, disruption of the myelin causing exposure of paranodal $K^+$ channels in RON has been suggested to occur as a result of nerve transection (Gordon et al., 1988). Yet, crushing the nerve end had little effect on $V_g$ until the nerve segment was injured in the area approaching the

gap (within 1.5 mm). The results showed that transection had no immediate effect on the properties determining the RMP including membrane resistance and ion transport systems because $V_g$ remained virtually unchanged.

### 5.2.3 Methods Utilized to Induce Glycolytic Inhibition and Chemical Anoxia

For technical reasons (aCSF/test well was exposed to $O_2$ present in the surrounding environment), the experimental design precluded the use of nitrogen to induce anoxia. As such, energy generated by glycolysis and oxidative phosphorylation was inhibited with chemical agents including the glycolytic enzyme inhibitors, IAA and DG, and $CN^-$ which disrupts mitochondrial ATP production. The issue concerns the validity of these agents to simulate an actual anoxic or ischemic insult.

Anoxia (reduction in $pO_2$) and $CN^-$ are reported to produce similar effects (Kauppinen and Nicholls, 1986a; Cummins et al., 1991). $R_g$ measurements were only affected by $CN^-$ treatment, remaining relatively constant during glycolytic inhibition, indicating that further investigation is required to elucidate the differences in the mechanisms of glycolytic block and chemical anoxia. It is also unlikely that IAA elicited significant non-specific effects because pyruvate prevented the typical depolarizing response produced by IAA, consistent with previous findings (Ochs and Smith, 1971; Sabri and Ochs, 1971).

## 5.3 Direction of Future Studies Examining CNS Axons

This research project explained certain mechanisms as well as raising other questions that deserve further study. The following experiments could examine these new questions.

### 5.3.1 Ion Channels and Membrane Transport Systems

There are several channels postulated to be present in the RON including a TTX-insensitive $Na^+$ channel and a $K_{Ca}$ channel, that must be localized and characterized with respect to gating mechanisms, kinetics, and ion specificity. The channel(s) sensitive to local anesthetics should also be studied since this could be another distinct population of $Na^+$ channels.

The possibility of an ATP dependent ion transport system that partially assists $Na^+$,$K^+$-ATPase in maintaining $V_m$ during normoxic conditions must be investigated.

### 5.3.2 Pathophysiological Conditions

Localization studies identifying the source of TCA cycle substrates, possibly amino acid pools, that are supplied to synthesize the mitochondrial ATP that is utilized to maintain $V_m$ (phase 1) during IAA application.

To estimate the contribution of internal $Ca^{2+}$ stores as a stimulus for $K_{Ca}$ channel activation, pharmacological manipulation causing or preventing release from stores may be performed prior to IAA exposure to observe if the response is enhanced or eliminated, respectively.

The potential protective role of the $Na^+/Ca^{2+}$ exchanger at the initial stage of metabolic stress could be examined with an experiment that blocks exchanger operation during the insult and then measure the level of $Ca^{2+}$ by electron probe at various times after the insult has been initiated.

Inhibiting phosphorylation of the $Na^+$ channel during metabolic stress may be used to investigate the hypothesis that $Na^+$ permeability is reduced, possibly by phosphorylation, in order to delay or prevent injury.

To explore the potential beneficial contribution of glial glycogen stores during anoxia or ischemia, the nerve could be exposed to insulin prior to an anoxic challenge with assessment of function to follow.

## 5.4 Conclusions

Central myelinated axons can function only with a continuous supply of energy. Disruption of ion homeostasis by a compromised metabolic state in the axon will cause impaired CNS signal transmission resulting in significant clinical morbidity.

One of the key promoters of anoxic/ischemic axonal injury is membrane depolarization. The findings of this research project have shown that during energy depletion, depolarization due to $K^+$ efflux is indirectly but tightly linked to electroneutral $Na^+$ influx. Transmembrane $Na^+$ flux occurs not only via TTX-sensitive $Na^+$ channels as previously thought, but also through additional TTX-insensitive pathway(s). The results have also demonstrated the potential use of $Na^+$ channel antagonists, such as procaine and QX-314, which were highly effective at reducing anoxic depolarization; such agents may be clinically applicable. The axon may also attempt to delay depolarization by activating $K^+$ conductance(s) during metabolic stress, as evidenced by the hyperpolarizing response (phase 1) during glycolytic inhibition. Finally, glycolytic inhibition and chemical anoxia produced strikingly different responses, thus indicating that distinct mechanisms are invoked depending on which energy synthesizing pathways are compromised. This is the first demonstration of unique effects of glycolytic versus mitochondrial failure in CNS axons. These observations may have important implications for our understanding of the relationship between energy production and ion homeostasis in normal and injured CNS myelinated axons.

## REFERENCES

Agrawal SK, Fehlings MG (1996) Mechanisms of secondary injury to spinal cord axons *in vitro*: role of $Na^+$, $Na^+$-$K^+$-ATPase, the $Na^+$-$H^+$ exchanger, and the $Na^+$-$Ca^{2+}$ exchanger. J Neurosci 16:545-552.

Albaum HG, Tepperman J, Bodansky O (1946) The *in vivo* inactivation by cyanide of brain cytochrome oxidase and its effect on glycolysis and on the high energy phosphorus compounds in the brain. J Biol Chem 164:45-51.

Alzheimer C, Schwindt PC, Crill WE (1993) Modal gating of $Na^+$ channels as a mechanism of persistent $Na^+$ current in pyramidal neurons from rat and cat sensorimotor cortex. J Neurosci 13:660-673.

Andreeva N, Khodorov B, Stelmashook E, Cragoe E, Victorov I (1991) Inhibition of $Na^+/Ca^{2+}$ exchange enhances delayed neuronal death elicited by glutamate in cerebellar granule cell cultures. Brain Res 548:322-325.

Baker M, Bostock H, Grafe P, Martius P (1987) Function and distribution of three types of rectifying channel in rat spinal root myelinated axons. J Physiol (Lond) 383:45-67.

Bamford J, Sandercock P, Warlow C (1987) The natural history of lacunar infarction: the oxfordshire community stroke project. Stroke 18:545-551.

Banik NL, Happel RD, Sostek MB, Chiu FC, Hogan EL (1987) $Ca^{2+}$-Mediated Degradation of Central Nervous System (CNS) Proteins: Topographic and Species Variation. Metabolic Brain Disease 2:117-126.

Belousov AB, Godfraind J-M, Krnjevic K (1995) Internal $Ca^{2+}$ stores involved in anoxic responses of rat hippocampal neurons. J Physiol (Lond) 486:547-556.

Benveniste H, Drejer J, Schousboe A, Diemer NH (1984) Elevation of the extracellular concentrations of glutamate and aspartate in rat hippocampus during transient cerebral ischemia monitored by intracerebral microdialysis. J Neurochem 43:1369-1374.

Black JA, Friedman B, Waxman SG, Elmer LW, Angelides KJ (1989) Immuno-ultrastructural localization of sodium channels at nodes of Ranvier and perinodal astrocytes in rat optic nerve. Proc R Soc Lond B 238:39-51.

Blatz AL, Magleby KL (1987) Calcium-activated potassium channels. Trends Neurosci 10:463-467.

Blaustein MP (1988) Calcium transport and buffering in neurons. Trends Neurosci 11:438-443.

Blaustein MP (1993) Physiologcial effects of endogenous ouabain: control of intracellular $Ca^{2+}$ stores and cell responsiveness. Am J Physiol 264:C1367-C1387.

Boening JA, Kass IS, Cottrell JE, Chambers G (1989) The effect of blocking sodium influx on anoxic damage in the rat hippocampal slice. Neuroscience 33:263-268.

Brismar T (1981) Potential clamp analysis of the effect of anoxia on the nodal function of rat peripheral nerve fibres. Acta Physiol Scand 112:495-496.

Brismar T (1983) Nodal function of pathological nerve fibers. Experientia 39:946-953.

Brismar T, Schwarz JR (1985) Potassium permeability in rat myelinated nerve fibres. Acta Physiol Scand 124:141-148.

Brorson JR, Manzolillo PA, Miller RJ (1994) $Ca^{2+}$ entry via AMPA/KA receptors and excitotoxicity in cultured cerebellar purkinje cells. J Neurosci 14:187-197.

Buchan A (1992) Advances in cerebral ischemia: experimental approaches. In: Cerebral Ischemia: Treatment and Prevention (Barnett HJM, Hachinski VC, eds), pp 54-55. Philadelphia: W. B. Saunders Co.

Cataldo AM, Broadwell RD (1986) Cytochemical identification of cerebral glycogen and glucose-6-phosphatase activity under normal and experimental conditions: I. neurons and glia. J Electron Microsc Tech 3:413-437.

Chiu SY, Kriegler S (1994) Neurotransmitter-mediated signaling between axons and glial cells. Glia 11:191-200.

Choi DW (1987) Ionic dependence of glutamate neurotoxicity. J Neurosci 7:369-379.

Choi DW (1988) Calcium-mediated neurotoxicity: relationship to specific channel types and role in ischemic damage. Trends Neurosci 11:465-469.

Choi DW (1992) Excitotoxic cell death. J Neurobiol 23:1261-1276.

Choi DW (1995) Calcium: still center-stage in hypoxic-ischemic neuronal death. Trends Neurosci 18:58-60.

Connors BW, Ransom BR (1984) Chloride conductance and extracellular potassium concentration interact to modify the excitability of rat optic nerve fibres. J Physiol (Lond) 355:619-633.

Cummins TR, Donnelly DF, Haddad GG (1991) Effect of metabolic inhibition on the excitability of isolated hippocampal CA1 neurons: developmental aspects. J Neurophysiol 66:1471-1482.

De Juan J, Cuenca N, Iniguez C, Fernandez E (1992) Axon types classified by morphometric and multivariate analysis in the rat optic nerve. Brain Res 585:431-434.

De Weer P, Geduldig D (1973) Electrogenic sodium pump in squid giant axon. Science 179:1326-1328.

Devlin TM (1992) Textbook of Biochemistry, p 308. New York: Wiley-Liss.

DiPolo R, Beaugé L (1988) $Ca^{2+}$ transport in nerve fibers. Biochim Biophys Acta 946:549-569.

DiPolo R, Rojas H, Beaugé L (1982) $Ca^{2+}$ entry at rest and during prolonged depolarization in dialyzed squid axons. Cell Calcium 3:19-41.

Douglas SM, Panizzon KL, Wallis RA (1996) Sodium channel blockers protect against traumatic neuronal injury in the adult rat spinal cord. Soc Neurosci Abstr 22:230.

Dringen R, Hamprecht B (1992) Glucose, insulin, and insulin-like growth factor I regulate the glycogen content of astroglia-rich primary cultures. J Neurochem 58:511-517.

Dringen R, Hamprecht B (1993) Inhibition by 2-deoxyglucose and 1.5-gluconolactone of glycogen mobilization in astroglia-rich primary cultures. J Neurochem 60:1498-1504.

Dugan LL, Bruno VMG, Amagasu SM (1995) Glia modulate the response of murine cortical neurons to excitotoxicity: glia exacerbate AMPA neurotoxicity. J Neurosci 15:4545-4555.

Dugan LL, Choi DW (1994) Excitotoxicity, free radicals, and cell membrane changes. Ann Neurol 35:S17-S21.

Dunham PB, Senyk O (1977) Lithium efflux through the Na/K pump in human erythrocytes. Proc Natl Acad Sci USA 74:3099-3103.

Eng DL, Gordon TR, Kocsis JD, Waxman SG (1990) Current-clamp analysis of a time-dependent rectification in rat optic nerve. J Physiol (Lond) 421:185-202.

Erecinska M, Dagani F (1990) Relationships between the neuronal sodium/potassium pump and energy metabolism. J Gen Physiol 95:591-616.

Erecinska M, Silver IA (1989) ATP and brain function. J Cereb Blood Flow Metab 9:2-19.

Erecinska M, Silver IA (1994) Ions and energy in mammalian brain. Prog Neurobiol 43:37-71.

Fern R, Ransom, BR, Stys PK, Waxman SG (1993) Pharmacological protection of CNS white matter during anoxia: actions of phenytoin, carbamazepine and diazepam. J Pharmacol Exp Ther 266:1549-1555.

Fern R, Ransom BR (1996) CNS axons from very young rats are highly resistant to energy deprivation. Soc Neurosci Abstr 22:1426.

Fern R, Ransom BR, Waxman SG (1995a) Voltage-gated calcium channels in CNS white matter: role in anoxic injury. J Neurophysiol 74:369-377.

Fern R, Ransom BR, Waxman SG (1996) Autoprotective mechanisms in the CNS - some new lessons from white matter. Molecular & Chemical Neuropathology 27:107-129.

Fern R, Waxman SG, Ransom BR (1994) Modulation of anoxic injury in CNS white matter by adenosine and interaction between adenosine and GABA. J Neurophysiol 72:2609-2616.

Fern R, Waxman SG, Ransom, BR (1995b) Endogenous GABA attenuates CNS white matter dysfunction following anoxia. J Neurosci 15:699-708.

Fisher CM (1982) Lacunar strokes and infarcts: a review. Neurology 32:871-876.

Foster RE, Connors BW, Waxman SG (1982) Rat optic nerve: electrophysiological, pharmacological and anatomical studies during development. Dev Brain Res 3:371-386.

Frandsen A, Drejer J, Schousboe A (1989) Direct evidence that excitotoxicity in cultured neurons is mediated via *N*-methyl-D-aspartate (NMDA) as well as non-NMDA receptors. J Neurochem 53:297-299.

Frandsen A, Schousboe A (1991) Dantrolene prevents glutamate cytotoxicity and $Ca^{2+}$ release from intracellular stores in cultured cerebral cortical neurons. J Neurochem 56:1075-1078.

French CR, Sah P, Buckett KJ, Gage PW (1990) A voltage-dependent persistent sodium current in mammalian hippocampal neurons. J Gen Physiol 95:1139-1157.

Fujiwara N, Higashi H, Shimoji K, Yoshimura M (1987) Effects of hypoxia on rat hippocampal neurones *in vitro*. J Physiol (Lond) 384:131-151.

Gallant PE (1988) Effects of the external ions and metabolic poisoning on the constriction of the squid giant axon after axotomy. J Neurosci 8:1479-1484.

Goldberg MP, Choi DW (1993) Combined oxygen and glucose deprivation in cortical cell culture: calcium-dependent and calcium-independent mechanisms of neuronal injury. J Neurosci 13:3510-3524.

Gordon TR, Kocsis JD, Waxman SG (1988) Evidence for the presence of two types of potassium channels in the rat optic nerve. Brain Res 447:1-9.

Gordon TR, Kocsis J , Waxman SG (1990) Electrogenic pump ($Na^+/K^+$-ATPase) activity in rat optic nerve. Neuroscience 37:829-837.

Gwag BJ, Lobner D, Koh JY, Wie MB, Choi DW (1995) Blockade of glutamate receptors unmasks neuronal apoptosis after oxygen-glucose deprivation *in vitro*. Neuroscience 68:615-619.

Haddad GG, Jiang C (1993) $O_2$ deprivation in the central nervous system: on mechanisms of neuronal response, differential sensitivity and injury. Prog Neurobiol 40:277-318.

Halm DR, Dawson DC (1983) Cation activation of the basolateral sodium-potassium pump in turtle colon. J Gen Physiol 82:315-329.

Hansen AJ (1985) Effect of anoxia on ion distribution in the brain. Physiol Rev 65:101-148.

Hansen AJ, Hounsgaard J, Jahnsen H (1982) Anoxia increases potassium conductance in hippocampal nerve cells. Acta Physiol Scand 115:301-310.

Hildebrand C, Waxman SG (1984) Postnatal differentiation of rat optic nerve fibers: electron microscopic observations on the development of nodes of ranvier and axoglial relations. J Comp Neurol 224:25-37.

Hille B (1992) Ionic channels of excitable membranes, pp 47-50, 72-74, 129-133, 351. Sunderland: Sinauer.

Hille B, Woodhull AM, Shapiro BI (1975) Negative surface charge near sodium channels of nerve: divalent ions, monovalent ions, and pH. Philos Trans R Soc Lond [Biol] 270:301-18.

Hirano A (1968) A confirmation of the oligodendroglial origin of myelin in the adult rat. J Cell. Biol 38:637-640.

Hirano A, Llena, JF (1995) Morphology of central nervous system axons. In: The Axon: Structure, Function and Pathophysiology (Waxman SG, Kocsis JD, Stys PK, eds), p 53. New York: Oxford University Press.

Hirano A, Levine S, Zimmerman HM (1967) Experimental cyanide encephalopathy: electron microscopic observations of early lesions in white matter. J Neuropathol Exp Neurol 26:200-213.

Hodgkin AL, Huxley AF (1952) A quantitative description of membrane current and its application to conduction and excitation in nerve. J Physiol (Lond) 117:500-544.

Horisberger JD, Lemas V, Kraehenbuhl JP, Rossier BC (1991) Structure-function relationship of $Na^+$, $K^+$-ATPase. Annu Rev Physiol 53:565-584.

Jiang C, Haddad GG (1991) Effect of anoxia on intracellular and extracellular potassium activity in hypoglossal neurons in vitro. J Neurophysiol 66:103-111.

Jirounek P, Jones GJ, Burckhardt CW, Straub RW (1981) The correction factors for sucrose gap measurements and their practical applications. Biophys J 33:107-120.

Jirounek P, Straub RW (1971) The potential distribution and the short-circuiting factor in the sucrose gap. Biophys J 11:1-10.

Jonas P, Koh D, Kampe K, Hermsteiner M, Vogel W (1991) ATP-sensitive and Ca-activated K channels in vertebrate axons: novel links between metabolism and excitability. Pflugers Arch 418:68-73.

Julian FJ, Moore JW, Goldman DE (1962) Membrane potentials of the lobster giant axon obtained by use of the sucrose-gap technique. J Gen Physiol 45:1195-1216.

Junge D (1981) Nerve and Muscle Excitation, pp 32-33. Sunderland: Sinauer.

Kandel ER, Schwartz JH (1991) Directly gated transmission at central synapses. In: Principles of Neural Science (Kandel ER, Schwartz JH, Jessell TM, eds), pp 158-160, 166. New York: Elsevier Science Publishing Co.

Karst H, Wadman WJ, Joels M (1993) Long-term control by corticosteroids of the inward rectifier in rat CA1 pyramidal neurons, *in vitro*. Brain Res 612:172-9.

Kauppinen RA, Nicholls DG (1986a) Failure to maintain glycolysis in anoxic nerve terminals. J Neurochem 47:1864-1869.

Kauppinen RA, Nicholls DG (1986b) Synaptosomal bioenergetics: the role of glycolysis, pyruvate oxidation and responses to hypoglycaemia. Eur J Biochem 158:159-165.

Khodorov B, Valkina O, Turovetsky V (1994) Mechanisms of stimulus-evoked intracellular acidification in frog nerve fibres. FEBS Lett 341:125-127.

Khodorov BI (1991) Role of inactivation in local anesthetic action. Ann NY Acad Sci 625:224-248.

Kiedrowski L, Brooker G, Costa E, Wroblewski JT (1994) Glutamate impairs neuronal calcium extrusion while reducing sodium gradient. Neuron 12:295-300.

Koester J (1991) Voltage-gated ion channels and the generation of the action potential. In: Principles of Neural Science (Kandel ER, Schwartz JH, Jessell TM, eds), pp 110-111. New York: Elsevier Science Publishing Co.

Koh D-S, Jonas P, Brau ME, Vogel W (1992) A TEA-insensitive flickering potassium channel active around the resting potential in myelinated nerve. J Membr Biol 130:149-162.

Koh D-S, Jonas P, Vogel W (1994) $Na^+$-activated $K^+$ channels localized in the nodal region of myelinated axons of *Xenopus*. J Physiol (Lond) 479:183-197.

Koh J-Y, Cotman CW (1992) Programmed cell death: its possible contribution to neurotoxicity mediated by calcium channel antagonists. Brain Res 587:233-240.

Koh J-Y, Goldberg MP, Hartley DM, Choi DW (1990) Non-NMDA receptor-mediated neurotoxicity in cortical culture. J Neurosci 10:693-705.

Kostyuk P, Verkhratsky A (1994) Calcium stores in neurons and glia. Neuroscience 63:381-404.

Kraig RP, Lascola CD, Caggiano A (1995) Glial response to brain ischemia. In: Neuroglia (Kettenmann H, Ransom BR, eds), pp 968-969. New York: Oxford University Press.

Krielger S, Chiu SY (1993) Calcium signaling of glial cells along mammalian axons. J Neurosci 13:4229-4245.

Leblond J, Krnjevic K (1989) Hypoxic changes in hippocampal neurons. J Neurophys 62:1-14.

Lee MR, Sakatani K, Young W (1993) Interaction of hypoxia and hypothermia on dorsal column conduction in adult rat spinal cord *in vitro*. Exp Neurol 119:140-145.

Leppanen LL, Stys PK (1996) Resting membrane potential during metabolic inhibition in central nervous system myelinated axons. Can J Physiol Pharmacol 74:Axx.

Lev-Ram V, Grinvald A (1987) Activity-dependent calcium transients in central nervous system myelinated axons revealed by the calcium indicator fura-2. Biophys J 52:571-576.

Li M, West JW, Numann R, Murphy BJ, Scheuer T, Catterall WA (1993) Convergent regulation of sodium channels by protein kinase C and cAMP-dependent protein kinase. Science 261:1439-1442.

LoPachin RM, Stys PK (1995) Elemental composition and water content of rat optic nerve myelinated axons and glial cells: effects of *in vitro* anoxia and reoxygenation. J Neurosci 15:6735-6746.

Lynch JJ, Yu SP, Canzoniero MT, Sensi SL, Choi DW (1995) Sodium channel blockers reduce oxygen-glucose deprivation-induced cortical neuronal injury when combined with glutamate receptor antagonists. J Pharmacol Exp Ther 273:554-560.

Martin AR, Levinson SR (1985) Contribution of the $Na^+$-$K^+$ pump to membrane potential in familial periodic paralysis. Muscle Nerve 8:359-362.

Martin RL, Lloyd HGE, Cowan AI (1994) The early events of oxygen and glucose deprivation: setting the scene for neuronal death? Trends Neurosci 17:251-257.

Mata M, Fink DJ (1989) $Ca^{++}$-ATPase in the central nervous system: an EM cytochemical study. J Histochem Cytochem 37:971-980.

Mata M, Fink DJ, Ernst SA, Siegel GJ (1991) Immunocytochemical demonstration of $Na^+$, $K^+$-ATPase in internodal axolemma of myelinated fibers of rat sciatic and optic nerves. J Neurochem 57:184-192.

Mattson MP, Guthrie PB, Kater SB (1989) A role for $Na^+$-dependent $Ca^{2+}$ extrusion in protection against neuronal excitotoxicity. FASEB J 3:2519-2526.

Mattson MP, Lovell MA, Furukawa K, Markesbery WR (1995) Neurotrophic factors attenuate glutamate-induced accumulation of peroxides, elevation of intracellular $Ca^{2+}$ concentration, and neurotoxicity and increase antioxidant enzyme activities in hippocampal neurons. J Neurochem 65:1740-1751.

Mody I, MacDonald J (1995) NMDA receptor-dependent excitotoxicity: the role of intracellular $Ca^{2+}$ release. Trends Pharmacol Sci 16:356-359.

Morita K, David G, Barrett JN, Barrett EF (1993) Posttetanic hyperpolarization produced by electrogenic $Na^+/K^+$ pump in lizard axons impaled near their motor terminals. J Neurophysiol 70:1874-1884.

Neumcke B, Schwarz JR, Stämpfli R (1987) A comparison of sodium currents in rat and frog myelinated nerve: normal and modified sodium inactivation. J Physiol (Lond) 382:175-191.

Nicholls D, Attwell D (1990) The release and uptake of excitatory amino acids. Trends Pharmacol Sci 11:462-468.

Nicolls JG, Martin AR, Wallace BG (1992) From Neuron to Brain, pp 76-77. Sunderland: Sinauer.

O'Reilly JP, Haddad GG (1996) Hypoxia reduces $Na^+$ current in hippocampal neurons via a kinase mediated pathway. Soc Neurosci Abstr 22:2151.

Obrenovitch TP, Urenjak J, Richards DA, Ueda Y, Curzon G, Symon L (1993) Extracellular neuroactive amino acids in the rat striatum during ischaemia: comparison between penumbral conditions and ischaemia with sustained anoxic depolarization. J Neurochem 61:178-186.

Ochs S, Smith CB (1971) Fast axoplasmic transport in mammalian nerve *in vitro* after block of glycolysis with iodoacetic acid. J Neurochem 18:833-43.

Orrenius S, McConkey DJ, Bellomo G, Nicotera P (1989) Role of $Ca^{2+}$ in toxic cell killing. Trends Pharmacol Sci 10:281-285.

Pappas CA, Ransom BR (1995) The effects of metabolic inhibition on the viability of cultured rat astrocytes. Proc Phys Soc 69P-70P.

Pauwels PJ, Opperdoes FR, Trouet A (1985) Effects of antimycin, glucose deprivation, and serum on cultures of neurons, astrocytes, and neuroblastoma cells. J Neurochem 44:143-148.

Poulter MO, Hashiguchi T, Padjen AL (1995) Evidence for a sodium-dependent potassium conductance in frog myelinated axon. Neuroscience 68:487-495.

Pulsinelli W (1996) Excitotoxic damage in global ischemia. In: Cellular and Molecular Mechanisms of Ischemic Brain Damage (Siesjö BK, Wieloch T, eds), pp 61-62. New York: Raven Press.

Ransom BR, Orkand RK (1996) Glial-neuronal interactions in non-synaptic areas of the brain: studies in the optic nerve. Trends Neurosci 19:352-358.

Ransom BR, Sontheimer H (1992) The neurophysiology of glial cells. J Clin Neurophysiol 9:224-251.

Ransom BR, Walz W, Davis PK, Carlini WG (1992) Anoxia-induced changes in extracellular $K^+$ and pH in mammalian central white matter. J Cereb Blood Flow Metab 12:593-602.

Ransom BR, Waxman SG, Davis PK (1990) Anoxic injury of CNS white matter: protective effect of ketamine. Neurology 40:1399-1403.

Ransom BR, Waxman SG, Stys PK (1994) Anoxic injury of central myelinated axons: nonsynaptic ionic mechanisms. In: Cerebral Ischemia and Basic Mechanisms (Hartmann A, Yatsu F, Kuschinsky W, eds), pp 77-90. Berlin: Springer-Verlag.

Ransom BR, Yamate CL, Connors BW (1985) Activity-dependent shrinkage of extracellular space in rat optic nerve: a development study. J Neurosci 5:532-535.

Rasgado-Flores H, Blaustein MP (1987) Na/Ca exchange in barnacle muscle cells has a stoichiometry of 3 $Na^+$/1 $Ca^{2+}$. Am J Physiol 252:C499-C504.

Richelson E (1977) Lithium ion entry through the sodium channel of cultured mouse neuroblastoma cells: a biochemical study. Science 196:1001-1002.

Ritchie JM (1967) The oxygen consumption of mammalian non-myelinated nerve fibres at rest and during activity. J Physiol 188:309-329.

Ritchie JM (1995) Physiology of axons. In: The Axon: Structure, Function and Pathophysiology (Waxman SG, Kocsis JD, Stys, PK eds), pp 70, 92. New York: Oxford University Press.

Ritchie JM, Rogart RB (1977) Density of sodium channels in mammalian myelinated nerve fibers and nature of the axonal membrane under the myelin sheath. Proc Natl Acad Sci USA 74:211-215.

Ritchie JM, Straub RW (1980) Observations on the mechanism for the active extrusion of lithium in mammalian non-myelinated nerve fibres. J Physiol (Lond) 304:123-134.

Roper J, Schwarz JR (1989) Heterogeneous distribution of fast and slow potassium channels in myelinated rat nerve fibres. J. Physiol (Lond) 416:93-110.

Rossier BC, Geering K, Kraehenbuhl JP (1987) Regulation of the sodium pump: how and why? Trends Biol Sci 12:483-487.

Rothman S (1984) Synaptic release of excitatory amino acid neurotransmitter mediates anoxic neuronal death. J Neurosci 4:1884-1891.

Rothman SM (1983) Synaptic activity mediates death of hypoxic neurons. Science 220:536-537.

Rothman SM (1985) The neurotoxicity of excitatory amino acids is produced by passive chloride influx. J Neurosci 5:1483-1489.

Rothman SM, Olney JW (1987) Excitotoxicity and the NMDA receptor. Trends Neurosci 10:299-302.

Russell JM, Boron WF (1990) Chloride transport in the squid giant axon. In: Chloride Channels and Carriers in Nerve, Muscle, and Glial Cells (Alvarez-Leefmans FJ, Russell JM, eds), pp 85-107. New York: Plenum Press.

Sabri MI, Ochs S (1971) Inhibition of glyceraldehyde-3-phosphate dehydrogenase in mammalian nerve by iodoacetic acid. J Neurochem 18:1509-1514.

Safronov BV, Kampe K, Vogel W (1993) Single voltage-dependent potassium channels in rat peripheral nerve membrane. J Physiol (Lond) 460:675-691.

Salamino F, Sparatore B, Melloni E, Michetti M, Viotti PL, Pontremoli S, Carafoli E (1994) The plasma membrane calcium pump is the preferred calpain substrate within the erythrocyte. Cell Calcium 15:28-35.

Schlaepfer WW, Zimmerman U-JP (1981) Calcium-mediated breakdown of glial filaments and neurofilaments in rat optic nerve and spinal cord. Neurochem Res 6:243-255.

Scholz A, Reid G, Vogel W, Bostock H (1993) Ion channels in human axons. J Neurophysiol 70:1274-1279.

Shimada N, Graf R, Rosner G, Heiss W-D (1993) Ischemia-induced accumulation of extracellular amino acids in cerebral cortex, white matter, and cerebrospinal fluid. J Neurochem 60:66-71.

Shyjan AW, Cena V, Klein DC, Levenson R (1990) Differential expression and enzymatic properties of the $Na^+,K^+$-ATPase $\alpha 3$ isoenzyme in rat pineal glands. Proc Natl Acad Sci USA 87:1178-1182.

Siesjö BK (1984) Cerebral circulation and metabolism. J Neurosurg 60:883-908.

Silver IA, Erecinska M (1990) Intracellular and extracellular changes of $[Ca^{2+}]$ in hypoxia and ischemia in rat brain *in vivo*. J Gen Physiol 95:837-866.

Siman R, Noszek JC, Kegerise C (1989) Calpain I activation is specifically related to excitatory amino acid induction of hippocampal damage. J Neurosci 9:1579-1590.

Simon RP, Swan JH, Griffiths T, Meldrum BS (1984) Blockade of *N*-methyl-D-aspartate receptors may protect against ischemic damage in the brain. Science 226:850-852.

Small DL, Monette R, Buchan AM, Morley P (1997) Identification of calcium channels involved in neuronal injury in rat hippocampal slices subjected to oxygen and glucose deprivation. Brain Res In press.

Solomon JS, Nerbonne JM (1993) Hyperpolarization-activated currents in isolated superior colliculus-projecting neurons from rat visual cortex. J Physiol (Lond) 462:393-420.

Srinivasan Y, Elmer L, Davis J, Bennett V, Angelides K (1988) Ankyrin and spectrin associate with voltage-dependent sodium channels in brain. Nature 333:177-180.

Stämpfli R (1954) A new method for measuring membrane potentials with external electrodes. Experientia 10:508-509.

Steffensen I, Stys PK (1995) Immunolocalization of the Na-Ca exchanger in central and peripheral myelinated axons of the rat. Soc Neurosci Abstr 21:60.

Steffensen I, Stys PK (1996) The $Na^{+}$-$Ca^{2+}$ exchanger in neurons and glial cells. The Neuroscientist 2:1-10.

Stryer L (1988) Biochemistry, pp 356-362, 410-413, 503. New York: W. H. Freeman.

Stys PK (1994) WaveTrak: a data acquisition system and waveform database for the Macintosh. Sci Comput Automation 10:19-24.

Stys PK (1995) Protective effects of antiarrhythmic agents against anoxic injury in CNS white matter. J Cereb Blood Flow Metab 15:425-432.

Stys PK (1996) Ions, channels, and transporters involved in anoxic injury of CNS white matter. In: Cellular and Molecular Mechanisms of Ischemic Brain Damage (Siesjö BK, Wieloch T, eds), pp 153-166. New York: Raven Press.

Stys PK, Hubatsch DA (1996) K channels modulate responses of rat optic nerves to metabolic inhibition. Soc Neurosci Abstr 22:2151.

Stys PK, Lehning EJ, Sauberman AJ, LoPachin RM (1997) Intracellular concentrations of major ions in rat central and peripheral myelinated axons and glia: calculations based on electron probe microanalysis studies. J Neurochem In press.

Stys PK, LoPachin RM (Submitted) Routes of $Ca^{2+}$ entry in anoxic myelinated CNS axons. Neuroscience.

Stys PK, Ransom BR, Black JA, Waxman SG (1995a) Anoxic/ischemic injury in axons. In: The Axon: Structure, Function and Pathophysiology (Waxman SG, Kocsis JD, Stys PK, eds), p 464. New York: Oxford University Press.

Stys PK, Ransom BR, Waxman SG (1990) Effects of polyvalent cations and dihydropyridine calcium channel blockers on recovery of CNS white matter from anoxia. Neurosci Lett 115:293-299.

Stys PK, Ransom BR, Waxman SG (1992a) Tertiary and quaternary local anesthetics protect CNS white matter from anoxic injury at concentrations that do not block excitability. J Neurophysiol 67:236-240.

Stys PK, Ransom BR, Waxman SG, Davis PK (1990) Role of extracellular calcium in anoxic injury of mammalian central white matter. Proc Natl Acad Sci USA 87:4212-4216.

Stys PK, Sontheimer H, Ransom BR, Waxman SG (1993) Noninactivating, tetrodotoxin-sensitive $Na^+$ conductance in rat optic nerve axons. Proc Natl Acad Sci USA 90:6976-6980.

Stys PK, Waxman SG, Ransom BR (1992b) Effects of temperature on evoked electrical activity and anoxic injury in CNS white matter. J Cereb Blood Flow Metab 12:977-986.

Stys PK, Waxman SG, Ransom BR (1992c) Ionic mechanisms of anoxic injury in mammalian CNS white matter: role of $Na^+$ channels and $Na^+$-$Ca^{2+}$ exchanger. J Neurosci 12:430-439.

Stys PK, Waxman SG, Ransom BR (1995b) Ion pumps and exchangers. In: The Axon: Structure, Function and Pathophysiology (Waxman SG, Kocsis JD, Stys PK, eds), pp 304-306. New York: Oxford University Press.

Swanson RA, Choi DW (1993) Glial glycogen stores affect neuronal survival during glucose deprivation *in vitro*. J Cereb Blood Flow Metab 13:162-169.

Sweadner KJ (1995) Na,K-ATPase and its isoforms. In: Neuroglia (Kettenmann H, Ransom BR, eds), pp 259-272. New York: Oxford University Press.

Sweeney MI, Yager JY, Walz W, Juurlink BHJ (1995) Cellular mechanisms involved in brain ischemia. Can J Physiol Pharmacol 73:1525-1535.

Tadic V (1992) The *in vivo* effects of cyanide and its antidotes on rat brain cytochrome oxidase activity. Toxicology 76:59-67.

Takei K, Stukenbrok H, Metcalf A, Mignery GA, Sudhof TC, Volpe P, De Camilli P (1992) $Ca^{2+}$ stores in Purkinje neurons: endoplasmic reticulum subcompartments demonstrated by the heterogeneous distribution of the $InsP_3$ receptor, $Ca(^{2+})$-ATPase, and calsequestrin. J Neurosci 12:489-505.

Tas PWL, Massa PT, Kress HG, Koschel K (1987) Characterization of an $Na^+/K^+/Cl^-$ co-transport in primary cultures of rat astrocytes. Biochim Biophys Acta 903:411-416.

Taylor C (1993) $Na^+$ currents that fail to inactivate. Trends Neurosci 16:455-460.

Taylor CP, Geer JJ, Burke SP (1992) Endogenous extracellular glutamate accumulation in rat neocortical cultures by reversal of the transmembrane sodium gradient. Neurosci Lett 145:197-200.

Thomas RC (1972) Electrogenic sodium pump in nerve and muscle cells. Physiol Rev 52:563-594.

Thomas RC, Simon W, Oehme M (1975) Lithium accumulation by snail neurones measured by a new $Li^+$-sensitive microelectrode. Nature 258:754-756.

Tsacopoulos M, Magistretti PJ (1996) Metabolic coupling between glia and neurons. J Neurosci 16:877-885.

Utzschneider DA, Kocsis JD, Waxman SG (1991) Differential sensitivity to hypoxia of the peripheral versus central trajectory of primary afferent axons. Brain Res 551:136-141.

Vibulsreth S, Hefti F, Ginsberg MD, Dietrich WD, Busto R (1987) Astrocytes protect cultured neurons from degeneration induced by anoxia. Brain Res 422:303-311.

Walz W (1995) Distribution and transport of chloride and bicarbonate ions across membranes. In: Neuroglia (Kettenmann H, Ransom BR, eds), pp 226-229. New York: Oxford University Press.

Walz W, Klimaszewski , Paterson IA (1993) Glial swelling in ischemia: a hypothesis. Dev Neurosci 15:216-225.

Wang GK, Brodwick MS, Eaton DC, Strichartz GR (1987) Inhibition of sodium currents by local anesthetics in chloramine-T-treated squid axons. The role of channel activation. J Gen Physiol 89:645-67.

Waxman SG (1983) Action potential propagation and conduction velocity - new perspectives and questions. Trends Neurosci 6:157-161.

Waxman SG (1995) Voltage-gated ion channels in axons: localization, function, and development. In: The Axon: Structure, Function and Pathophysiology (Waxman SG, Kocsis JD, Stys PK, eds), pp 224-225. New York: Oxford University Press.

Waxman SG, Black JA (1984) Freeze-fracture ultrastructure of the perinodal astrocyte and associated glial junctions. Brain Res 308:77-87.

Waxman SG, Black JA, Ransom BR, Stys PK (1993) Protection of the axonal cytoskeleton in anoxic optic nerve by decreased extracellular calcium. Brain Res 614:137-145.

Waxman SG, Black JA, Ransom BR, Stys PK (1994) Anoxic injury of rat optic nerve: ultrastructural evidence for coupling between $Na^+$ influx and $Ca^{2+}$ mediated injury in myelinated CNS axons. Brain Res 644:197-204.

Waxman SG, Black JA, Stys PK, Ransom BR (1992a) Ultrastructural concomitants of anoxic injury and early post-anoxic recovery in rat optic nerve. Brain Res 574:105-119.

Waxman SG, Davis PK, Black JA, Ransom BR (1990) Anoxic injury of mammalian central white matter: decreased susceptibility in myelin-deficient optic nerve. Ann Neurol 28:335-340.

Waxman SG, Ransom BR, Stys PK (1991) Non-synaptic mechanisms of $Ca^{2+}$-mediated injury of CNS white matter. Trends Neurosci 14:461-468.

Waxman SG, Ritchie JM (1993) Molecular dissection of the myelinated axon. Ann Neurol 33:121-136.

Waxman SG, Stys PK, Black JA, Ransom BR (1992b) Role of $Na^{+}$ conductance and the $Na^{+}$-$Ca^{2+}$ exchanger in anoxic injury of CNS white matter. In: Pharmacology of Cerebral Ischemia (Krieglstein J, Oberpichler-Schwenk H, eds), pp 13-31. Stuttgart: Wissenschaftliche Verlagsgesellschaft.

Weiss JH, Hartley DM, Koh J, Choi DW (1990) The calcium channel blocker nifedipine attenuates slow excitatory amino acid neurotoxicity. Science 247:1474-1477.

White RJ, Reynolds IJ (1995) Mitochondria and $Na^{+}/Ca^{2+}$ exchange buffer glutamate-induced calcium loads in cultured cortical neurons. J Neurosci 15:1318-1328.

Woodhull AM (1973) Ionic blockage of sodium channels in nerve. J Gen Physiol 61:687-708.

Xie Y, Dengler K, Zacharias E, Wilffert B, Tegtmeier F (1994) Effects of the sodium channel blocker tetrodotoxin (TTX) on cellular ion homeostasis in rat brain subjected to complete ischemia. Brain Res 652:216-224.

Xu KY, Zweier JL, Becker LC (1995) Functional coupling between glycolysis and sarcoplasmic reticulum $Ca^{2+}$ transport. Circ Res 77:88-97.

Zhang L, Krnjevic K (1993) Whole - cell recording of anoxic effects on hippocampal neurons in slices. J Neurophysiol 69:118-127.